LIQUID-GAS PHASE TRANSITIONS IN NUCLEAR MATTER

A (hopefully) pedagogical introduction and overview of experimental achievements in the field

John FRANKLAND

GANIL

cnrs NUCLÉAIRE & PARTICULES

cea

LIQUID-GAS PHASE TRANSITIONS IN NUCLEAR MATTER

A (hopefully) pedagogical introduction and overview of experimental achievements in the field

John FRANKLAND

GANIL

cnrs NUCLÉAIRE & PARTICULES

cea

"If it were possible to experiment with neutrons or protons of energies above a hundred million volts, several charged or uncharged particles would eventually leave the nucleus as a result of the encounter; with particles of energies of about a thousand million volts, we must even be prepared for the collision to lead to an explosion of the whole nucleus"

Niels Bohr, Nature 137 (1936) 351

LIQUID-GAS PHASE TRANSITIONS IN NUCLEAR MATTER

A (hopefully) pedagogical introduction and overview of experimental achievements in the field

John FRANKLAND

GANIL

cnrs NUCLÉAIRE & PARTICULES

cea

1. INTRODUCTION

- a few “reminders” on equations of state & LGPT in classical systems, associated critical phenomena, realistic nuclear matter EoS & link to multifragmentation, and statistical models in HIC

2. SOME EXPERIMENTAL OBSERVATIONS

- a historical tour from the earliest experiments suggesting strong links between multifragmentation and a liquid-gas phase transition of nuclear matter

3. INDRA RESULTS

- characterizing the gas phase, now including in-medium effects & link to QCD phase diagram
- characterizing the phase transition: convex entropy intruder & all that entails

The Equation of State of Ideal Fluids

IDEAL FLUID EoS (Clapeyron*, 1834)

**combination of Boyle (1662) and Charles (1787)*

$$pV = NT$$

Or: $p = \rho T$ with $\rho = \frac{N}{V}$

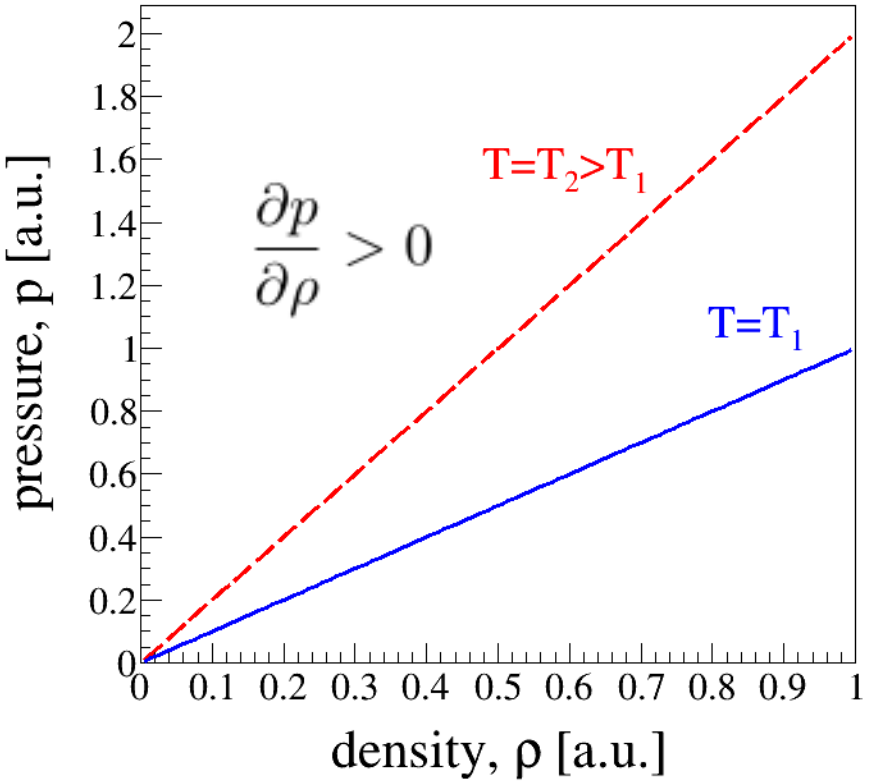

The Equation of State of Ideal Fluids

IDEAL FLUID EoS (Clapeyron*, 1834)

**combination of Boyle (1662) and Charles (1787)*

$$pV = NT$$

Or: $p = \rho T$ with $\rho = \frac{N}{V}$

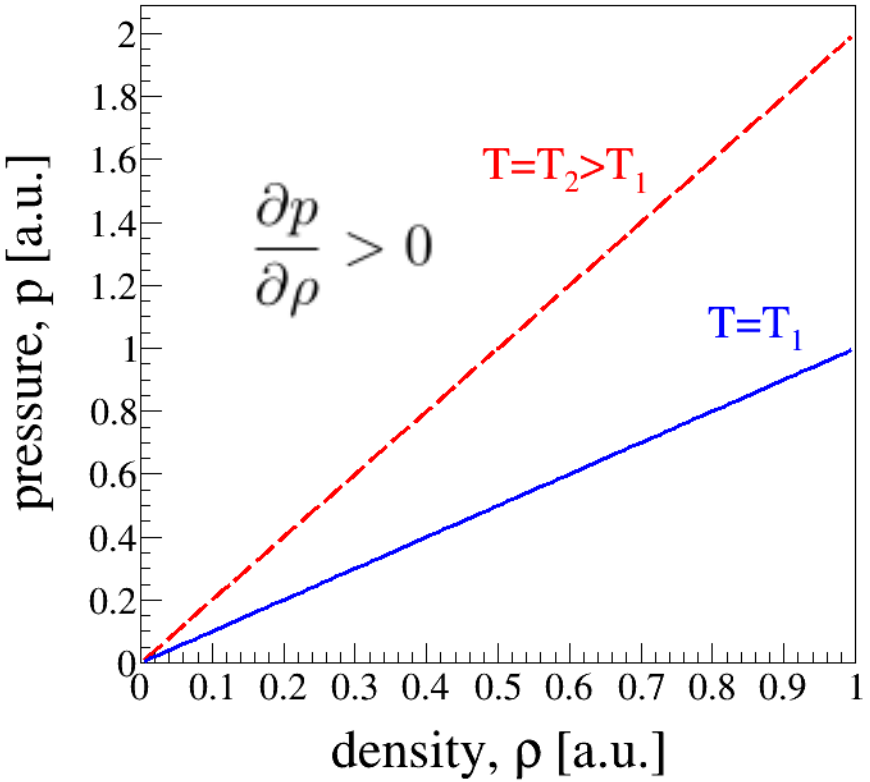

But real fluids (e.g. H_2O) exhibit phase transitions (liquid, gas) at different temperatures/ densities/pressures...

Introduction: Classical EoS & LGPT

(An) Equation of State for Non-Ideal Fluids

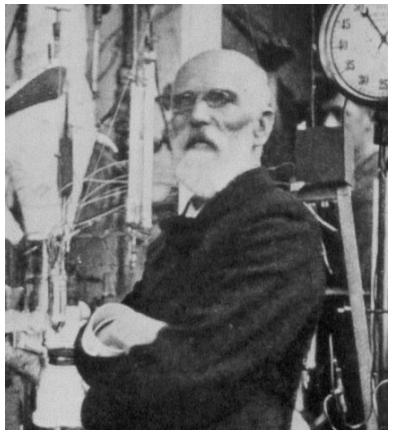

NON-IDEAL FLUID EoS (Van der Waals, 1873)

$$\left(p + a\rho^2\right)(V - Nb) = NT$$

Introduction: Classical EoS & LGPT

(An) Equation of State for Non-Ideal Fluids

NON-IDEAL FLUID EoS (Van der Waals, 1873)

$$\left(p + a\rho^2\right)\left(V - Nb\right) = NT$$

(long-range) intermolecular attraction

excluded volume → short-range repulsion

Johannes Diderik van der Waals theorised his EoS as part of his Ph.D thesis. It was the first theory to explain the existence of liquid and gas phases of the same substance.

At the time, the 'molecular hypothesis' was not widely believed; it was also thought possible that different phases could be chemically different.

It earned him the Nobel prize in 1910.

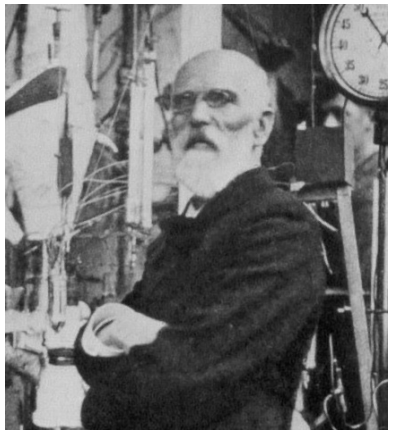

(An) Equation of State for Non-Ideal Fluids

NON-IDEAL FLUID EoS (Van der Waals, 1873)

$$\left(p + a\rho^2\right)\left(V - Nb\right) = NT$$

(long-range) intermolecular attraction

excluded volume → short-range repulsion

New 'rich' phase structure of EoS :
- low- & high-density regions separated by forbidden (thermodynamically unstable) region → spinodal
- 'critical' temperature marks end of liquid/gas coexistence
- critical point (p_c,ρ_c,T_c) with special properties...

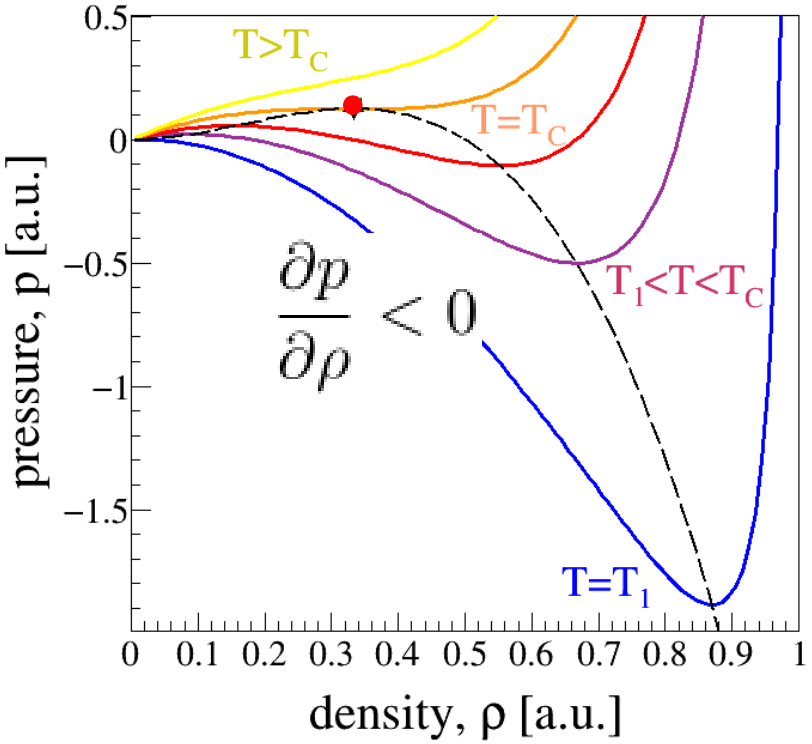

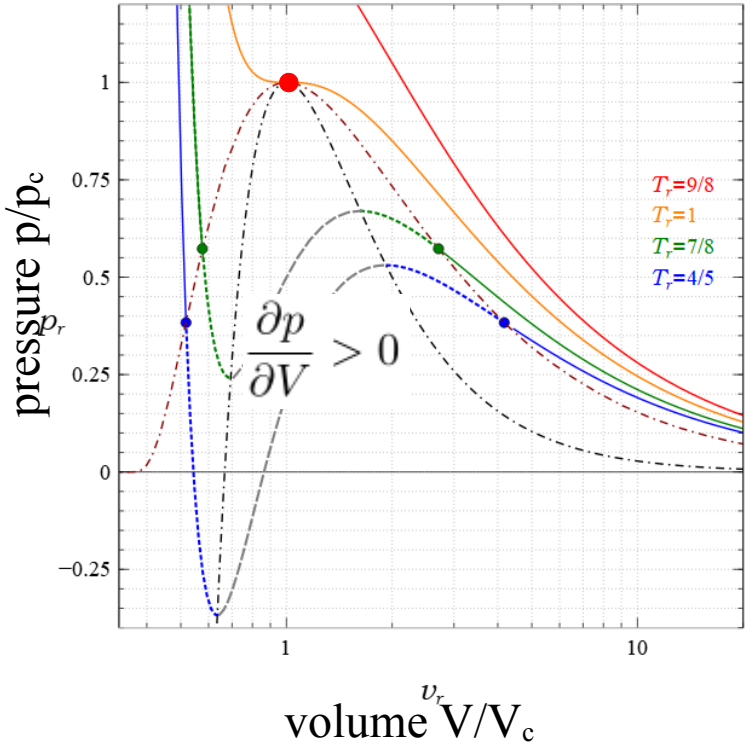

Critical phenomena

Many different systems exhibit ‘critical’ phenomena
(LGPT, percolation, Ising/magnetization, ⋯)

Close to a critical point, ‘universal’ features,
independent of the underlying microscopic interactions,
are determined by ‘critical exponents’:

Introduction: Classical EoS & LGPT

Critical phenomena

Many different systems exhibit ‘critical’ phenomena (LGPT, percolation, Ising/magnetization, ⋯)

Close to a critical point, ‘universal’ features, independent of the underlying microscopic interactions, are determined by ‘critical exponents’:

Order parameter → 0 $\quad \Psi \sim \epsilon^{\beta}$

Correlation length → ∞ $\quad \xi \sim |\epsilon|^{-1/\nu}$

		LGPT	**Percolation**
Distance to critical point	ϵ	$T_C - T$	$p - p_C$
Order parameter	Ψ	$\rho_l - \rho_g$	s_{max}
$\chi \to \infty$ $\quad \chi \sim \lvert\epsilon\rvert^{-\gamma}$		$\chi = K_T = \left(\rho \left.\frac{\partial p}{\partial \rho}\right\rvert_T\right)^{-1}$ isothermal compressibility	$\chi = M_2 = \sum_s s^2 n(s)$ variance of cluster sizes

$$\tau = 2 + \frac{\beta}{\beta + \gamma},$$

$$\sigma = \frac{1}{\beta + \gamma}.$$

Quantity	Value for percolation on a 3D lattice [7]	Value for liquid–gas systems [6]
τ	2.18	2.21
β	0.41	0.33
γ	1.8	1.23
ν	0.88	0.63
σ	0.45	0.64

Introduction: Classical EoS & LGPT

Critical phenomena

Many different systems exhibit ‘critical’ phenomena (LGPT, percolation, Ising/magnetization, ⋯)

Close to a critical point, ‘universal’ features, independent of the underlying microscopic interactions, are determined by ‘critical exponents’

Order parameter → 0 $\quad \Psi \sim \epsilon^{\beta}$

Correlation length → ∞ $\quad \xi \sim |\epsilon|^{-1/\nu}$

		LGPT	Percolation
Distance to critical point	ϵ	$T_C - T$	$p - p_C$
Order parameter	Ψ	$\rho_l - \rho_g$	s_{max}
$\chi \to \infty$ $\chi \sim \lvert\epsilon\rvert^{-\gamma}$		$\chi = K_T = \left(\rho \left.\frac{\partial p}{\partial \rho}\right\rvert_T\right)^{-1}$ isothermal compressibility	$\chi = M_2 = \sum_s s^2 n(s)$ variance of cluster sizes

$$\tau = 2 + \frac{\beta}{\beta+\gamma},$$

$$\sigma = \frac{1}{\beta+\gamma}.$$

Quantity	Value for percolation on a 3D lattice [7]	Value for liquid–gas systems [6]
τ	2.18	2.21
β	0.41	0.33
γ	1.8	1.23
ν	0.88	0.63
σ	0.45	0.64

Fisher droplet model

M.E. Fisher, Physics 3(1967)255

$$n_A = q_0 A^{-\tau} \exp\left[\frac{\Delta\mu A}{T} - \frac{c_0 \varepsilon A^{\sigma}}{T}\right]$$

- liquid droplets forming in near-critical fluid
- reduces to power law at critical point

Introduction:
Nuclear Matter EoS & LGPT

Nuclear Matter

Nuclear Matter

Dominant features of the (isoscalar) nucleon-nucleon interaction are short-range repulsion & long-range attraction...

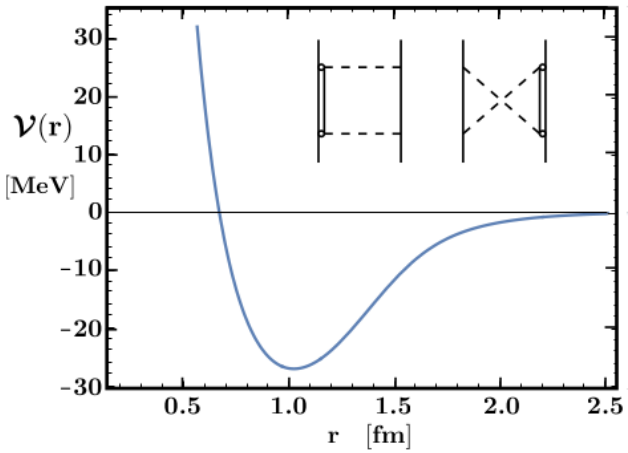

2-Pion exchange in Chiral Effective Field Theory (ChEFT)

N. Kaiser, W. Weise, arXiv:2602.09916v2

Nuclear Matter

Dominant features of the (isoscalar) nucleon-nucleon interaction are short-range repulsion & long-range attraction…

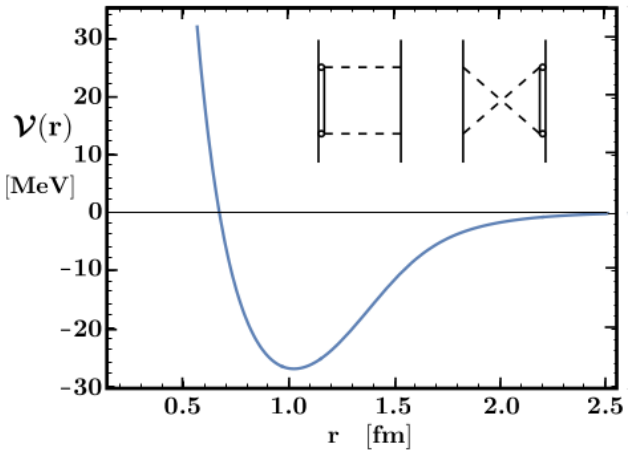

2-Pion exchange in Chiral Effective Field Theory (ChEFT)

N. Kaiser, W. Weise, arXiv:2602.09916v2

…so unsurprisingly (?) the thermodynamics of nuclear matter bears a striking resemblance to the Van der Waals EoS

Thermal Hartree-Fock calculation
(Skyrme interaction)
Infinite nuclear matter

G. Sauer et al., Nucl. Phys. A264(1976)221

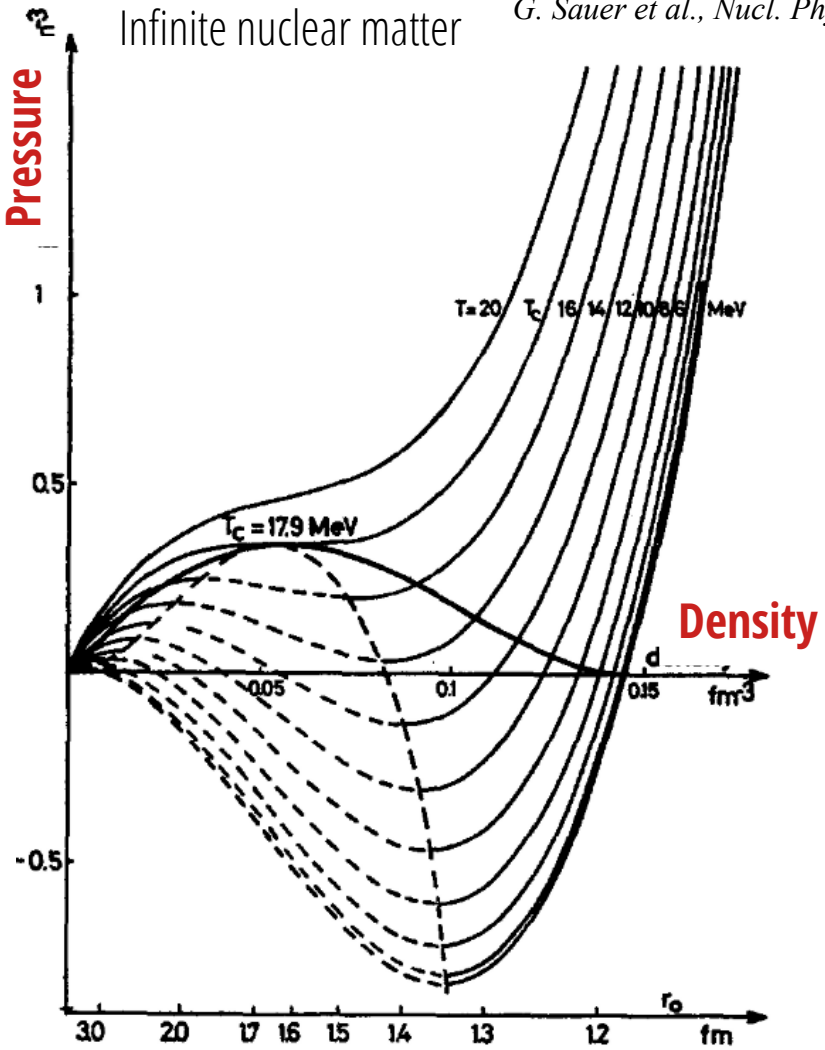

Introduction:
Nuclear Matter EoS & LGPT

Nuclear Matter

Dominant features of the (isoscalar) nucleon-nucleon interaction are short-range repulsion & long-range attraction…

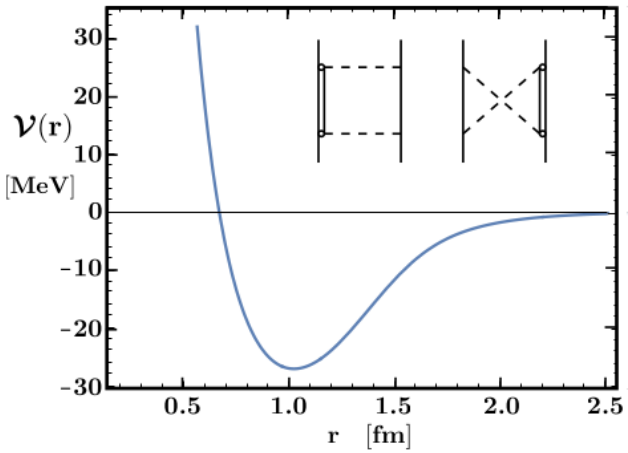

2-Pion exchange in Chiral Effective Field Theory (ChEFT)

N. Kaiser, W. Weise, arXiv:2602.09916v2

…so unsurprisingly (?) the thermodynamics of nuclear matter bears a striking resemblance to the Van der Waals EoS

Thermal Hartree-Fock calculation
(Skyrme interaction)
Infinite nuclear matter

G. Sauer et al., Nucl. Phys. A264(1976)221

A. Rios / Nuclear Physics A 845 (2010) 58–87

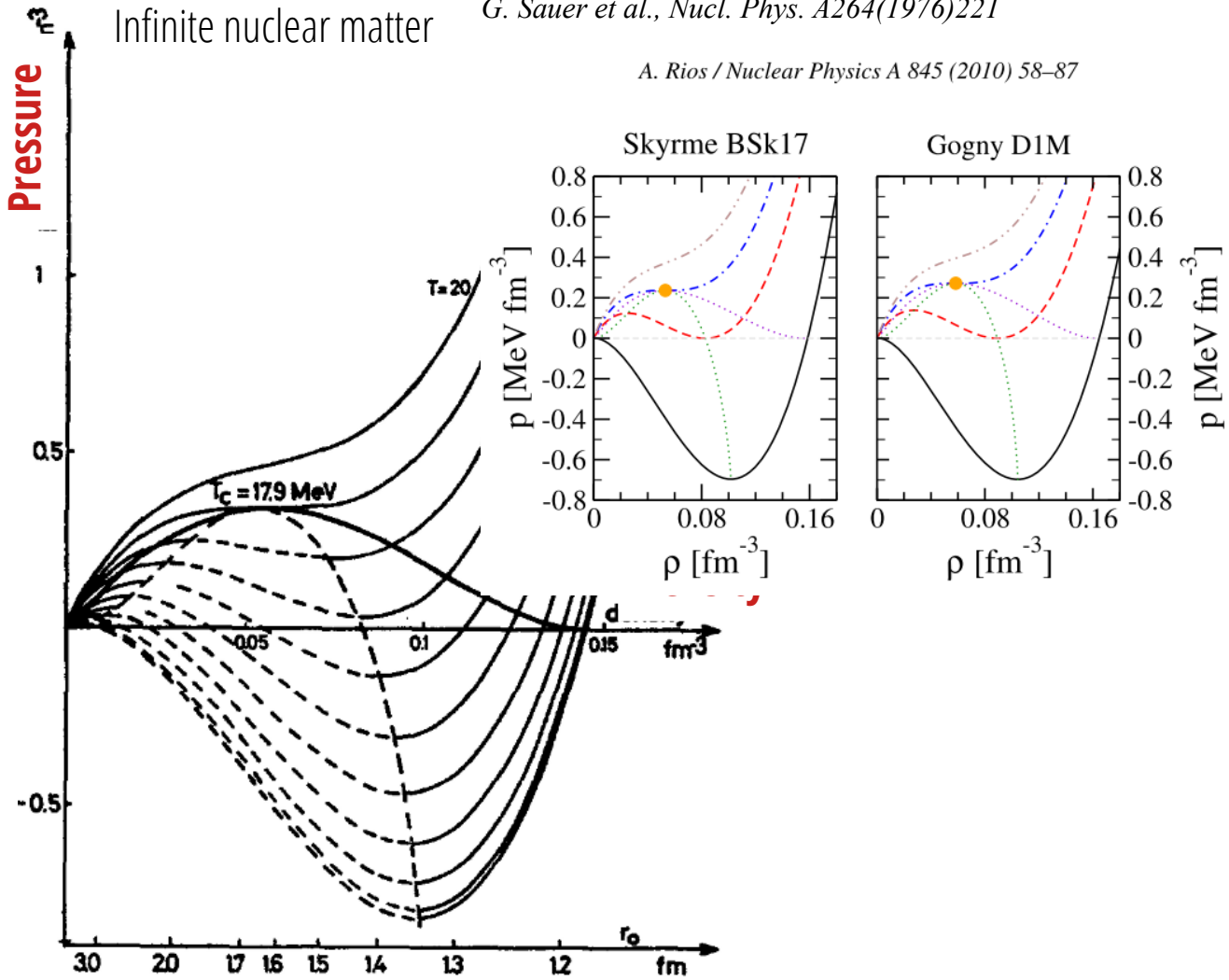

Introduction:
Nuclear Matter EoS & LGPT

Nuclear Matter

Dominant features of the (isoscalar) nucleon-nucleon interaction are short-range repulsion & long-range attraction…

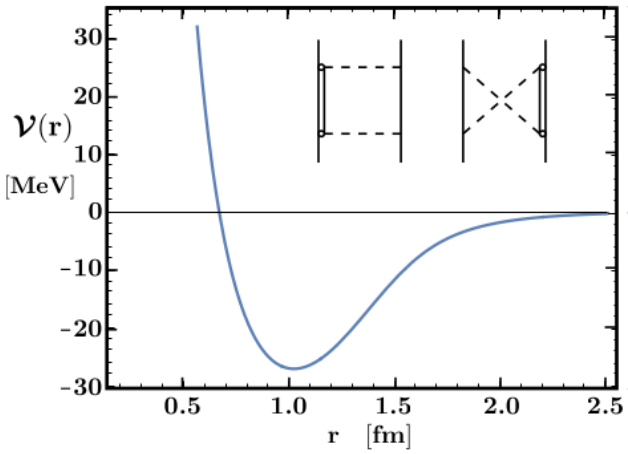

2-Pion exchange in Chiral Effective Field Theory (ChEFT)

N. Kaiser, W. Weise, arXiv:2602.09916v2

…so unsurprisingly (?) the thermodynamics of nuclear matter bears a striking resemblance to the Van der Waals EoS

Thermal Hartree-Fock calculation
(Skyrme interaction)
Infinite nuclear matter

G. Sauer et al., Nucl. Phys. A264(1976)221

A. Rios / Nuclear Physics A 845 (2010) 58–87

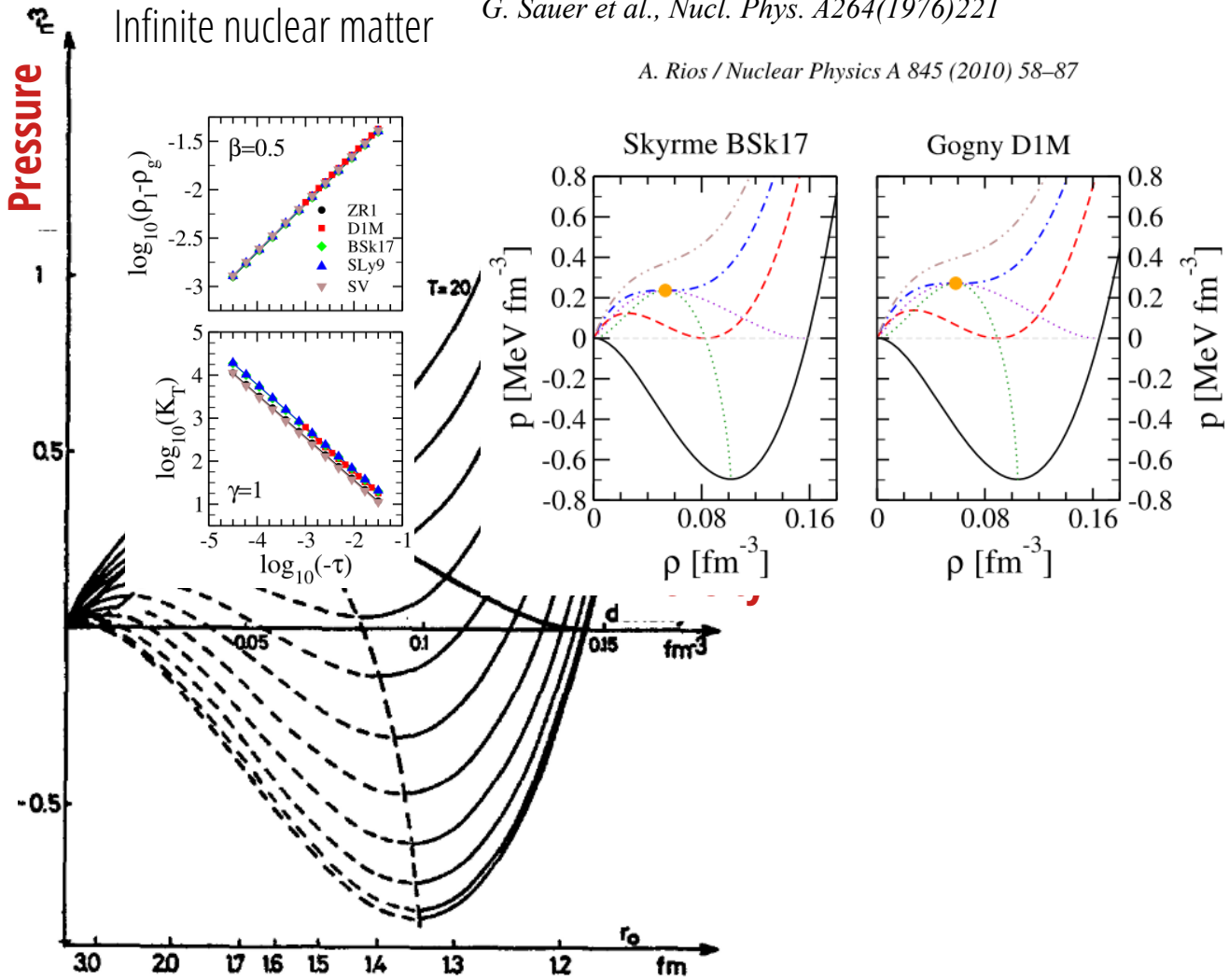

Introduction:
Nuclear Matter EoS & LGPT

Nuclear Matter

Dominant features of the (isoscalar) nucleon-nucleon interaction are short-range repulsion & long-range attraction…

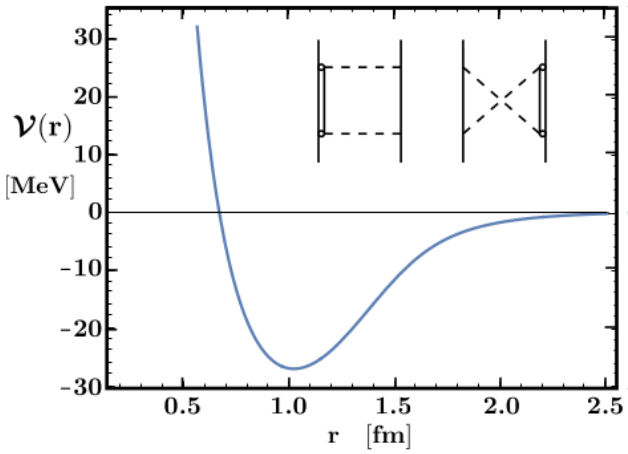

2-Pion exchange in Chiral Effective Field Theory (ChEFT)

N. Kaiser, W. Weise, arXiv:2602.09916v2

…so unsurprisingly (?) the thermodynamics of nuclear matter bears a striking resemblance to the Van der Waals EoS

Thermal Hartree-Fock calculation
(Skyrme interaction)
Infinite nuclear matter

G. Sauer et al., Nucl. Phys. A264(1976)221

A. Rios / Nuclear Physics A 845 (2010) 58–87

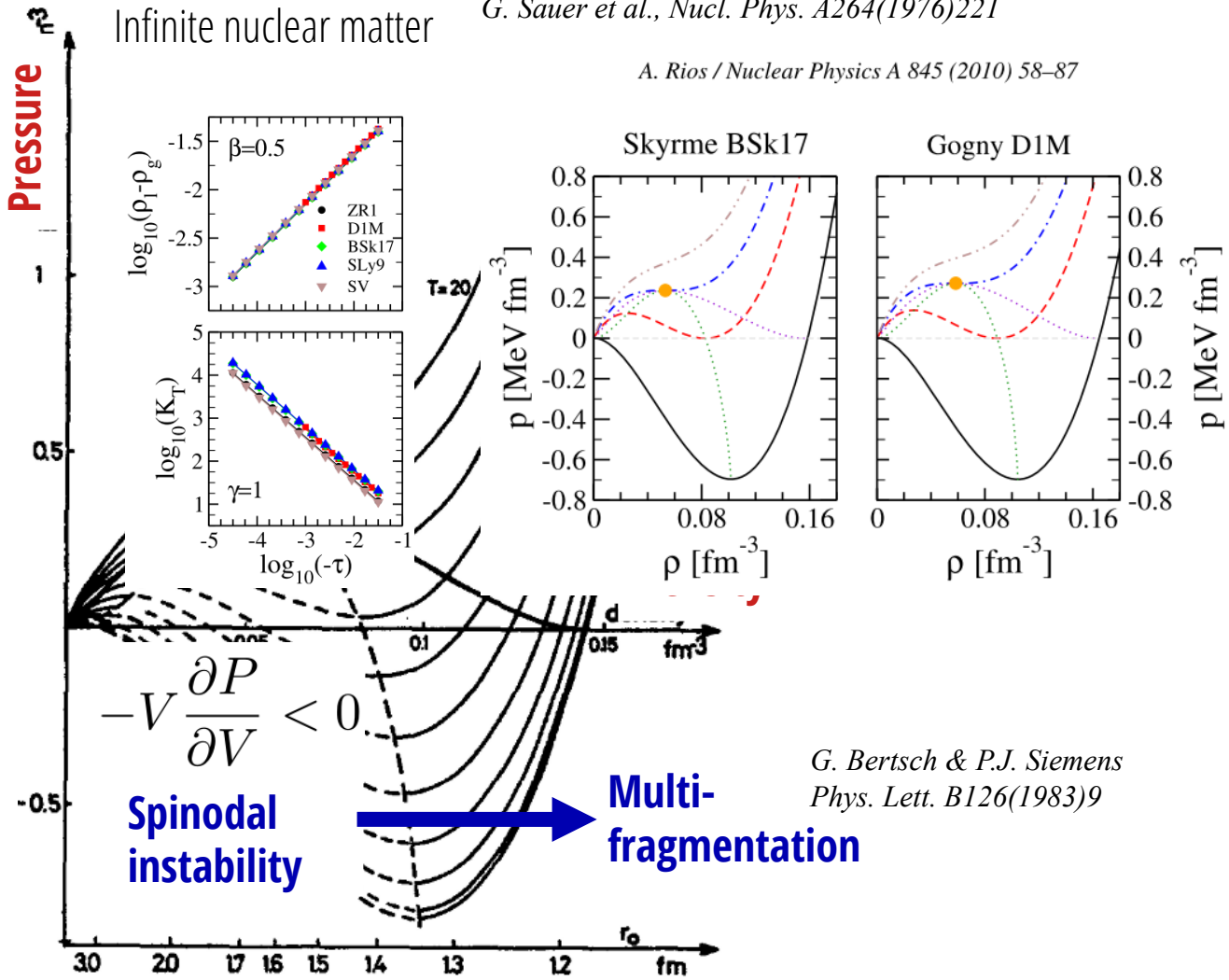

G. Bertsch & P.J. Siemens
Phys. Lett. B126(1983)9

Hot nuclei & multifragmentation

Statistical models for multifragmentation of hot nuclei:
statistical ensembles of break-up configurations

System - A_0, Z_0, E_0, V

Ensemble of partitions - $\{f\colon N_{AZ}, 1 \le A \le A_0, 0 \le Z \le Z_0\}$

Microcanonical description	Canonical description	Macrocanonical description
$\sum A \cdot N_{AZ} = A_0$	$\sum A \cdot N_{AZ} = A_0$	$\sum A \cdot \langle N_{AZ} \rangle = A_0$
$\sum Z \cdot N_{AZ} = Z_0$	$\sum Z \cdot N_{AZ} = Z_0$	$\sum Z \cdot \langle N_{AZ} \rangle = Z_0$
$E_f(N_{AZ}, T_f, V) = E_0$	$\langle E_f(N_{AZ}, T, V) \rangle = E_0$	$\langle E_f(\langle N_{AZ} \rangle, T, V) \rangle = E_0$
$W_f^{mic} \sim \exp S_f(E_0, V, A_0, Z_0)$	$W_f^{can} \sim \exp\left(-\frac{F_f(T,V,A_0,Z_0)}{T}\right)$	$W_f^{mac} \sim \exp\left(-\frac{F_f(T,V,A_0,Z_0)-\mu\sum A-\nu\sum Z}{T}\right)$

Hot nuclei & multifragmentation

Statistical models for multifragmentation of hot nuclei:
statistical ensembles of break-up configurations

System - A_0, Z_0, E_0, V

Ensemble of partitions - $\{f: N_{AZ}, 1 \le A \le A_0, 0 \le Z \le Z_0\}$

Microcanonical description	Canonical description	Macrocanonical description
$\sum A \cdot N_{AZ} = A_0$	$\sum A \cdot N_{AZ} = A_0$	$\sum A \cdot \langle N_{AZ} \rangle = A_0$
$\sum Z \cdot N_{AZ} = Z_0$	$\sum Z \cdot N_{AZ} = Z_0$	$\sum Z \cdot \langle N_{AZ} \rangle = Z_0$
$E_f(N_{AZ}, T_f, V) = E_0$	$\langle E_f(N_{AZ}, T, V) \rangle = E_0$	$\langle E_f(\langle N_{AZ} \rangle, T, V) \rangle = E_0$
$W_f^{mic} \sim \exp S_f(E_0, V, A_0, Z_0)$	$W_f^{can} \sim \exp\left(-\frac{F_f(T,V,A_0,Z_0)}{T}\right)$	$W_f^{mac} \sim \exp\left(-\frac{F_f(T,V,A_0,Z_0)-\mu\sum A-\nu\sum Z}{T}\right)$

Statistical Multifragmentation Model (SMM)

Volume 162B, number 1,2,3 PHYSICS LETTERS 7 November 1985

ENERGY THRESHOLDS FOR FRAGMENTATION AND VAPORIZATION OF THE ATOMIC NUCLEUS

J.P. BONDORF, R. DONANGELO [1], H. SCHULZ [2] and K. SNEPPEN
The Niels Bohr Institute, Blegdamsvej 17, DK 2100 Copenhagen, Denmark

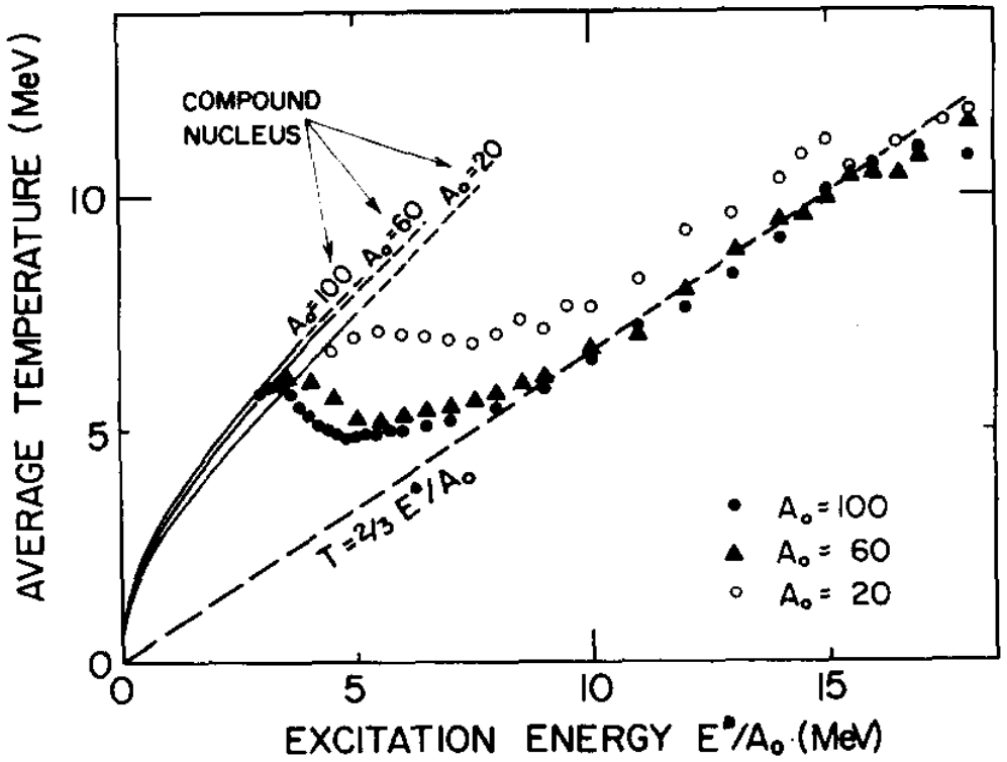

Hot nuclei & multifragmentation

Statistical models for multifragmentation of hot nuclei:
statistical ensembles of break-up configurations

System - A_0, Z_0, E_0, V

Ensemble of partitions - $\{f: N_{AZ}, 1 \le A \le A_0, 0 \le Z \le Z_0\}$

Microcanonical description	Canonical description	Macrocanonical description
$\sum A \cdot N_{AZ} = A_0$	$\sum A \cdot N_{AZ} = A_0$	$\sum A \cdot \langle N_{AZ} \rangle = A_0$
$\sum Z \cdot N_{AZ} = Z_0$	$\sum Z \cdot N_{AZ} = Z_0$	$\sum Z \cdot \langle N_{AZ} \rangle = Z_0$
$E_f(N_{AZ}, T_f, V) = E_0$	$\langle E_f(N_{AZ}, T, V) \rangle = E_0$	$\langle E_f(\langle N_{AZ} \rangle, T, V) \rangle = E_0$
$W_f^{mic} \sim \exp S_f(E_0, V, A_0, Z_0)$	$W_f^{can} \sim \exp\left(-\frac{F_f(T,V,A_0,Z_0)}{T}\right)$	$W_f^{mac} \sim \exp\left(-\frac{F_f(T,V,A_0,Z_0)-\mu\sum A-\nu\sum Z}{T}\right)$

Statistical Multifragmentation Model (SMM)

Volume 162B, number 1,2,3 PHYSICS LETTERS 7 November 1985

ENERGY THRESHOLDS FOR FRAGMENTATION AND VAPORIZATION OF THE ATOMIC NUCLEUS

J.P. BONDORF, R. DONANGELO [1], H. SCHULZ [2] and K. SNEPPEN
The Niels Bohr Institute, Blegdamsvej 17, DK 2100 Copenhagen, Denmark

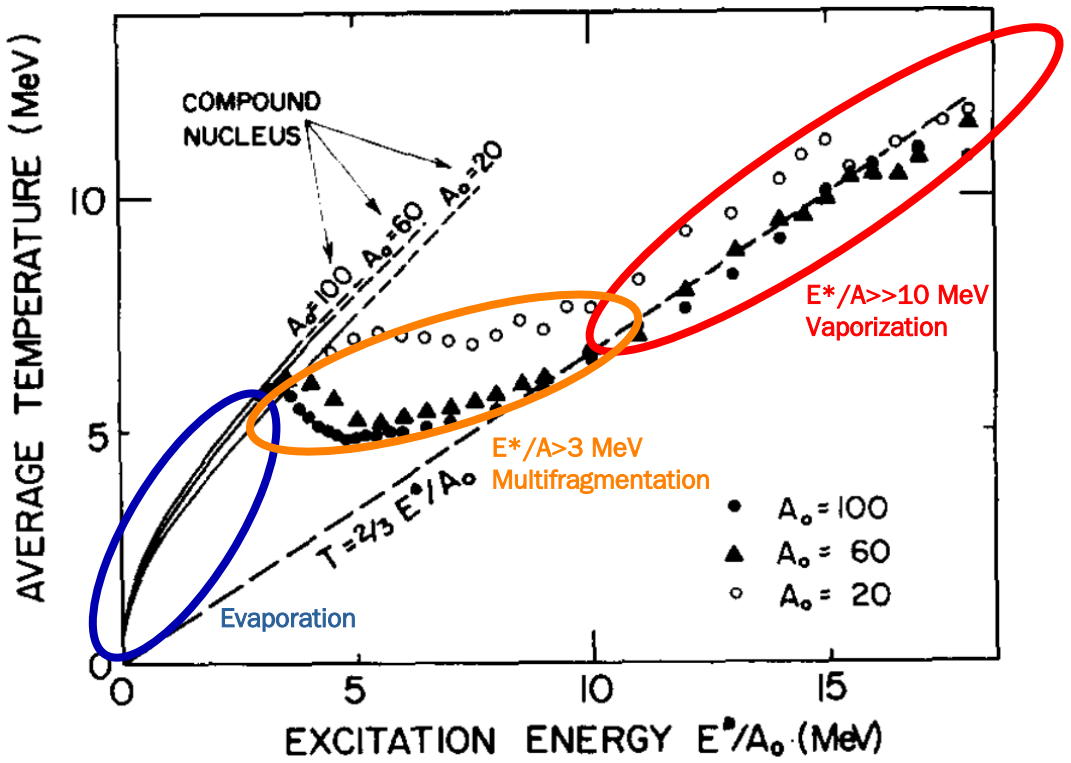

Introduction: Nuclear Matter EoS & LGPT

Hot nuclei & multifragmentation

Statistical models for multifragmentation of hot nuclei: statistical ensembles of break-up configurations

System - A_0, Z_0, E_0, V

Ensemble of partitions - $\{f: N_{AZ}, 1 \le A \le A_0, 0 \le Z \le Z_0\}$

Microcanonical description	Canonical description	Macrocanonical description
$\sum A \cdot N_{AZ} = A_0$	$\sum A \cdot N_{AZ} = A_0$	$\sum A \cdot \langle N_{AZ} \rangle = A_0$
$\sum Z \cdot N_{AZ} = Z_0$	$\sum Z \cdot N_{AZ} = Z_0$	$\sum Z \cdot \langle N_{AZ} \rangle = Z_0$
$E_f(N_{AZ}, T_f, V) = E_0$	$\langle E_f(N_{AZ}, T, V) \rangle = E_0$	$\langle E_f(\langle N_{AZ} \rangle, T, V) \rangle = E_0$
$W_f^{mic} \sim \exp S_f(E_0, V, A_0, Z_0)$	$W_f^{can} \sim \exp\left(-\frac{F_f(T,V,A_0,Z_0)}{T}\right)$	$W_f^{mac} \sim \exp\left(-\frac{F_f(T,V,A_0,Z_0)-\mu\sum A-\nu\sum Z}{T}\right)$

Justification for statistical approach?

It is natural to think that an intensive exchange of mass, charge and energy between different parts of the system takes place in the course of expansion. That is why we assume that at least partial thermodynamic equilibrium is established prior to the break-up. The process of fragment formation takes place in an unstable medium and, therefore, has a chaotic character. One may expect large

Volume 162B, number 1,2,3 PHYSICS LETTERS 7 November 1985

Statistical Multifragmentation Model (SMM)

ENERGY THRESHOLDS FOR FRAGMENTATION AND VAPORIZATION OF THE ATOMIC NUCLEUS

J.P. BONDORF, R. DONANGELO [1], H. SCHULZ [2] and K. SNEPPEN

The Niels Bohr Institute, Blegdamsvej 17, DK 2100 Copenhagen, Denmark

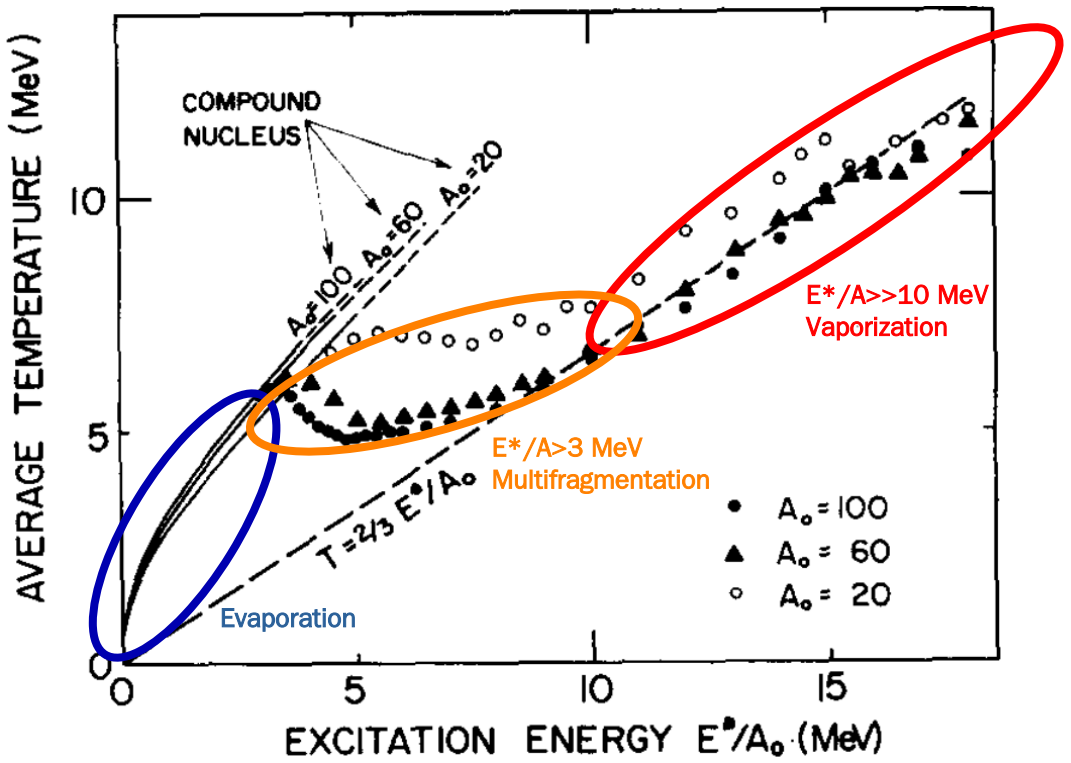

HIC & statistical (even thermodynamical) approaches

Equilibrium thermodynamics

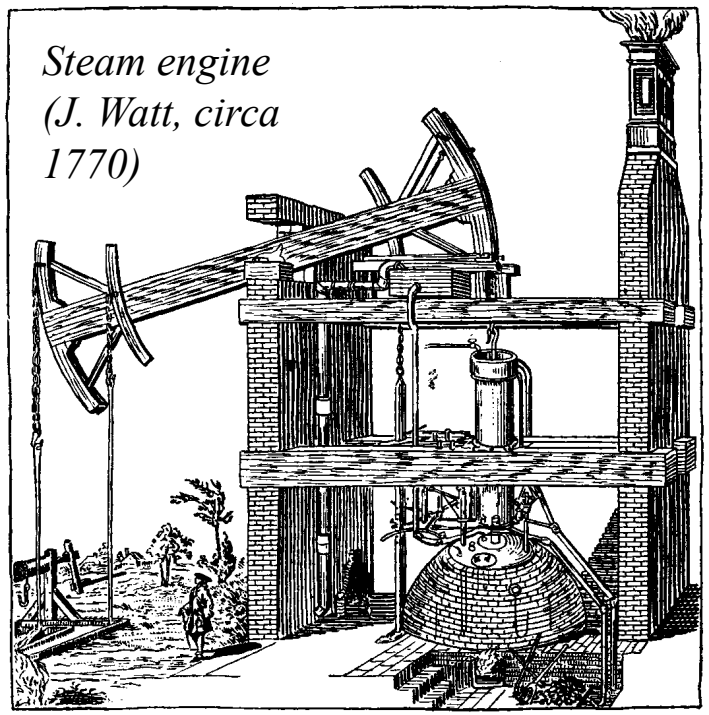

Single system, time-averaged observable properties

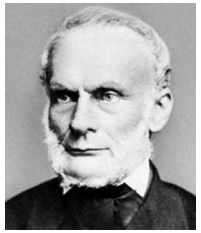

$$dS = \frac{\delta Q}{T}$$

Introduction: HIC & LGPT

Equilibrium thermodynamics

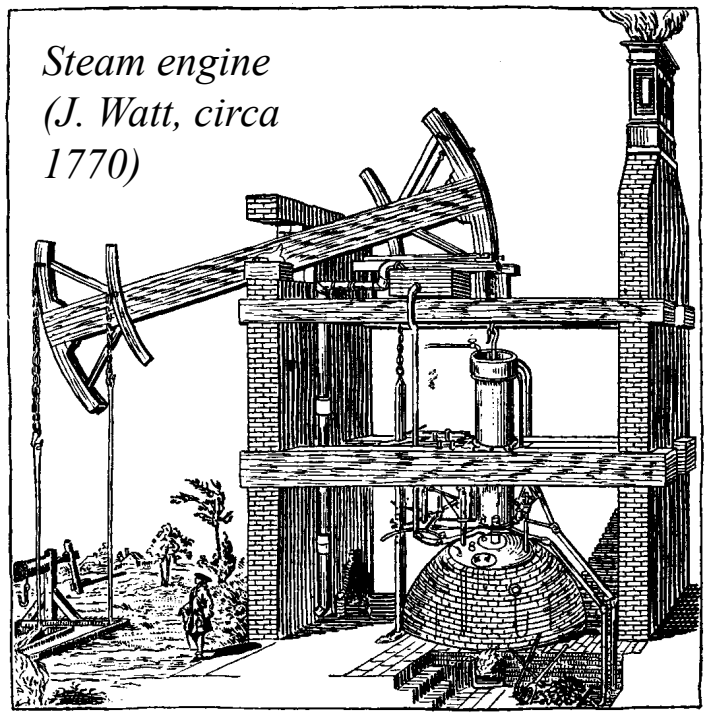

Single system, time-averaged observable properties

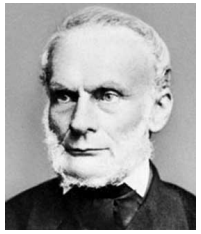

$$dS = \frac{\delta Q}{T}$$

Equilibrium statistical mechanics

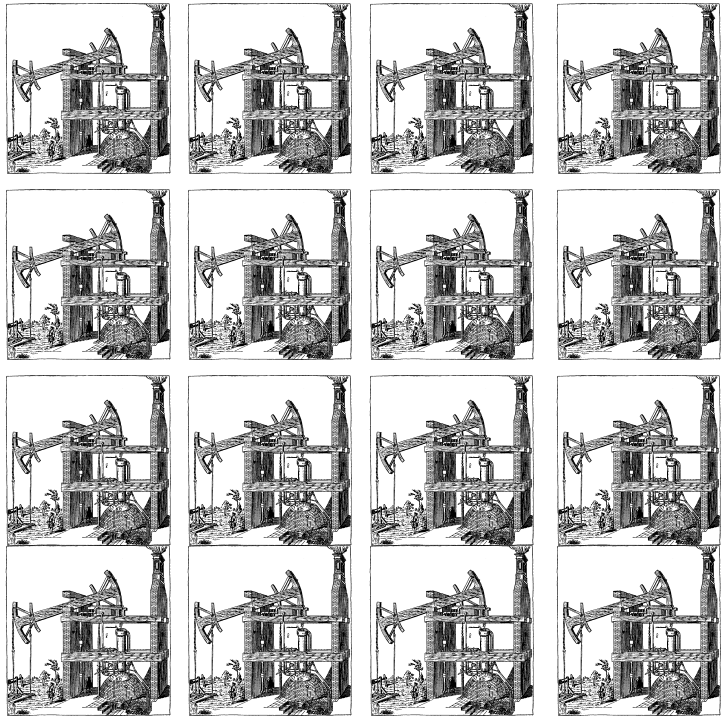

Fictitious ensemble of system replicates at different (fixed) times in its evolution

Microstate population constrained by observable properties

$$S = k \log W$$

HIC & statistical (even thermodynamical) approaches

Fermi energy heavy-ion collisions

Each collision is a highly dynamical, far-from-equilibrium, process leading to hugely many different final states (freeze-out)

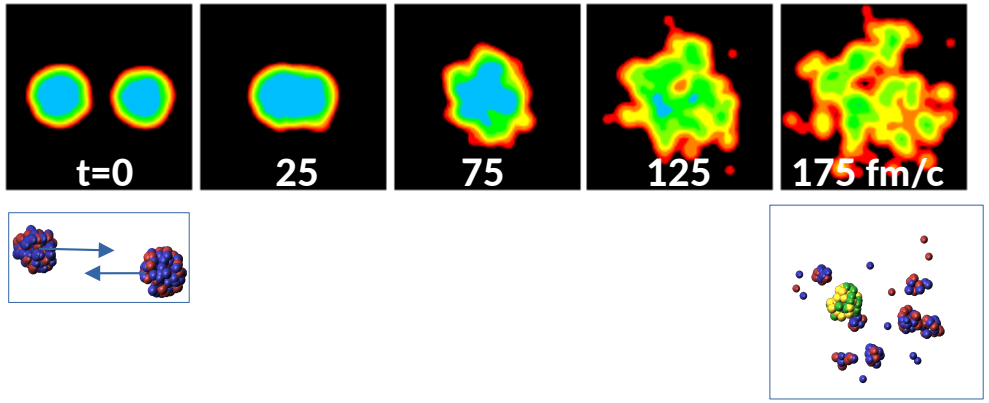

Antisymmetrized Molecular Dynamics calculation (AMD) for Xe+Sn 50 MeV/u collisions (b=0) (A. Ono et al)

HIC & statistical (even thermodynamical) approaches

Fermi energy heavy-ion collisions

Each collision is a highly dynamical, far-from-equilibrium, process leading to hugely many different final states (freeze-out)

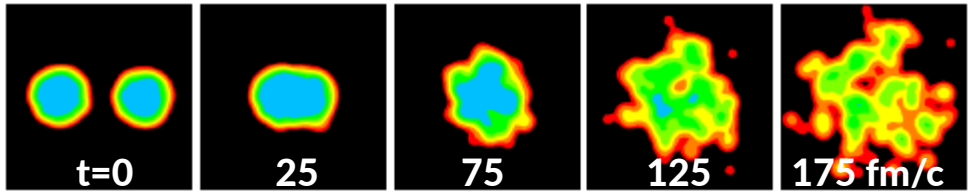

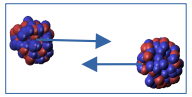

Antisymmetrized Molecular Dynamics calculation (AMD) for Xe+Sn 50 MeV/u collisions (b=0) (A. Ono et al)

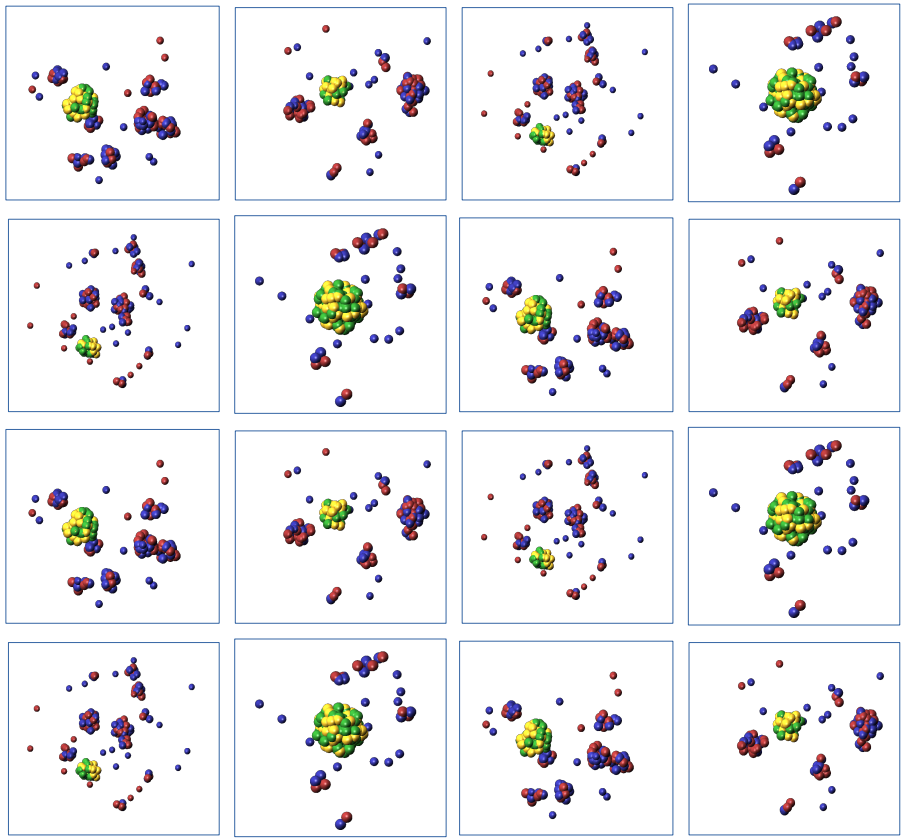

Recording the outcome of many millions of collisions leads to the measured population of all accessible final states (not a statistical ensemble *per se*)

HIC & statistical (even thermodynamical) approaches

Fermi energy heavy-ion collisions

Each collision is a highly dynamical, far-from-equilibrium, process leading to hugely many different final states (freeze-out)

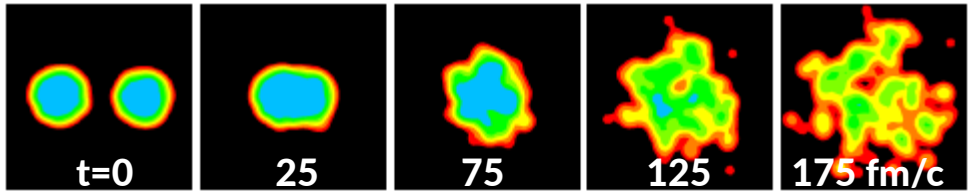

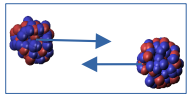

Antisymmetrized Molecular Dynamics calculation (AMD) for Xe+Sn 50 MeV/u collisions (b=0) (A. Ono et al)

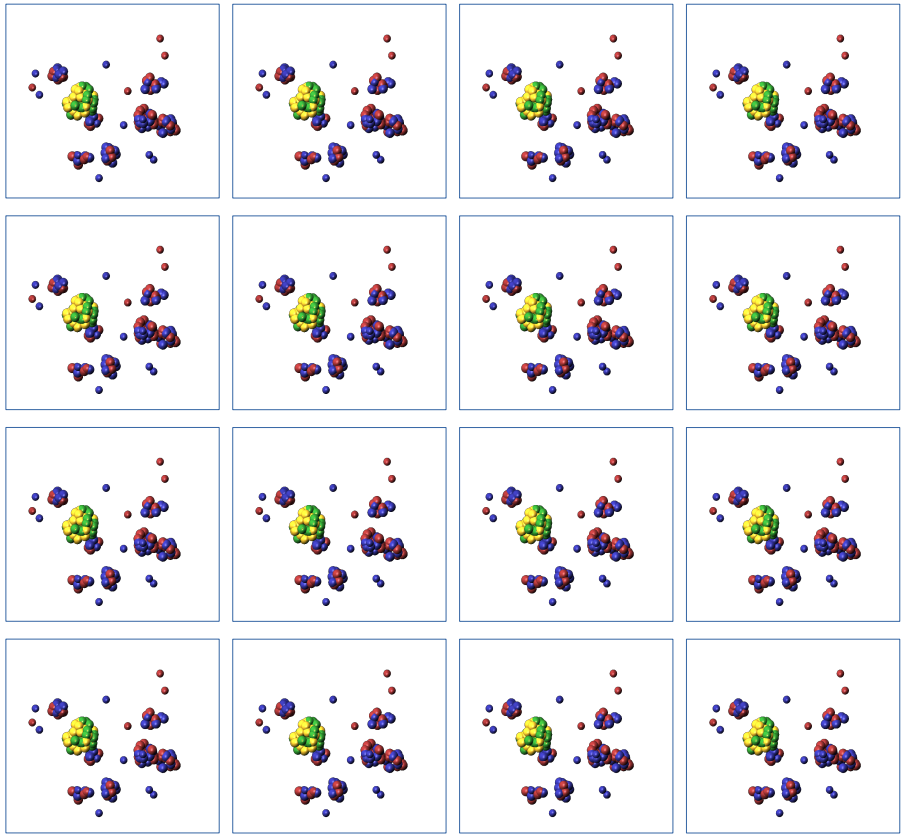

Recording the outcome of many millions of collisions leads to the measured population of all accessible final states (not a statistical ensemble *per se*)

The outcomes of carefully-selected similar collisions reweighted according to the observable constraints *may* populate a statistical ensemble according to equilibrium statistical mechanics

$$S = -\sum_i p_i \log p_i + \sum_X \lambda_X \langle X \rangle$$



HIC & statistical (even thermodynamical) approaches

Fermi energy heavy-ion collisions

Each collision is a highly dynamical, far-from-equilibrium, process leading to hugely many different final states (freeze-out)

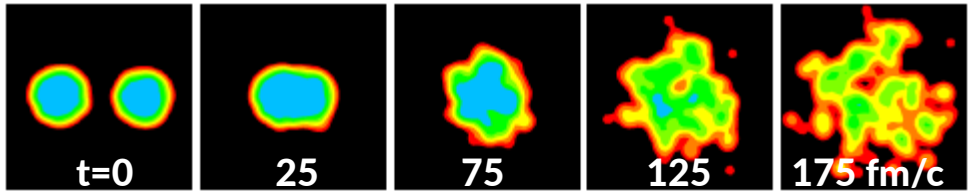

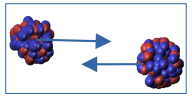

Antisymmetrized Molecular Dynamics calculation (AMD) for Xe+Sn 50 MeV/u collisions (b=0) (A. Ono et al)

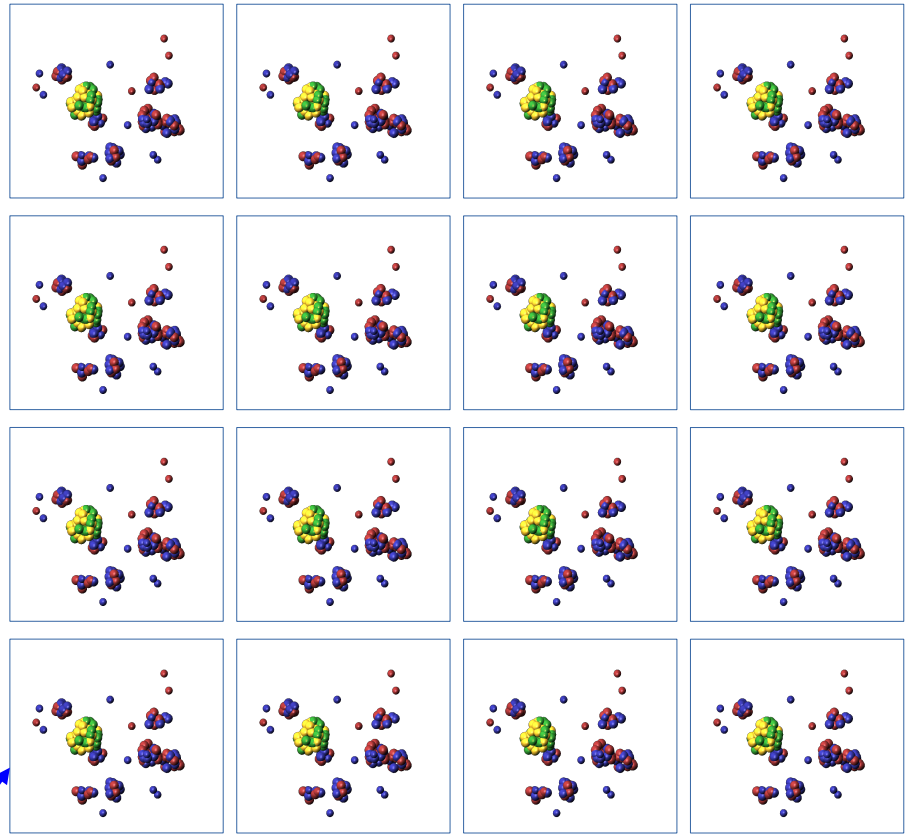

Recording the outcome of many millions of collisions leads to the measured population of all accessible final states (not a statistical ensemble *per se*)

The outcomes of carefully-selected similar collisions reweighted according to the observable constraints *may* populate a statistical ensemble according to equilibrium statistical mechanics

➡ **Only meaningful definition of equilibrium in this context**

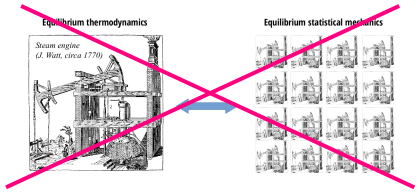

WARNING: no equivalent "system" evolving in time (non-ergodic)

Statistical models of multifragmentation etc. describe this ensemble not a hypothetic equilibrated system

$$S = -\sum_i p_i \log p_i + \sum_X \lambda_X \langle X \rangle$$

LIQUID-GAS PHASE TRANSITIONS IN NUCLEAR MATTER

A (hopefully) pedagogical introduction and overview of experimental achievements in the field

John FRANKLAND

GANIL

cnrs NUCLÉAIRE & PARTICULES

cea

1. INTRODUCTION

- a few “reminders” on equations of state & LGPT in classical systems, associated critical phenomena, realistic nuclear matter EoS & link to multifragmentation, and statistical models in HIC

2. SOME EXPERIMENTAL OBSERVATIONS

- a historical tour from the earliest experiments suggesting strong links between multifragmentation and a liquid-gas phase transition of nuclear matter

3. INDRA RESULTS

- characterizing the gas phase, now including in-medium effects & link to QCD phase diagram
- characterizing the phase transition: convex entropy intruder & all that entails

A historic experiment: Purdue/Fermilab 1981

Nuclear Fragment Mass Yields from High-Energy Proton-Nucleus Interactions

J. E. Finn, S. Agarwal, A. Bujak, J. Chuang,[a] L. J. Gutay, A. S. Hirsch, R. W. Minich,[b] N. T. Porile, R. P. Scharenberg, and B. C. Stringfellow
Departments of Physics and Chemistry, Purdue University, West Lafayette, Indiana 47907

and

F. Turkot
Fermi National Accelerator Laboratory, Batavia, Illinois 60510

(Received 11 January 1982)

Isotopically resolved nuclear fragments (A_f, Z_f), $3 \leq Z_f \leq 14$, produced by protons in the energy range $80 \leq E_{inc} \leq 350$ GeV incident on krypton and xenon targets have been studied at the Internal Target Laboratory of the Fermi National Accelerator. A power-law dependence, isobaric yield $\propto A_f^{-\tau}$, was found to describe the data over a broad range of yields. The particular value of τ is a signature for the fragment formation mechanism.

J.E. Finn et al., Phys. Rev. Lett. 49(1982)1321

A historic experiment: Purdue/Fermilab 1981

Nuclear Fragment Mass Yields from High-Energy Proton-Nucleus Interactions

J. E. Finn, S. Agarwal, A. Bujak, J. Chuang,[a] L. J. Gutay, A. S. Hirsch, R. W. Minich,[b] N. T. Porile, R. P. Scharenberg, and B. C. Stringfellow
Departments of Physics and Chemistry, Purdue University, West Lafayette, Indiana 47907

and

F. Turkot
Fermi National Accelerator Laboratory, Batavia, Illinois 60510

(Received 11 January 1982)

Isotopically resolved nuclear fragments (A_f, Z_f), $3 \leq Z_f \leq 14$, produced by protons in the energy range $80 \leq E_{inc} \leq 350$ GeV incident on krypton and xenon targets have been studied at the Internal Target Laboratory of the Fermi National Accelerator. A power-law dependence, isobaric yield $\propto A_f^{-\tau}$, was found to describe the data over a broad range of yields. The particular value of τ is a signature for the fragment formation mechanism.

proton beam 80-350 GeV

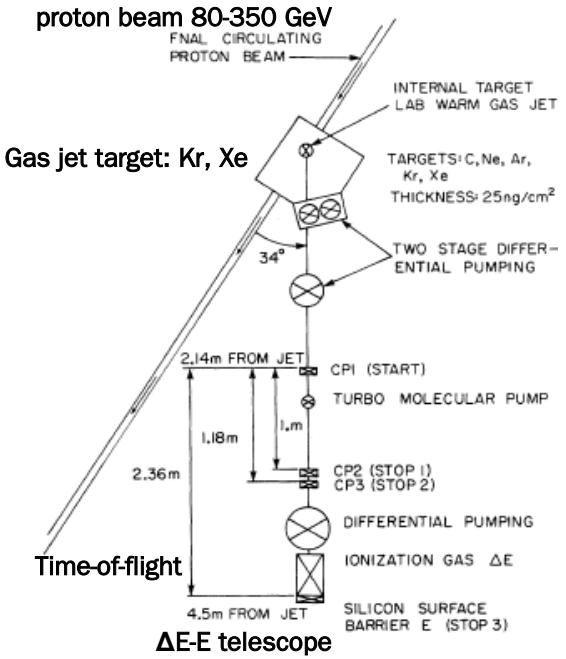

Gas jet target: Kr, Xe

Time-of-flight

ΔE-E telescope

J.E. Finn et al., Phys. Rev. Lett. 49(1982)1321

A historic experiment: Purdue/Fermilab 1981

Nuclear Fragment Mass Yields from High-Energy Proton-Nucleus Interactions

J. E. Finn, S. Agarwal, A. Bujak, J. Chuang,[a] L. J. Gutay, A. S. Hirsch, R. W. Minich,[b] N. T. Porile, R. P. Scharenberg, and B. C. Stringfellow
Departments of Physics and Chemistry, Purdue University, West Lafayette, Indiana 47907

and

F. Turkot
Fermi National Accelerator Laboratory, Batavia, Illinois 60510

(Received 11 January 1982)

Isotopically resolved nuclear fragments (A_f, Z_f), $3 \leq Z_f \leq 14$, produced by protons in the energy range $80 \leq E_{inc} \leq 350$ GeV incident on krypton and xenon targets have been studied at the Internal Target Laboratory of the Fermi National Accelerator. A power-law dependence, isobaric yield $\propto A_f^{-\tau}$, was found to describe the data over a broad range of yields. The particular value of τ is a signature for the fragment formation mechanism.

proton beam 80-350 GeV

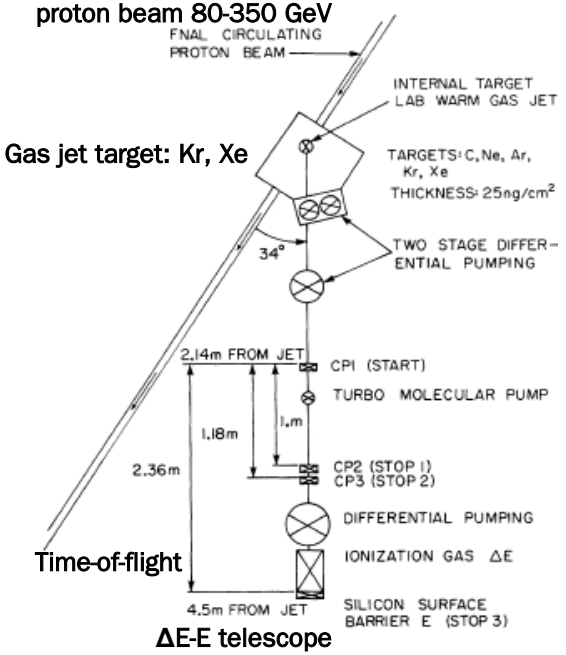

Gas jet target: Kr, Xe

Time-of-flight

ΔE-E telescope

Low-threshold inclusive Z, A, E measurements at 34° & 76°

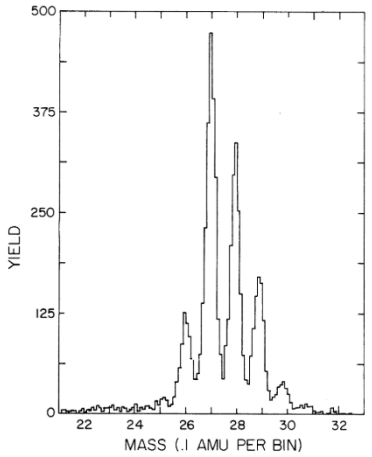

FIG. 2. Aluminum mass spectrum from krypton.

J.E. Finn et al., Phys. Rev. Lett. 49(1982)1321

LGPT & HIC: Experimental observations

A historic experiment: Purdue/Fermilab 1981

Nuclear Fragment Mass Yields from High-Energy Proton-Nucleus Interactions

J. E. Finn, S. Agarwal, A. Bujak, J. Chuang,[a] L. J. Gutay, A. S. Hirsch, R. W. Minich,[b] N. T. Porile, R. P. Scharenberg, and B. C. Stringfellow
Departments of Physics and Chemistry, Purdue University, West Lafayette, Indiana 47907

and

F. Turkot
Fermi National Accelerator Laboratory, Batavia, Illinois 60510

(Received 11 January 1982)

Isotopically resolved nuclear fragments (A_f, Z_f), $3 \leq Z_f \leq 14$, produced by protons in the energy range $80 \leq E_{inc} \leq 350$ GeV incident on krypton and xenon targets have been studied at the Internal Target Laboratory of the Fermi National Accelerator. A power-law dependence, isobaric yield $\propto A_f^{-\tau}$, was found to describe the data over a broad range of yields. The particular value of τ is a signature for the fragment formation mechanism.

proton beam 80-350 GeV

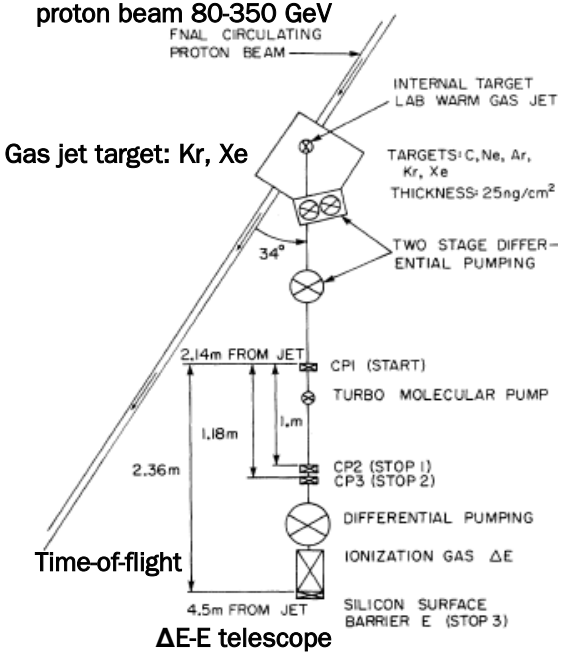

Gas jet target: Kr, Xe

Time-of-flight

ΔE-E telescope

Low-threshold inclusive Z, A, E measurements at 34° & 76°

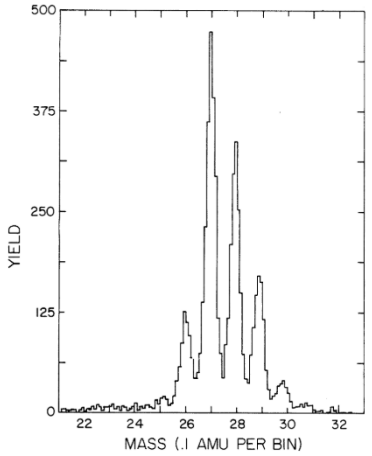

FIG. 2. Aluminum mass spectrum from krypton.

J.E. Finn et al., Phys. Rev. Lett. 49(1982)1321

- Power law mass distribution for fragments!
- Just like Fisher droplet model at $T=T_c$!

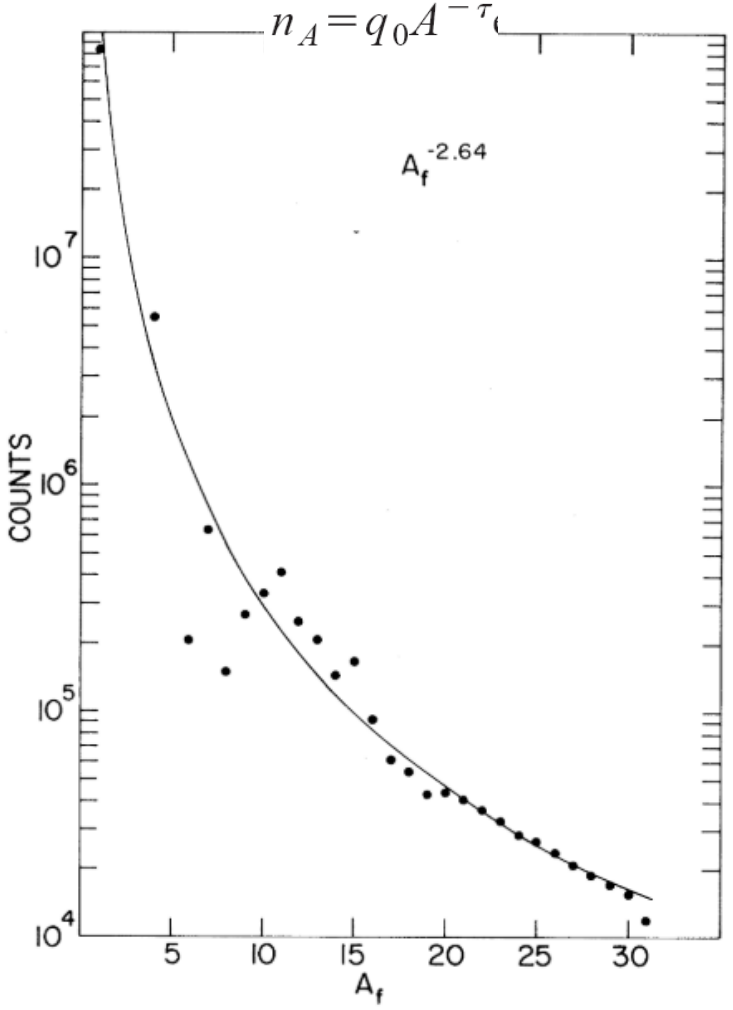

LGPT & HIC: Experimental observations

Multifragmentation in spectator decay @ E/A > 100 MeV

Exclusive
(event-by-event) measurements

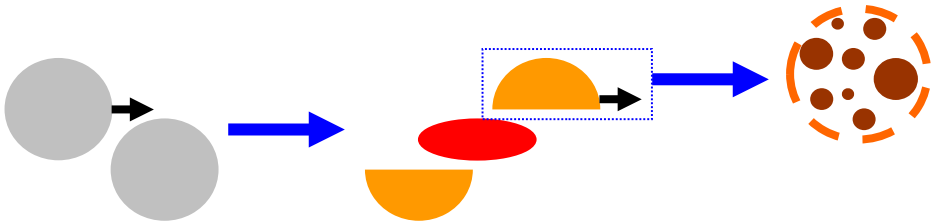

EOS@BEVALAC

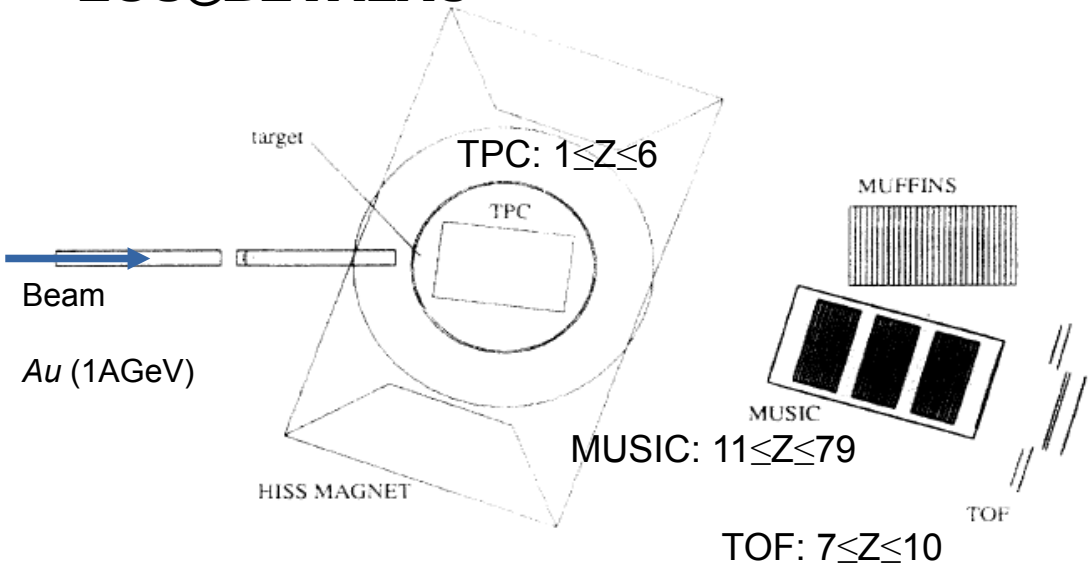

TPC: 1≤Z≤6

MUSIC: 11≤Z≤79

TOF: 7≤Z≤10

VOLUME 73, NUMBER 12 PHYSICAL REVIEW LETTERS 19 SEPTEMBER 1994

Determination of Critical Exponents from the Multifragmentation of Gold Nuclei

M. L. Gilkes,[1] S. Albergo,[2] F. Bieser,[6] F. P. Brady,[3] Z. Caccia,[2] D. A. Cebra,[3] A. D. Chacon,[7] J. L. Chance,[3] Y. Choi,[1,*] S. Costa,[2] J. B. Elliott,[1] J. A. Hauger,[1] A. S. Hirsch,[1] E. L. Hjort,[1] A. Insolia,[2] M. Justice,[5] D. Keane,[5] J. C. Kintner,[3] V. Lindenstruth,[4] M. A. Lisa,[6] U. Lynen,[4] H. S. Matis,[6] M. McMahan,[6] C. McParland,[6] W. F. J. Müller,[4] D. L. Olson,[6]

LGPT & HIC: Experimental observations

Multifragmentation in spectator decay @ E/A > 100 MeV

Exclusive
(event-by-event) measurements

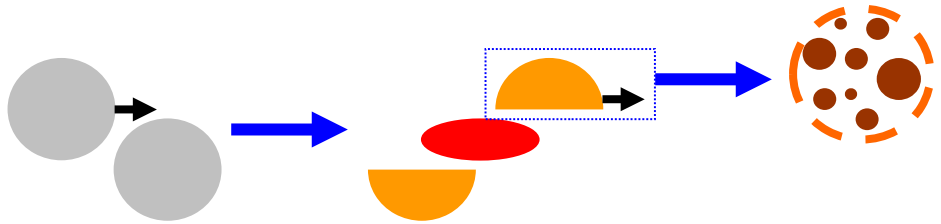

EOS@BEVALAC

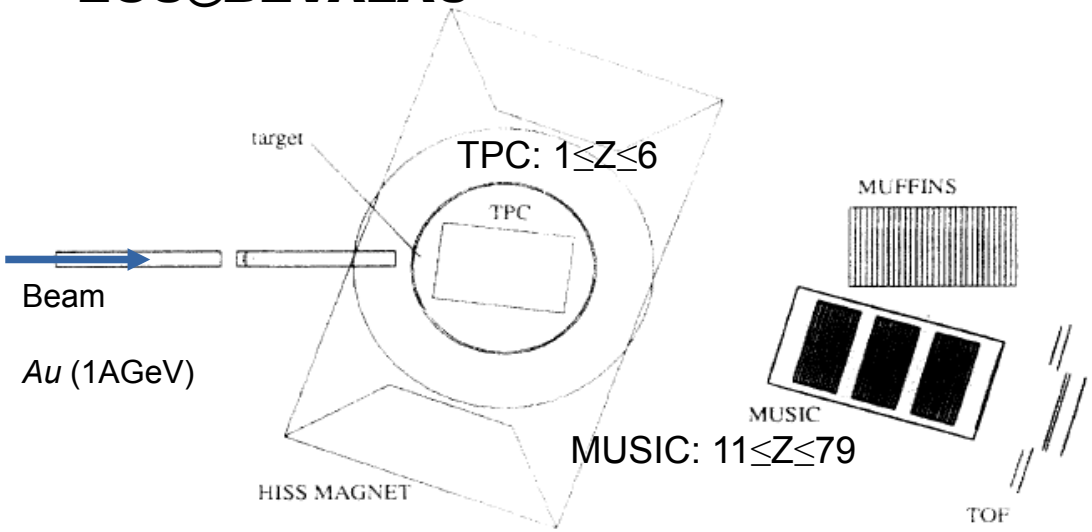

TPC: 1≤Z≤6

MUSIC: 11≤Z≤79

TOF: 7≤Z≤10

M.L. Gilkes et al.,
Phys. Rev. Lett. 73(1994)1590
J.B. Elliott et al.,
Phys. Lett. B381(1996)35

VOLUME 73, NUMBER 12 PHYSICAL REVIEW LETTERS 19 SEPTEMBER 1994

Determination of Critical Exponents from the Multifragmentation of Gold Nuclei

M. L. Gilkes,[1] S. Albergo,[2] F. Bieser,[6] F. P. Brady,[3] Z. Caccia,[2] D. A. Cebra,[3] A. D. Chacon,[7] J. L. Chance,[3] Y. Choi,[1,*] S. Costa,[2] J. B. Elliott,[1] J. A. Hauger,[1] A. S. Hirsch,[1] E. L. Hjort,[1] A. Insolia,[2] M. Justice,[5] D. Keane,[5] J. C. Kintner,[3] V. Lindenstruth,[4] M. A. Lisa,[6] U. Lynen,[4] H. S. Matis,[6] M. McMahan,[6] C. McParland,[6] W. F. J. Müller,[4] D. L. Olson,[6]

- Critical exponents extracted from fits to moments of fragment charge distributions à la percolation

$$M_k = \sum_Z n_Z(m) Z^k$$

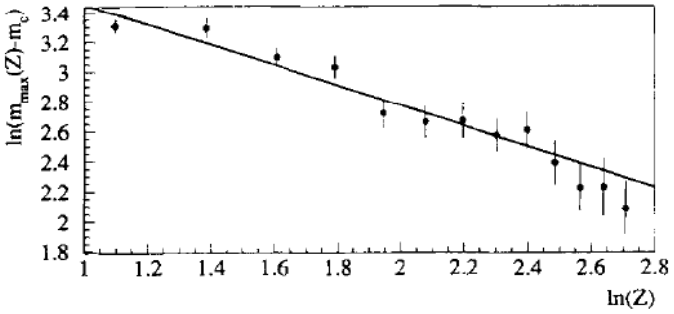

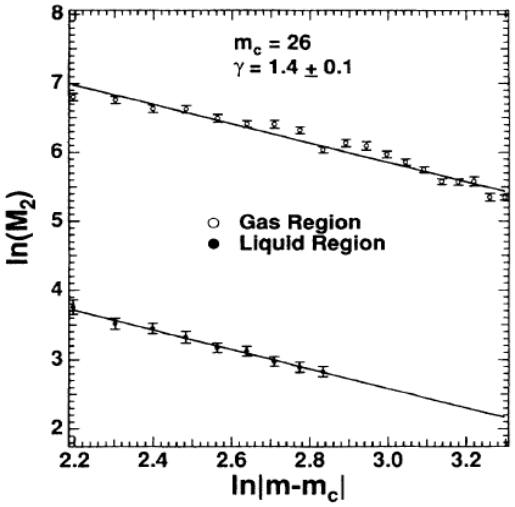

Table 1
Critical exponents for multifragmentation of gold and other three-dimensional systems.

Exponent	Experiment	Liquid-gas	Liquid-gas mean-field	Percolation
γ	1.4 ± 0.1	1.23	1	1.8
β	0.29 ± 0.02	0.33	1/2	0.41
σ	0.68 ± 0.05	0.64	2/3	0.45

- Values are close to liquid-gas...?

LGPT & HIC: Experimental observations

Multifragmentation in spectator decay @ E/A > 100 MeV

Exclusive
(event-by-event) measurements

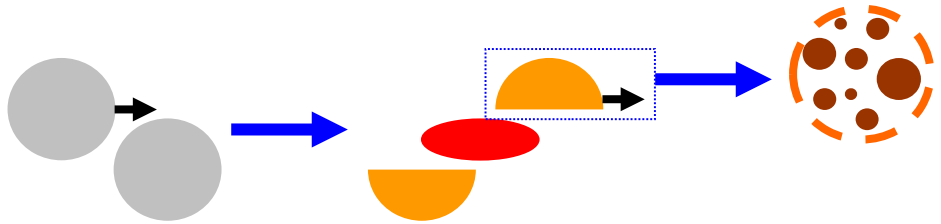

EOS@BEVALAC

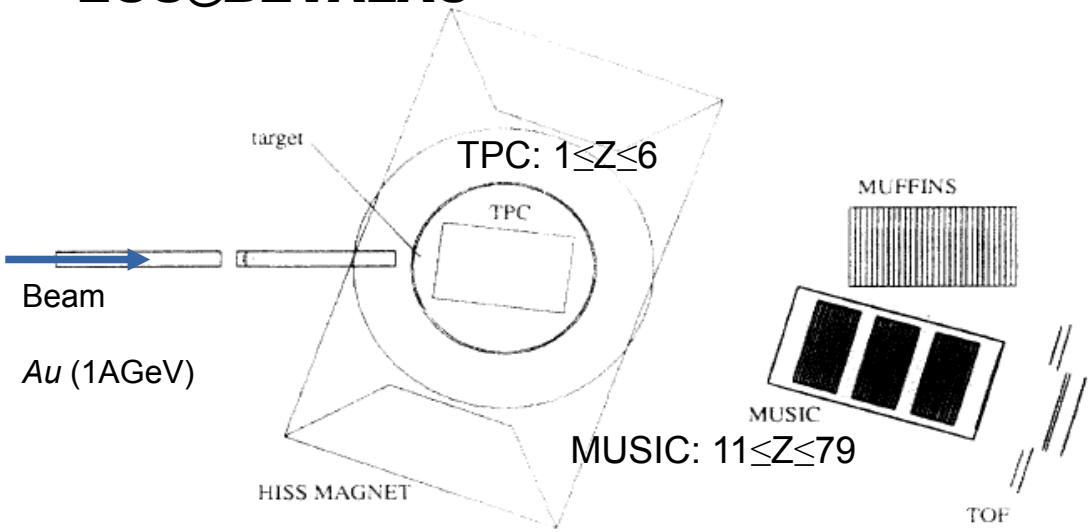

M.L. Gilkes et al.,
Phys. Rev. Lett. 73(1994)1590
J.B. Elliott et al.,
Phys. Lett. B381(1996)35

VOLUME 73, NUMBER 12 PHYSICAL REVIEW LETTERS 19 SEPTEMBER 1994

Determination of Critical Exponents from the Multifragmentation of Gold Nuclei

M. L. Gilkes,[1] S. Albergo,[2] F. Bieser,[6] F. P. Brady,[3] Z. Caccia,[2] D. A. Cebra,[3] A. D. Chacon,[7] J. L. Chance,[3] Y. Choi,[1,*] S. Costa,[2] J. B. Elliott,[1] J. A. Hauger,[1] A. S. Hirsch,[1] E. L. Hjort,[1] A. Insolia,[2] M. Justice,[5] D. Keane,[5] J. C. Kintner,[3] V. Lindenstruth,[4] M. A. Lisa,[6] U. Lynen,[4] H. S. Matis,[6] M. McMahan,[6] C. McParland,[6] W. F. J. Müller,[4] D. L. Olson,[6]

- Critical exponents extracted from fits to moments of fragment charge distributions à la percolation

$$M_k = \sum_Z n_Z(m) Z^k$$

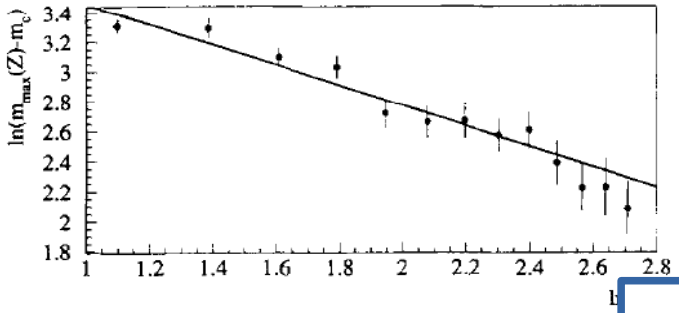

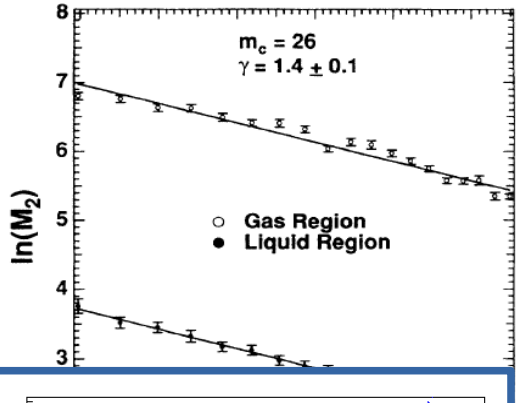

Table 1
Critical exponents for multifragmentation of gold and othe
dimensional systems.

Exponent	Experiment	Liquid-gas	Liquid-gas mean-field	Percol
γ	1.4 ± 0.1	1.23	1	1.8
β	0.29 ± 0.02	0.33	1/2	0.41
σ	0.68 ± 0.05	0.64	2/3	0.45

- Values are close to liquid-gas...?

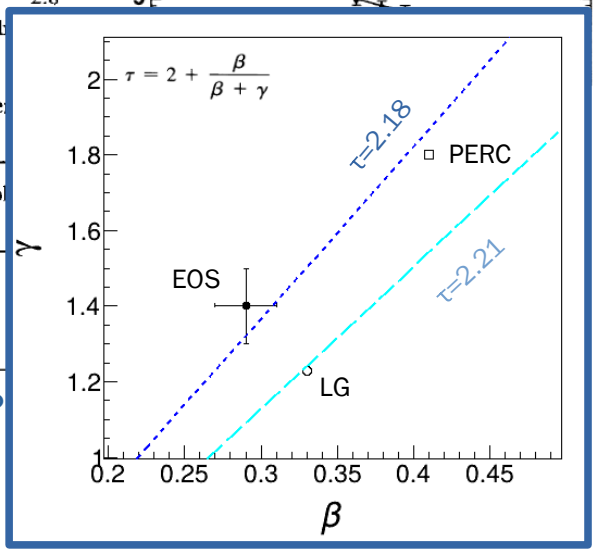

Multifragmentation in spectator decay @ E/A > 100 MeV

Exclusive
(event-by-event) measurements

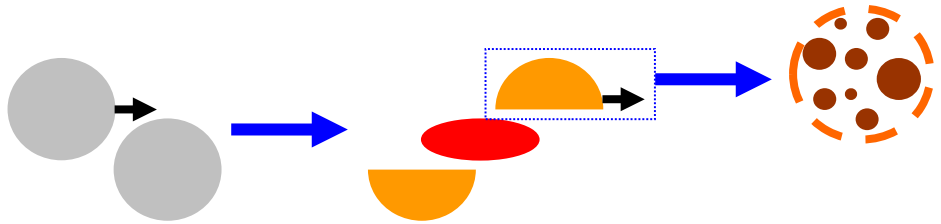

ALADIN@GSI

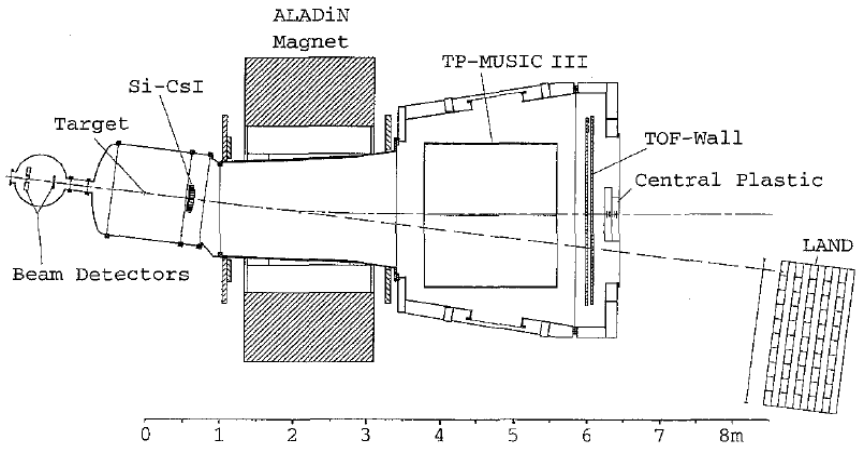

A. Schütthauf et al, Nucl. Phys. A607, 457 (1996)

LGPT & HIC: Experimental observations

Multifragmentation in spectator decay @ E/A > 100 MeV

Exclusive
(event-by-event) measurements

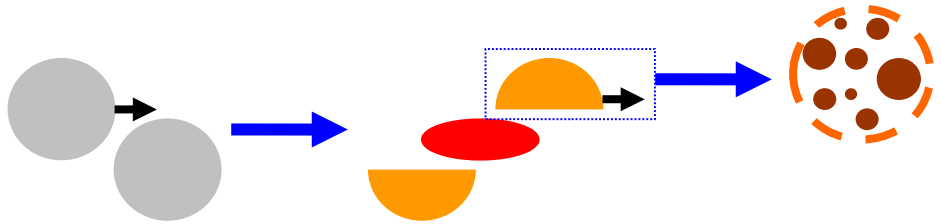

ALADIN@GSI

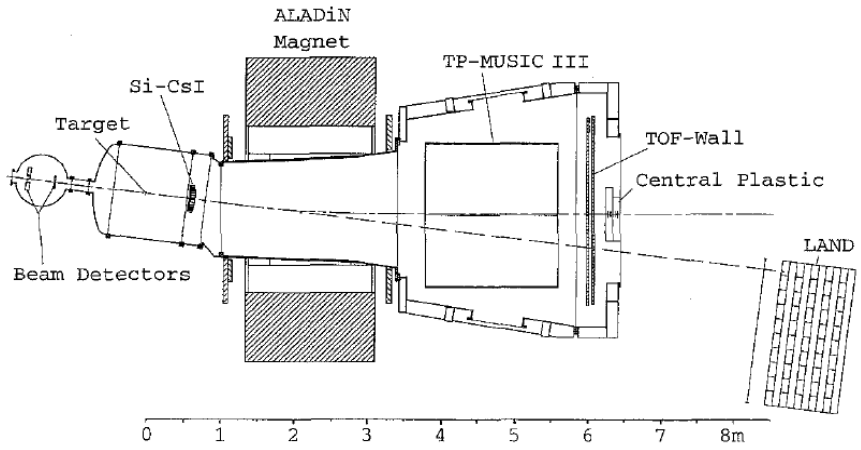

A. Schütthauf et al, Nucl. Phys. A607, 457 (1996)

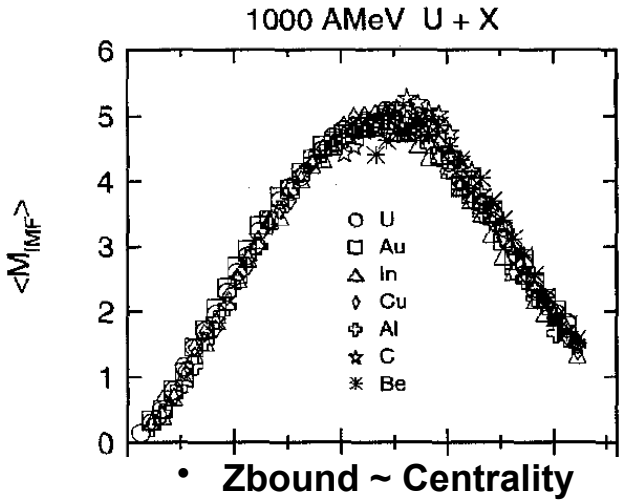

"rise and fall"
of
fragment production

Universality of spectator fragmentation

↓

statistical equilibrium

LGPT & HIC: Experimental observations

Multifragmentation in spectator decay @ E/A > 100 MeV

Exclusive
(event-by-event) measurements

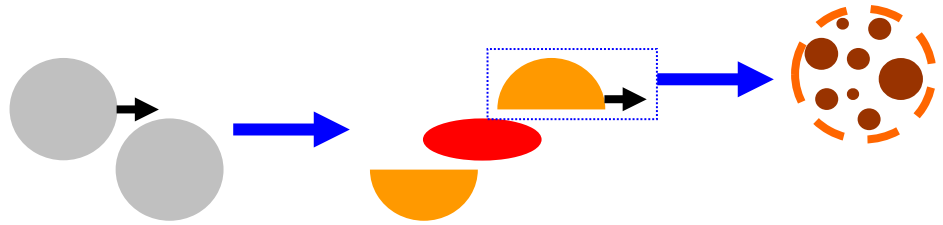

ALADIN@GSI

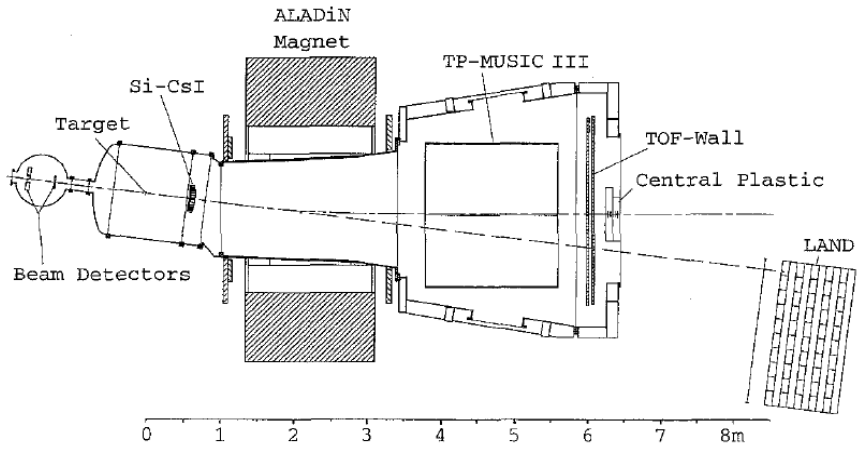

J. Pochodzalla et al., Phys. Rev. Lett. 75, 1040 (1995)

"caloric curve"

$$T_{HeLi} := 16/\ln\left(2.18 \times \frac{Y_{6Li}/Y_{7Li}}{Y_{3He}/Y_{4He}}\right)$$

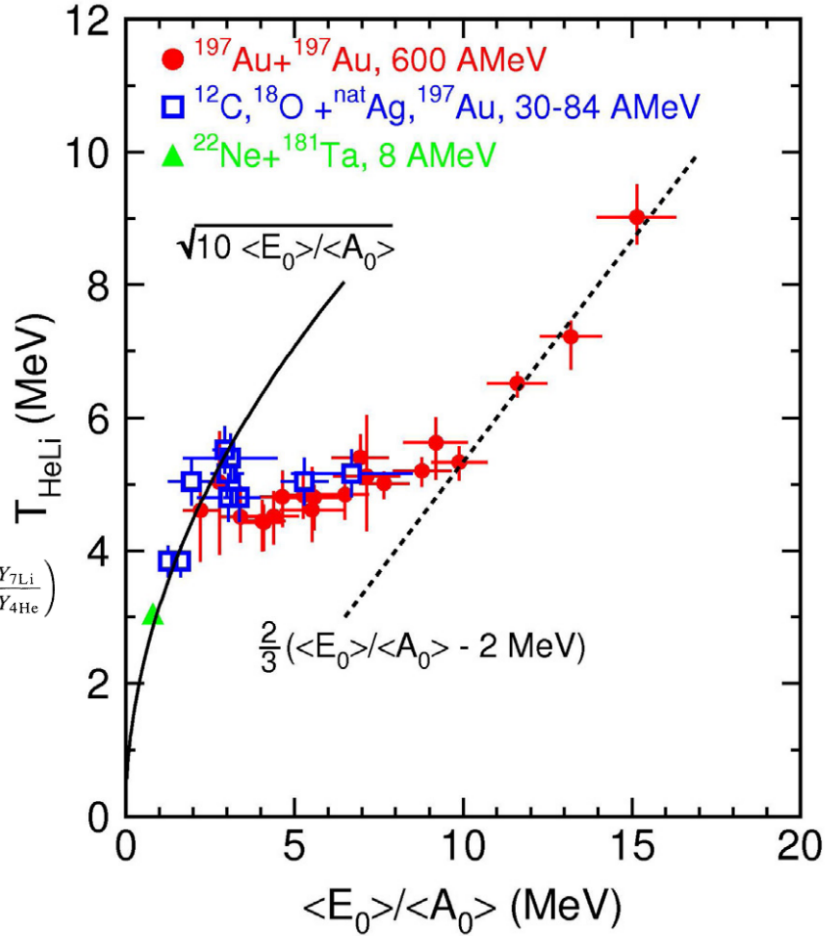

LGPT & HIC: Experimental observations

Multifragmentation in spectator decay @ E/A > 100 MeV

Exclusive
(event-by-event) measurements

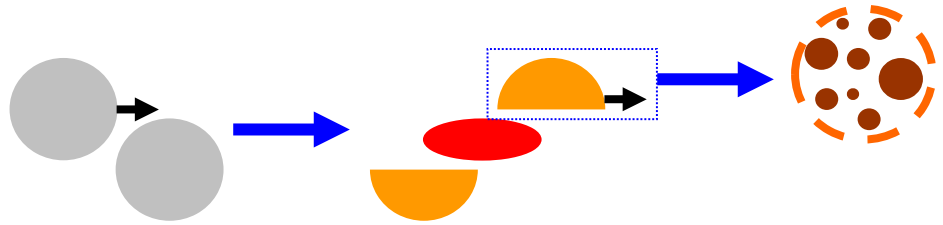

ALADIN@GSI

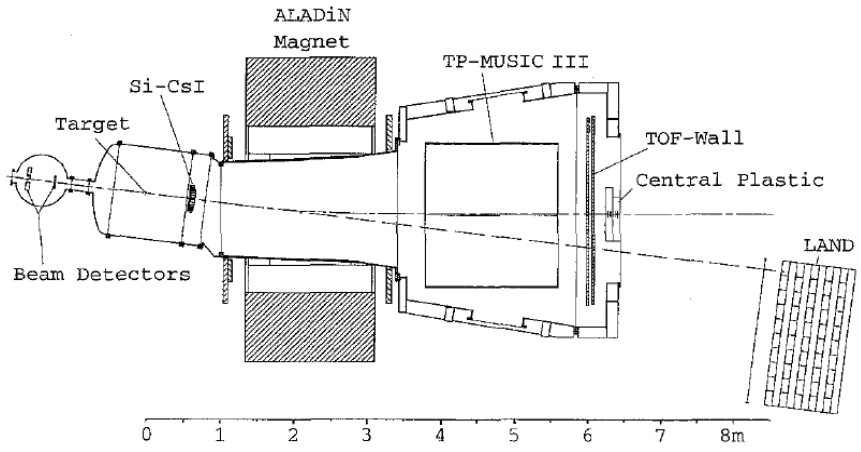

J. Pochodzalla et al., Phys. Rev. Lett. 75, 1040 (1995)

"caloric curve"

$$T_{HeLi} := 16/\ln\left(2.18 \times \frac{Y_{6Li}/Y_{7Li}}{Y_{3He}/Y_{4He}}\right)$$

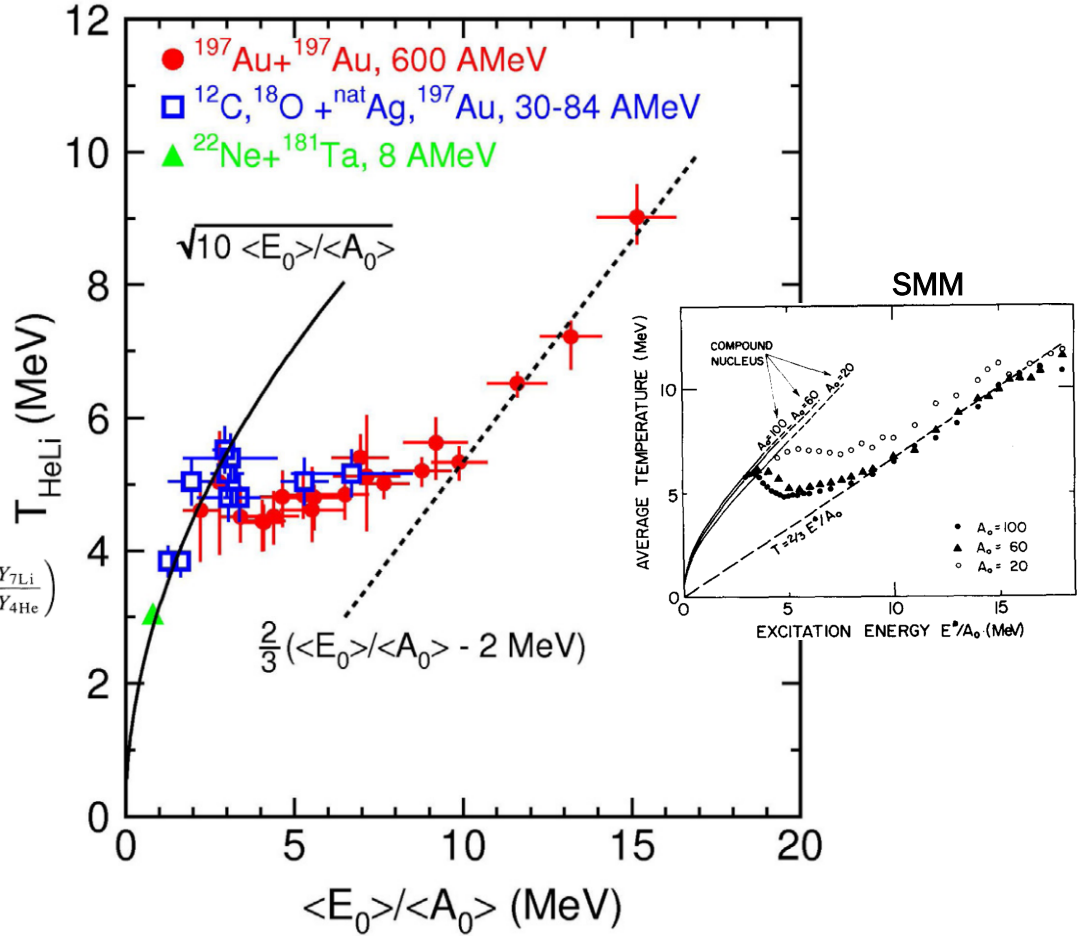

LGPT & HIC: Experimental observations

Multifragmentation in spectator decay @ E/A > 100 MeV

Exclusive
(event-by-event) measurements

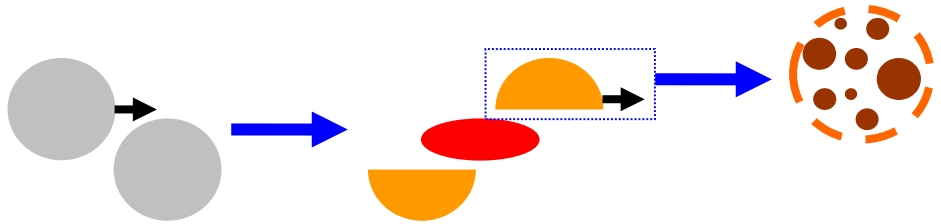

ALADIN@GSI

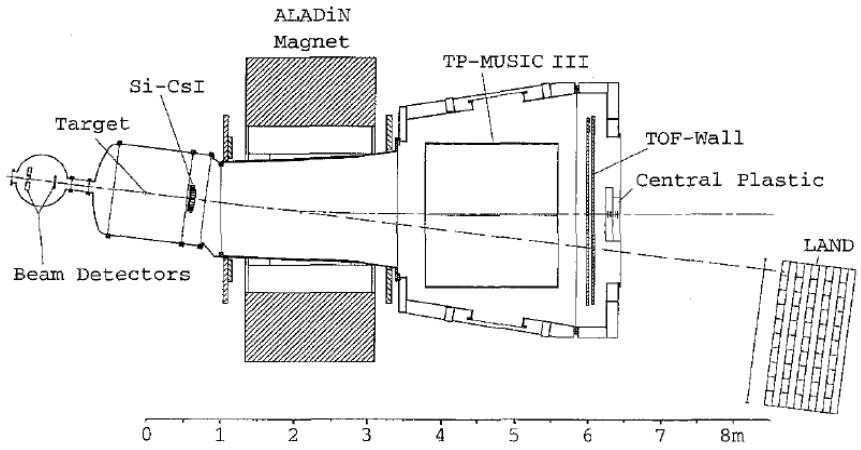

J. Pochodzalla et al., Phys. Rev. Lett. 75, 1040 (1995)

"caloric curve"

$$T_{HeLi} := 16/\ln\left(2.18 \times \frac{Y_{6Li}/Y_{7Li}}{Y_{3He}/Y_{4He}}\right)$$

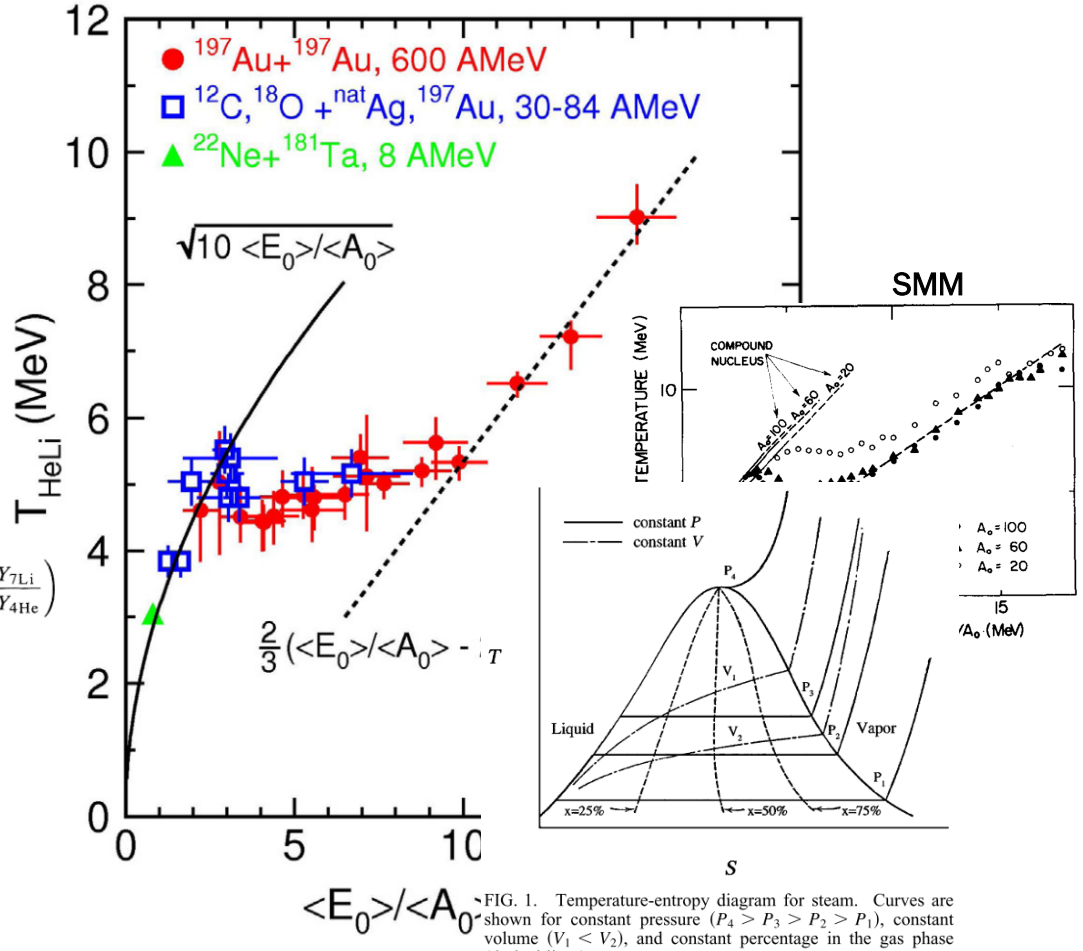

FIG. 1. Temperature-entropy diagram for steam. Curves are shown for constant pressure ($P_4 > P_3 > P_2 > P_1$), constant volume ($V_1 < V_2$), and constant percentage in the gas phase (dashed lines).

L.G. Moretto et al., Phys. Rev. Lett. 76, 2822 (1996)

(more about this later on...)

Light-hadron induced reactions: “clean” preparation of hot nuclei

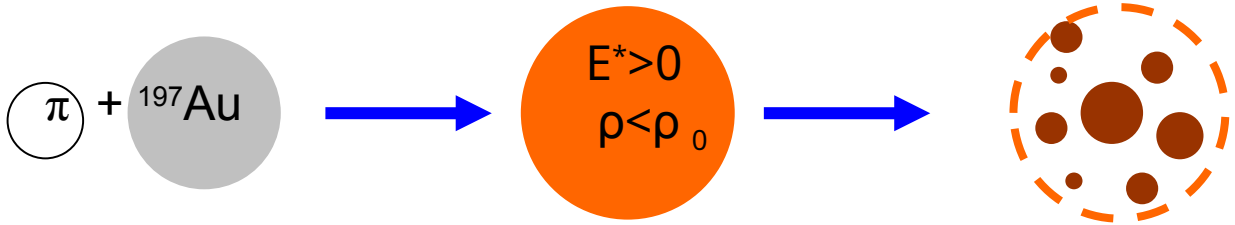

ISiS@INDIANA

(Indiana Silicon Sphere)

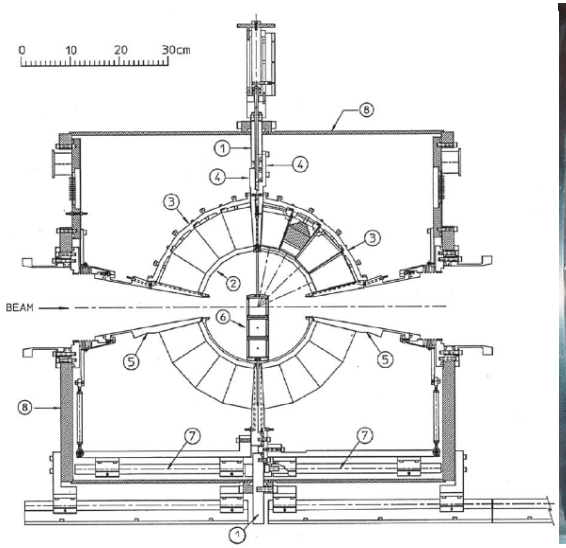

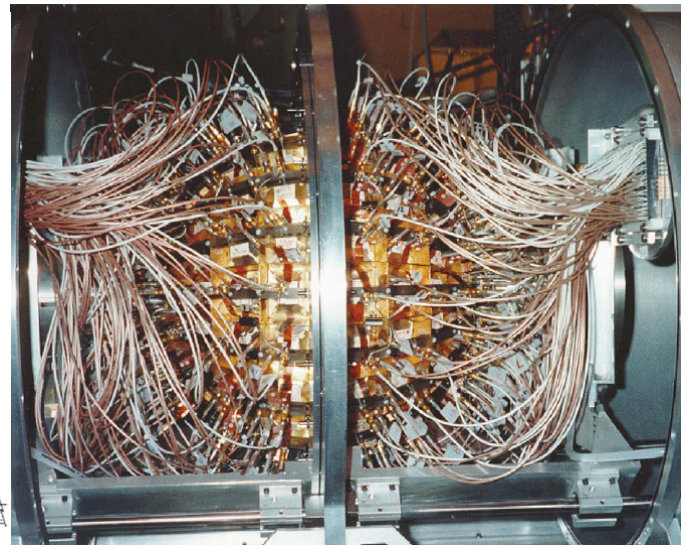

V.E. Viola et al., Phys. Rep. 434, 1 (2006)

LGPT & HIC: Experimental observations

Light-hadron induced reactions: “clean” preparation of hot nuclei

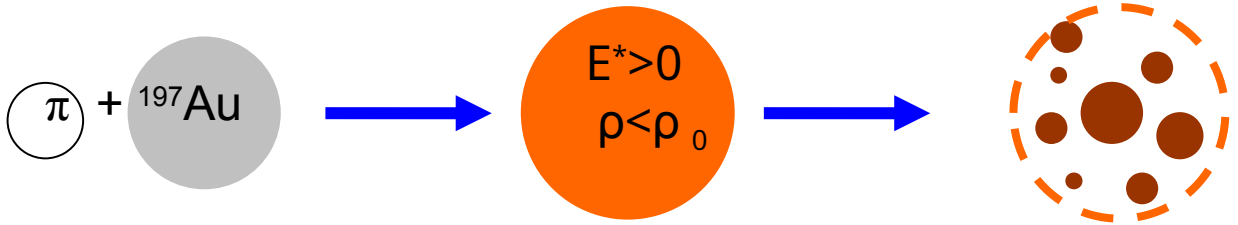

isotropic emission patterns in velocity space

ISiS@INDIANA

(Indiana Silicon Sphere)

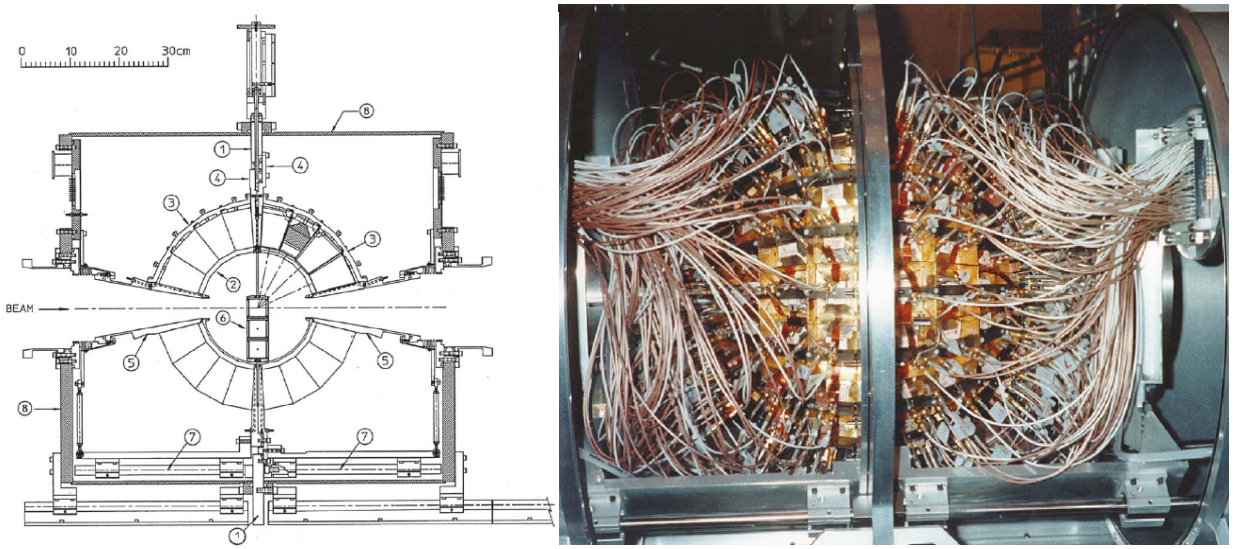

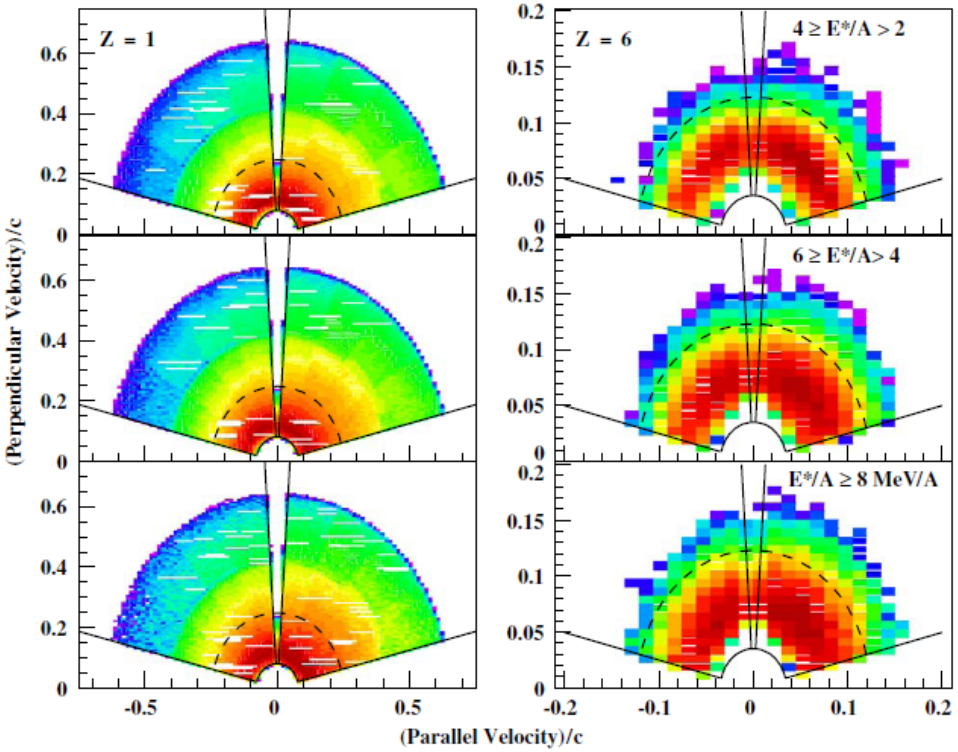

V.E. Viola et al., Phys. Rep. 434, 1 (2006)

Light-hadron induced reactions: “clean” preparation of hot nuclei

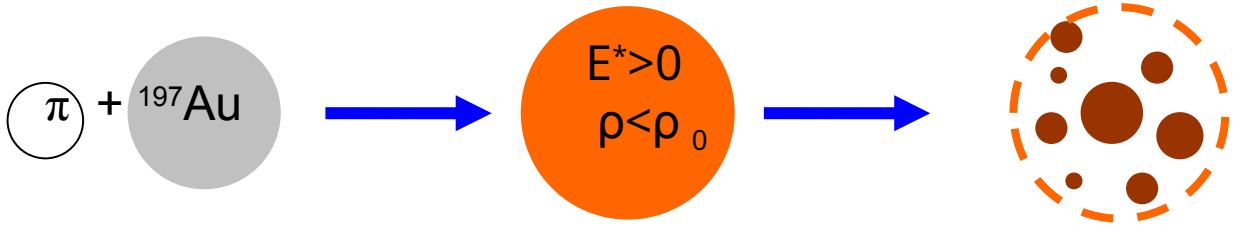

ISIS@INDIANA

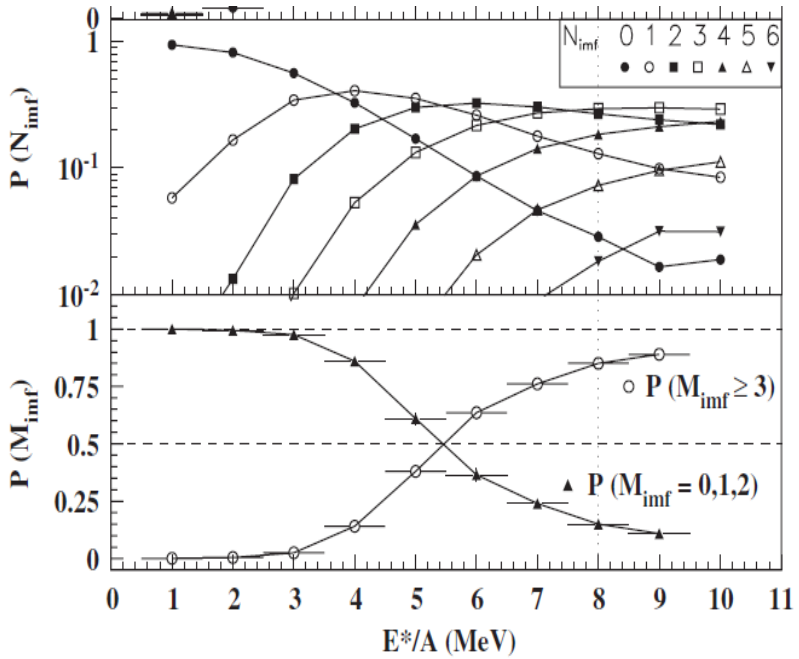

V.E. Viola et al., Phys. Rep. 434, 1 (2006)

Light-hadron induced reactions: "clean" preparation of hot nuclei

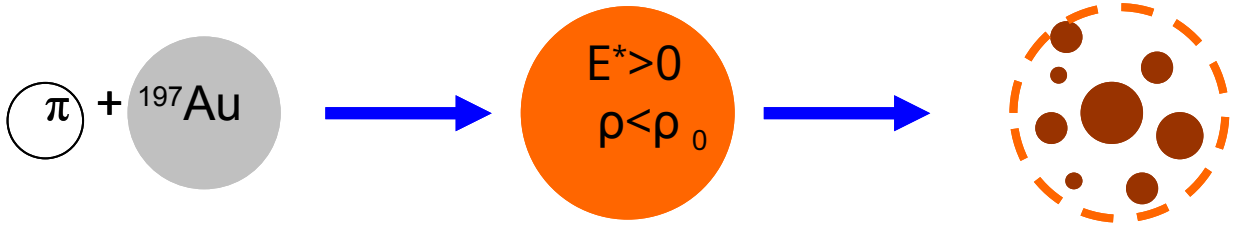

ISIS@INDIANA

E*/A ~ 3 MeV
≥3 fragment
emission onset

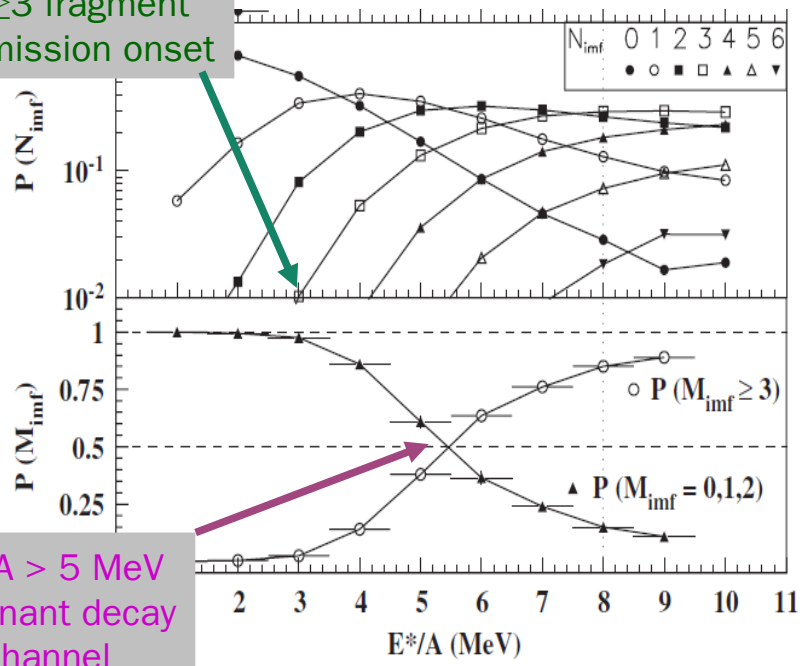

E*/A > 5 MeV
dominant decay
channel

V.E. Viola et al., Phys. Rep. 434, 1 (2006)

LGPT & HIC: Experimental observations

Light-hadron induced reactions: "clean" preparation of hot nuclei

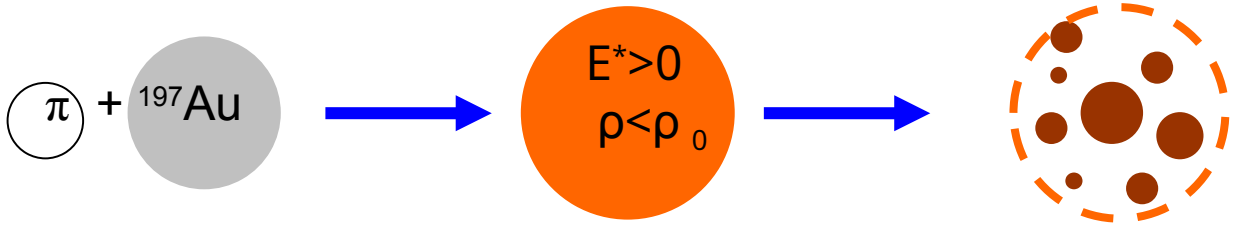

IMF velocity correlation functions → emission timescale : rapid decrease E*/A~3 MeV

ISIS@INDIANA

E*/A ~ 3 MeV
≥3 fragment
emission onset

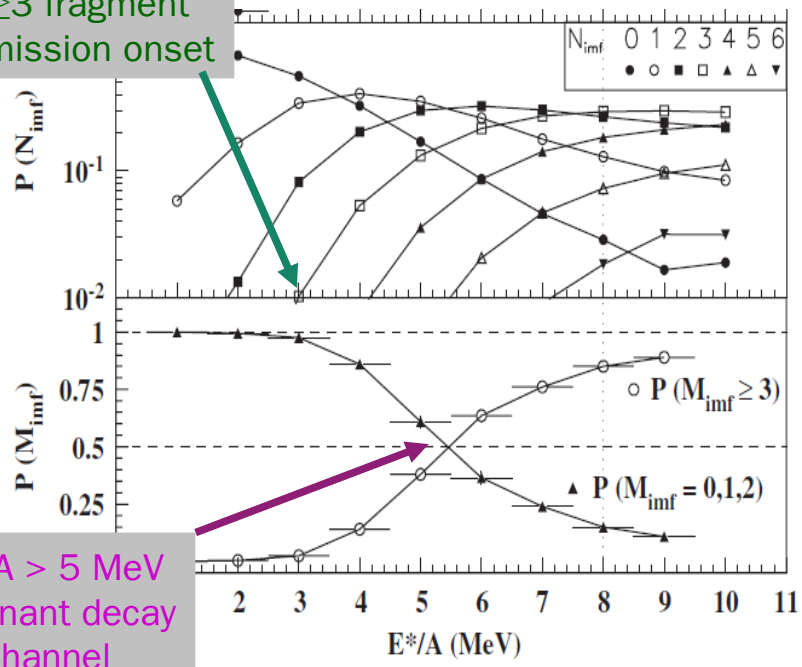

E*/A > 5 MeV
dominant decay
channel

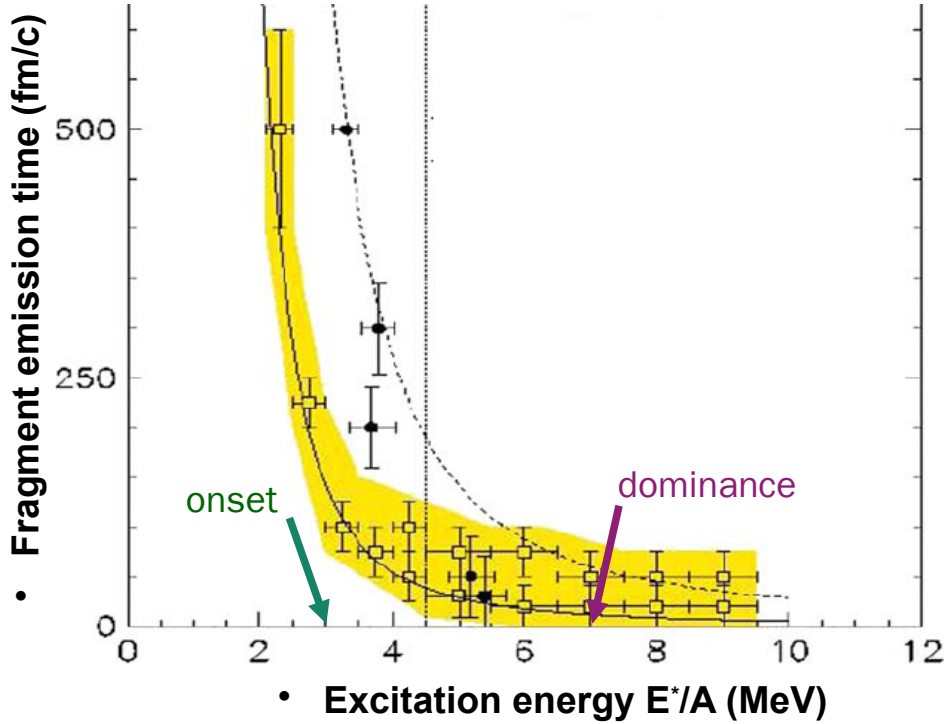

V.E. Viola et al., Phys. Rep. 434, 1 (2006)

LGPT & HIC: Experimental observations

Light-hadron induced reactions: "clean" preparation of hot nuclei

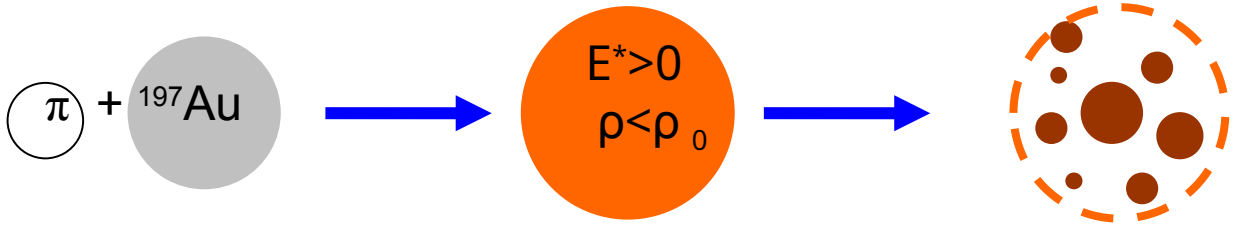

IMF velocity correlation functions → emission timescale : rapid decrease E*/A~3 MeV

Reduced fragment emission barriers → Break-up of low-density system

ISIS@INDIANA

E*/A ~ 3 MeV
≥3 fragment
emission onset

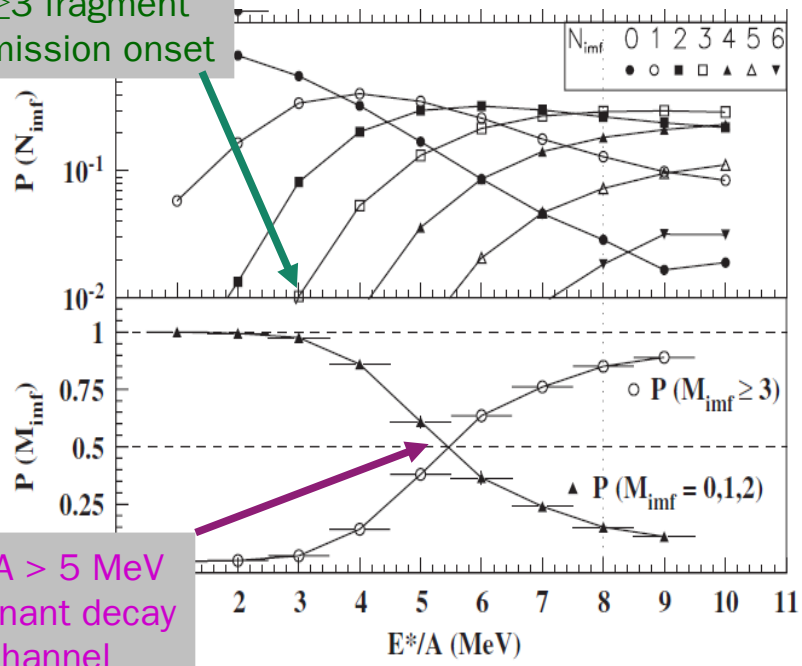

E*/A > 5 MeV
dominant decay
channel

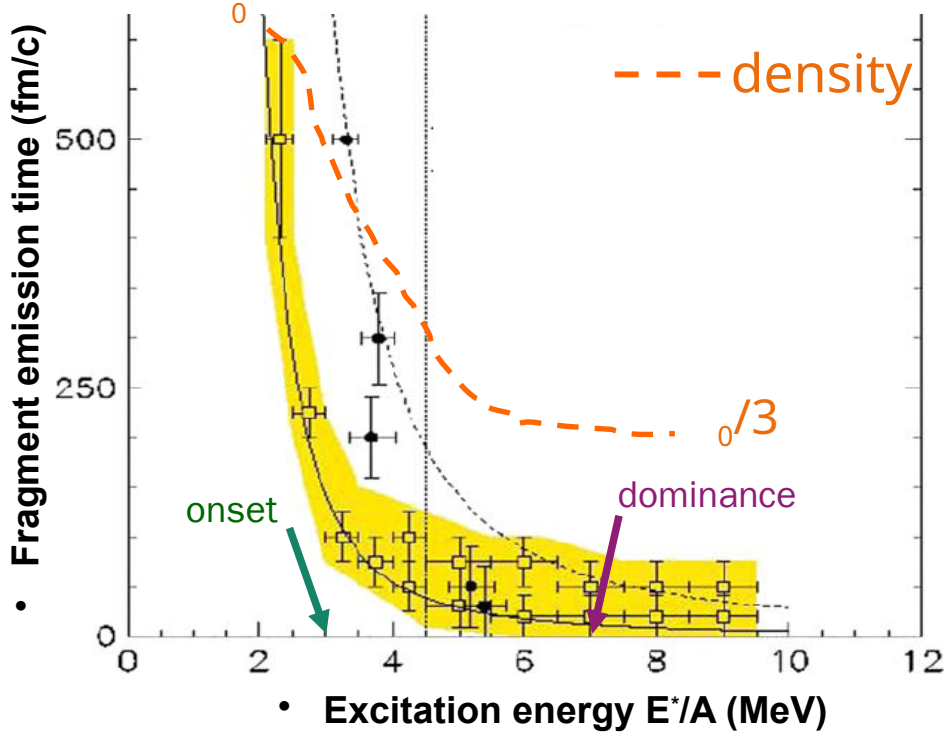

V.E. Viola et al., Phys. Rep. 434, 1 (2006)

LIQUID-GAS PHASE TRANSITIONS IN NUCLEAR MATTER

A (hopefully) pedagogical introduction and overview of experimental achievements in the field

John FRANKLAND

GANIL

cnrs NUCLÉAIRE & PARTICULES

cea

1. INTRODUCTION

- a few “reminders” on equations of state & LGPT in classical systems, associated critical phenomena, realistic nuclear matter EoS & link to multifragmentation, and statistical models in HIC

2. SOME EXPERIMENTAL OBSERVATIONS

- a historical tour from the earliest experiments suggesting strong links between multifragmentation and a liquid-gas phase transition of nuclear matter

3. INDRA RESULTS

- characterizing the gas phase, now including in-medium effects & link to QCD phase diagram
- characterizing the phase transition: convex entropy intruder & all that entails

INDRA Results: The gas phase

Vaporization

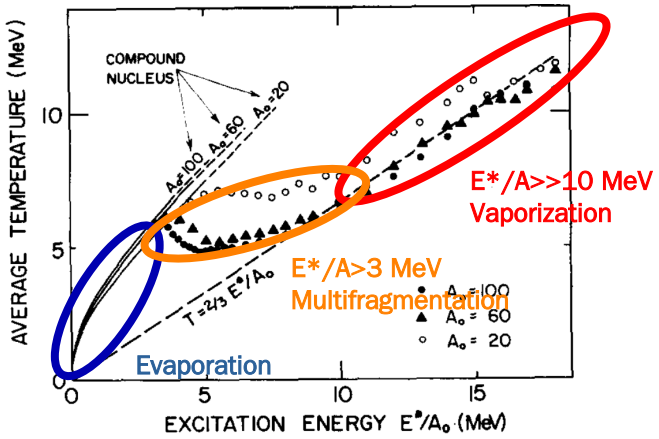

Onset of vaporization events with only Z=1,2 seen for central Ar+Ni collisions @52AMeV

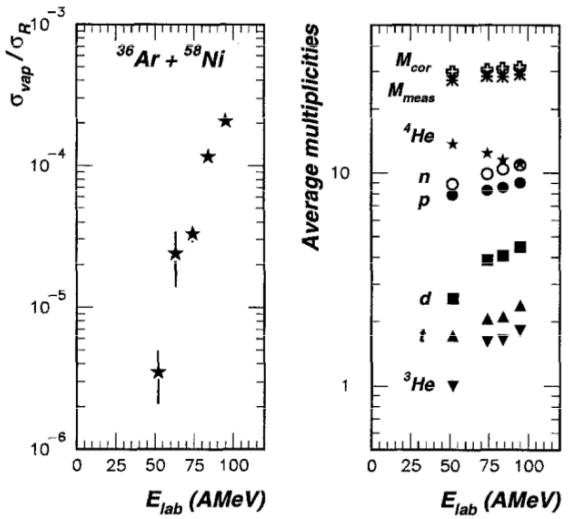

Ch.-O. Bacri & al. (INDRA), Phys. Lett. B353, 27(1995)

INDRA Results: The gas phase

Vaporization

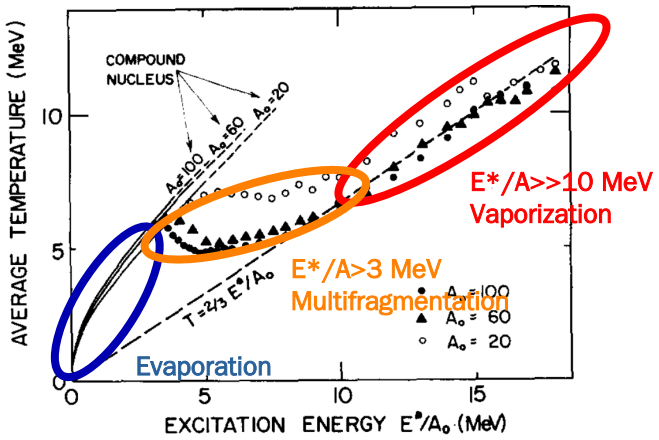

Onset of vaporization events with only Z=1,2 seen for central Ar+Ni collisions @52AMeV

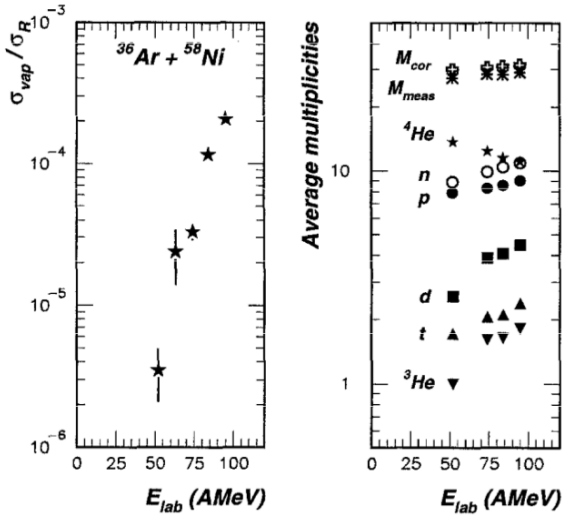

Ch.-O. Bacri & al. (INDRA), Phys. Lett. B353, 27(1995)

Further studies with vaporized Ar projectiles @95AMeV on composition & nature of gas

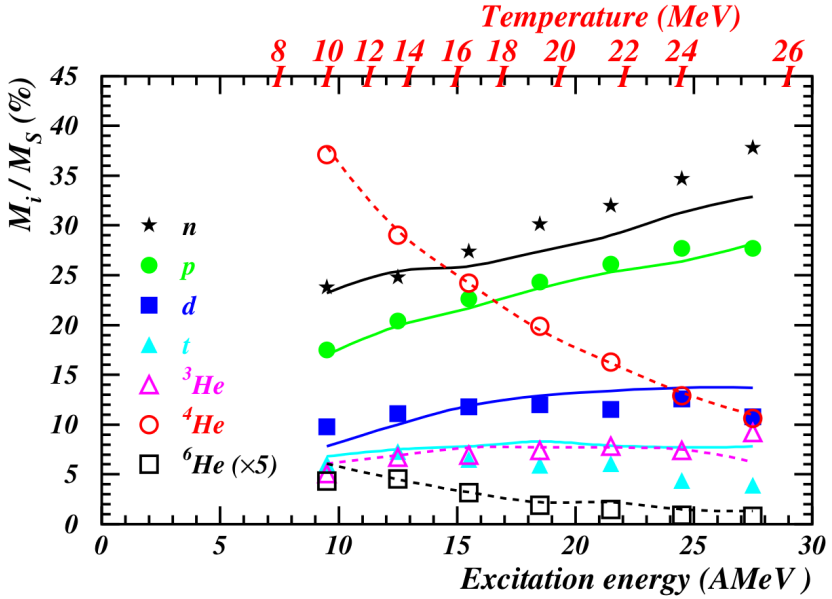

B. Borderie & al. (INDRA), Eur. Phys. J. A 6(1999)197

INDRA Results: The gas phase

Vaporization

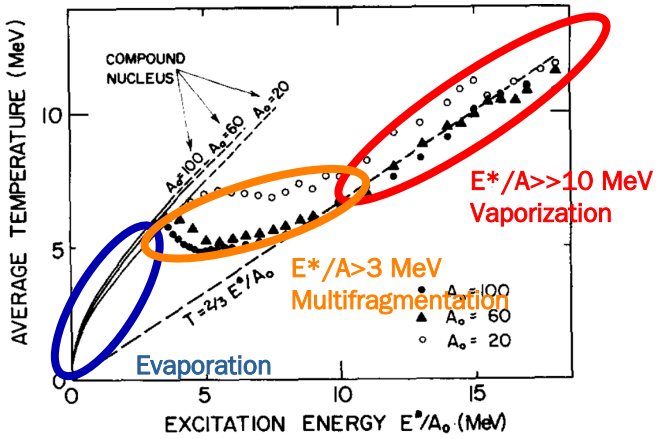

Onset of vaporization events with only Z=1,2 seen for central Ar+Ni collisions @52AMeV

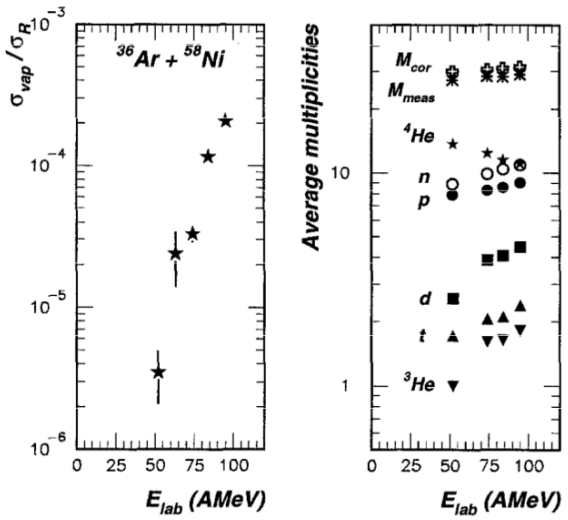

Ch.-O. Bacri & al. (INDRA), Phys. Lett. B353, 27(1995)

Further studies with vaporized Ar projectiles @95AMeV on composition & nature of gas

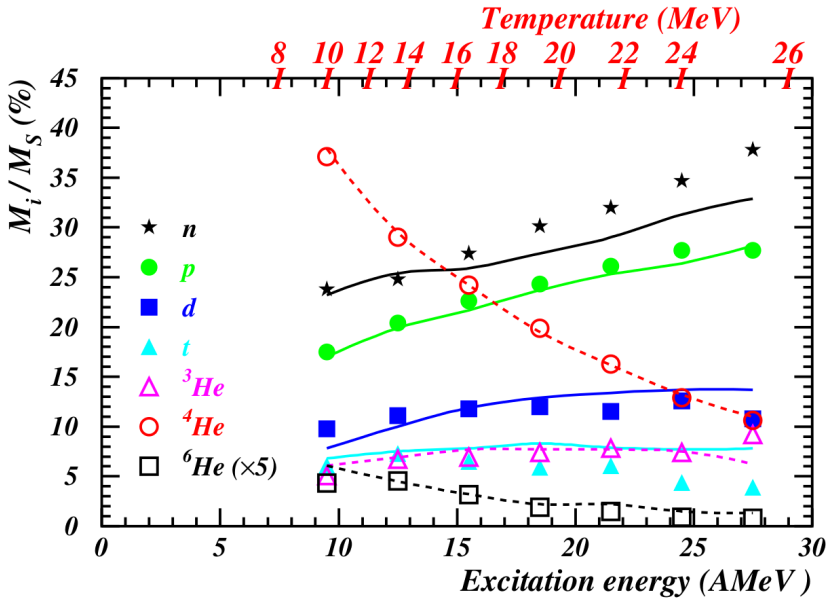

B. Borderie & al. (INDRA), Eur. Phys. J. A 6(1999)197

Quantum Statistical Model reproduces data as a weakly-interacting non-ideal gas of fermions and bosons in thermal/chemical equilibrium, taking into account excitation of particle-unstable levels, side-feeding from resonance decays, and a species-dependent excluded volume

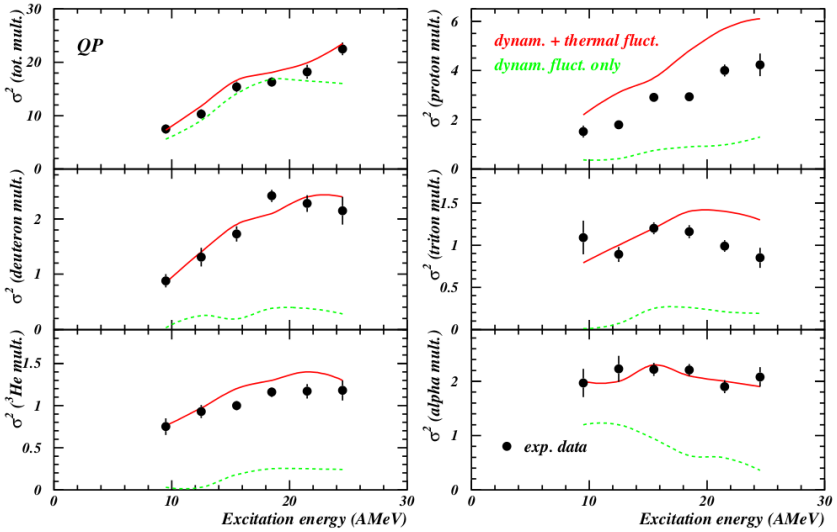

F. Gulminelli, D. Durand, Nucl. Phys. A615(1997)117

Chemical constants and in-medium effects

- Astrophysical importance of low-density nuclear matter
  - Neutron star crusts (cold)
  - Core-collapse supernova (warm)
- Clusters in low-density nuclear matter
  - CCSN dynamics ([anti]neutrino opacity)
  - Cooling of protoneutron stars
  - Symmetry energy density-dependence
- Determine cluster contributions to EoS (wide range density & temperature) ?

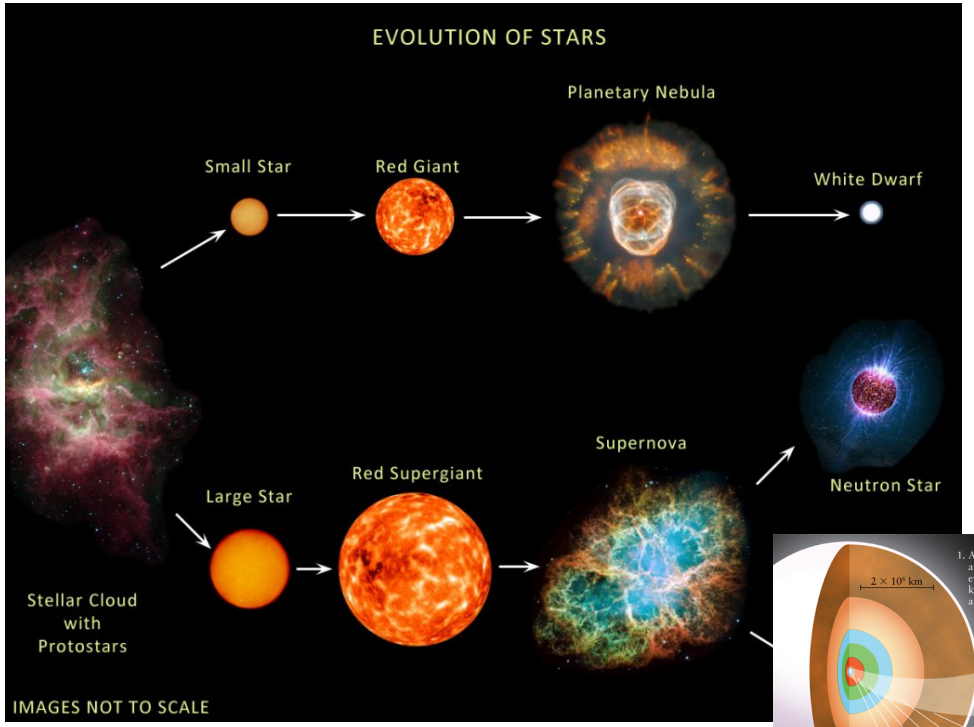

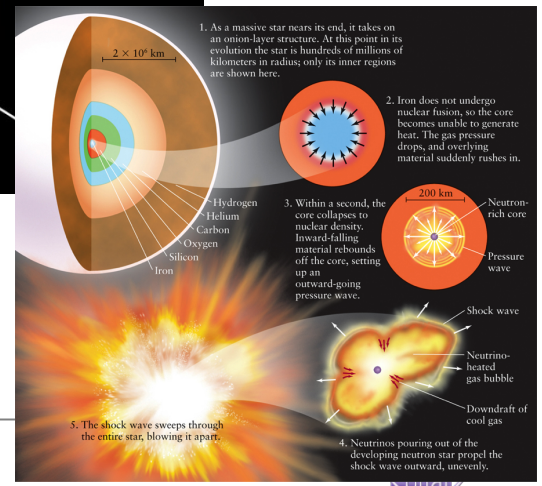

INDRA Results: The gas phase

Chemical constants and in-medium effects

Equilibrium constants for different (A,Z):
- *depend only on (ρ,T)*

$$K_c(A,Z) = \frac{\rho(A,Z)}{\rho_p^Z \rho_n^{(A-Z)}}$$

Analysis method: NIMROD/Texas, Qin et al. PRL(2012)

IOP Publishing Journal of Physics G: Nuclear and Particle Physics
J. Phys. G: Nucl. Part. Phys. **47** (2020) 025103 (15pp) https://doi.org/10.1088/1361-6471/ab56ba

Equilibrium constants of hydrogen and helium isotopes at low nuclear densities

R Bougault[1,10], E Bonnet[2], B Borderie[3], A Chbihi[4], J D Frankland[4], E Galichet[3,5], D Gruyer[1], M Henri[4], M La Commara[6], N Le Neindre[1], I Lombardo[7], O Lopez[1], L Manduci[1,8], M Parlôg[1], R Roy[9], G Verde[7] and M Vigilante[6]

[1] Normandie Univ, ENSICAEN, UNICAEN, CNRS/IN2P3, LPC Caen, F-14000 Caen, France

INDRA Results: The gas phase

Chemical constants and in-medium effects

Equilibrium constants for different (A,Z):
- *depend only on (ρ,T)*

$$K_c(A,Z) = \frac{\rho(A,Z)}{\rho_p^Z \rho_n^{(A-Z)}}$$

Analysis method: NIMROD/Texas, Qin et al. PRL(2012)

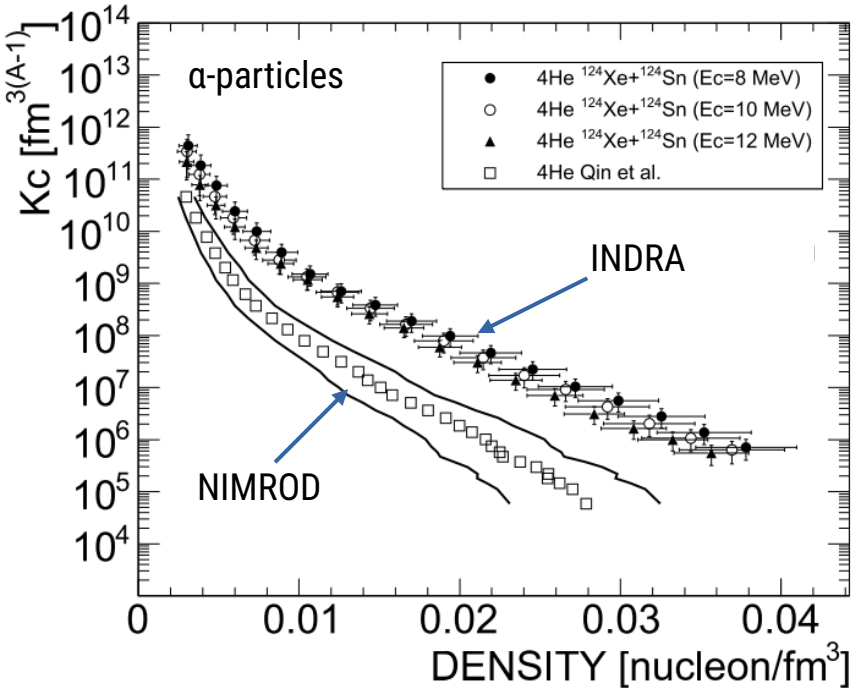

IOP Publishing Journal of Physics G: Nuclear and Particle Physics
J. Phys. G: Nucl. Part. Phys. **47** (2020) 025103 (15pp) https://doi.org/10.1088/1361-6471/ab56ba

Equilibrium constants of hydrogen and helium isotopes at low nuclear densities

R Bougault[1,10], E Bonnet[2], B Borderie[3], A Chbihi[4], J D Frankland[4], E Galichet[3,5], D Gruyer[1], M Henri[4], M La Commara[6], N Le Neindre[1], I Lombardo[7], O Lopez[1], L Manduci[1,8], M Parlôg[1], R Roy[9], G Verde[7] and M Vigilante[6]

[1] Normandie Univ, ENSICAEN, UNICAEN, CNRS/IN2P3, LPC Caen, F-14000 Caen, France

INDRA Results: The gas phase

Chemical constants and in-medium effects

Equilibrium constants for different (A,Z):
- *depend only on (ρ,T)*

$$K_c(A,Z) = \frac{\rho(A,Z)}{\rho_p^Z \rho_n^{(A-Z)}}$$

Analysis method: NIMROD/Texas, Qin et al. PRL(2012)

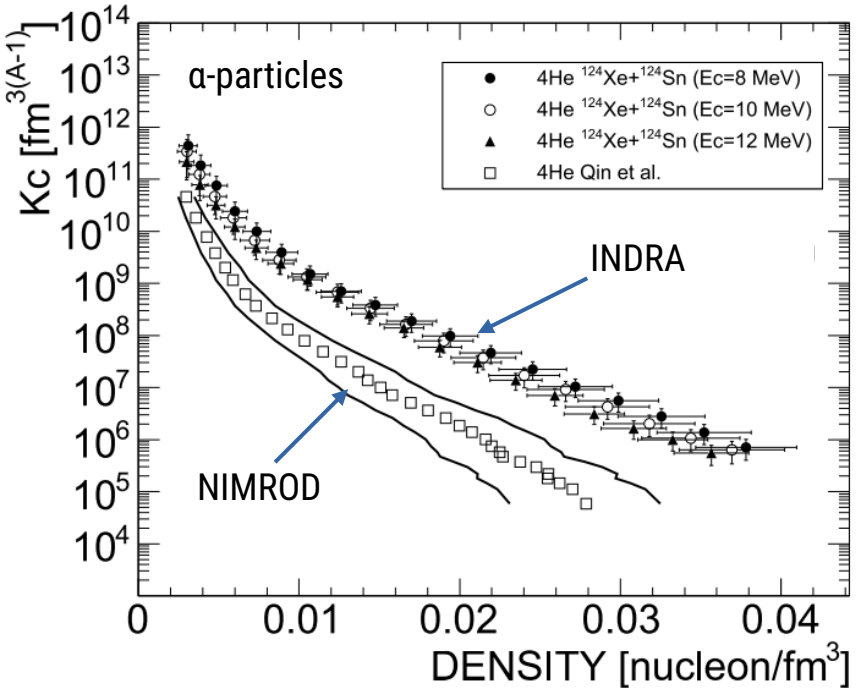

INDRA/NIMROD consistent results
- *INDRA lower temperatures → higher K_c*

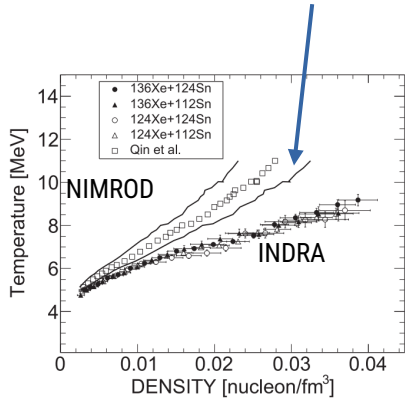

IOP Publishing Journal of Physics G: Nuclear and Particle Physics
J. Phys. G: Nucl. Part. Phys. **47** (2020) 025103 (15pp) https://doi.org/10.1088/1361-6471/ab56ba

Equilibrium constants of hydrogen and helium isotopes at low nuclear densities

R Bougault[1,10], E Bonnet[2], B Borderie[3], A Chbihi[4], J D Frankland[4], E Galichet[3,5], D Gruyer[1], M Henri[4], M La Commara[6], N Le Neindre[1], I Lombardo[7], O Lopez[1], L Manduci[1,8], M Parlôg[1], R Roy[9], G Verde[7] and M Vigilante[6]

[1] Normandie Univ, ENSICAEN, UNICAEN, CNRS/IN2P3, LPC Caen, F-14000 Caen, France

INDRA Results: The gas phase

Chemical constants and in-medium effects

Equilibrium constants for different (A,Z):
- *depend only on (ρ,T)*

$$K_c(A,Z) = \frac{\rho(A,Z)}{\rho_p^Z \rho_n^{(A-Z)}}$$

Analysis method: NIMROD/Texas, Qin et al. PRL(2012)

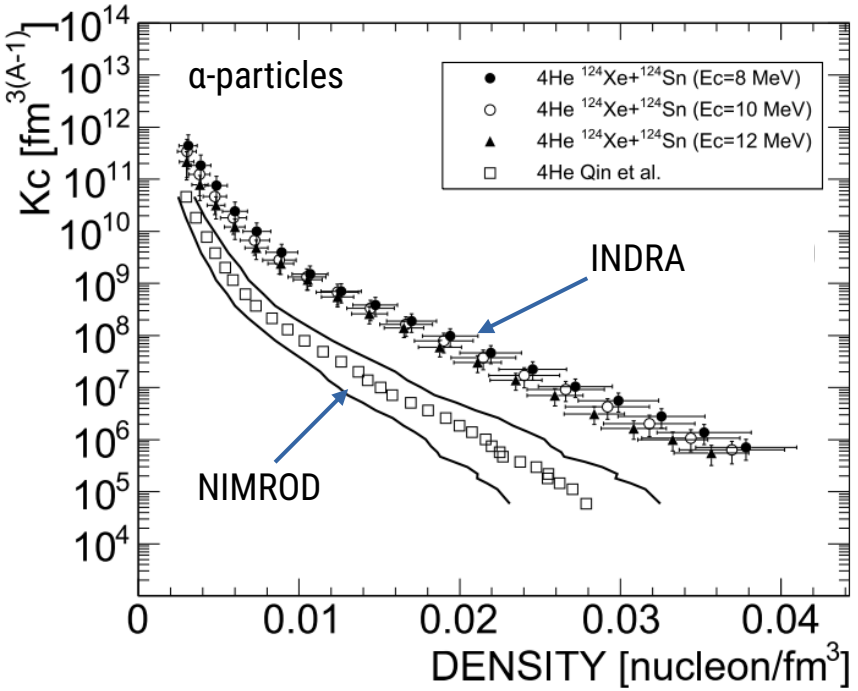

INDRA/NIMROD consistent results
- *INDRA lower temperatures → higher K_c*

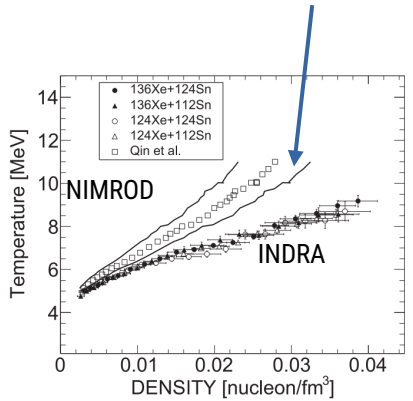

IOP Publishing Journal of Physics G: Nuclear and Particle Physics
J. Phys. G: Nucl. Part. Phys. **47** (2020) 025103 (15pp) https://doi.org/10.1088/1361-6471/ab56ba

Equilibrium constants of hydrogen and helium isotopes at low nuclear densities

R Bougault[1,10], E Bonnet[2], B Borderie[3], A Chbihi[4], J D Frankland[4], E Galichet[3,5], D Gruyer[1], M Henri[4], M La Commara[6], N Le Neindre[1], I Lombardo[7], O Lopez[1], L Manduci[1,8], M Parlôg[1], R Roy[9], G Verde[7] and M Vigilante[6]

[1] Normandie Univ, ENSICAEN, UNICAEN, CNRS/IN2P3, LPC Caen, F-14000 Caen, France

Analysis inconsistency: volume/density depends on cluster...

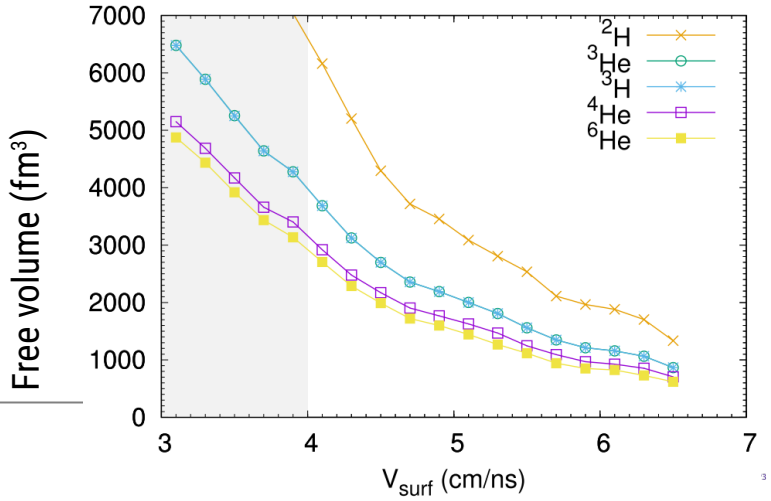

Chemical constants and in-medium effects

Inconsistency due to use of ideal-gas prescription for volume (no medium):

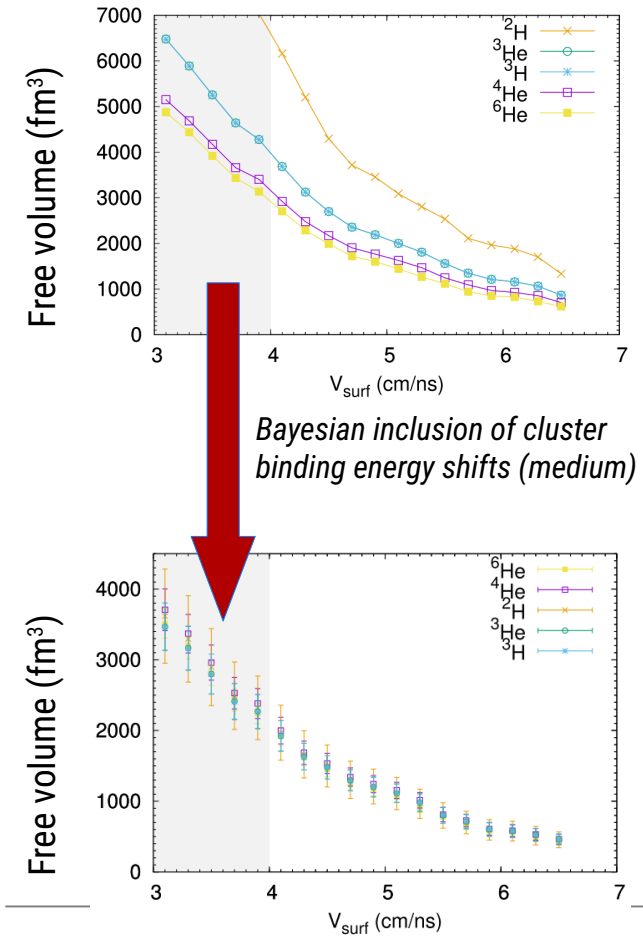

PHYSICAL REVIEW LETTERS **125,** 012701 (2020)

Low Density In-Medium Effects on Light Clusters from Heavy-Ion Data

Helena Pais,[1] Rémi Bougault,[2] Francesca Gulminelli,[2] Constança Providência,[1] Eric Bonnet,[3] Bernard Borderie,[4] Abdelouahad Chbihi,[5] John D. Frankland,[5] Emmanuelle Galichet,[4,6] Diégo Gruyer,[2] Maxime Henri,[5] Nicolas Le Neindre,[2] Olivier Lopez,[2] Loredana Manduci,[2,7] Marian Parlôg,[2] and Giuseppe Verde[8]
[1]*CFisUC, Department of Physics, University of Coimbra, 3004-516 Coimbra, Portugal*
[2]*Normandie University, ENSICAEN, UNICAEN, CNRS/IN2P3, LPC Caen, F-14000 Caen, France*

IOP Publishing — Journal of Physics G: Nuclear and Particle Physics
J. Phys. G: Nucl. Part. Phys. **47** (2020) 105204 (24pp) https://doi.org/10.1088/1361-6471/aba561

Improved method for the experimental determination of in-medium effects from heavy-ion collisions

Helena Pais[1,9], Rémi Bougault[2], Francesca Gulminelli[2], Constança Providência[1], Eric Bonnet[3], Bernard Borderie[4], Abdelouahad Chbihi[5], John D Frankland[5], Emmanuelle Galichet[4,6], Diégo Gruyer[2], Maxime Henri[5], Nicolas Le Neindre[2], Olivier Lopez[2], Loredana Manduci[2,7], Marian Parlôg[2] and Giuseppe Verde[8]

INDRA Results: The gas phase

Chemical constants and in-medium effects

Inconsistency due to use of ideal-gas prescription for volume (no medium):

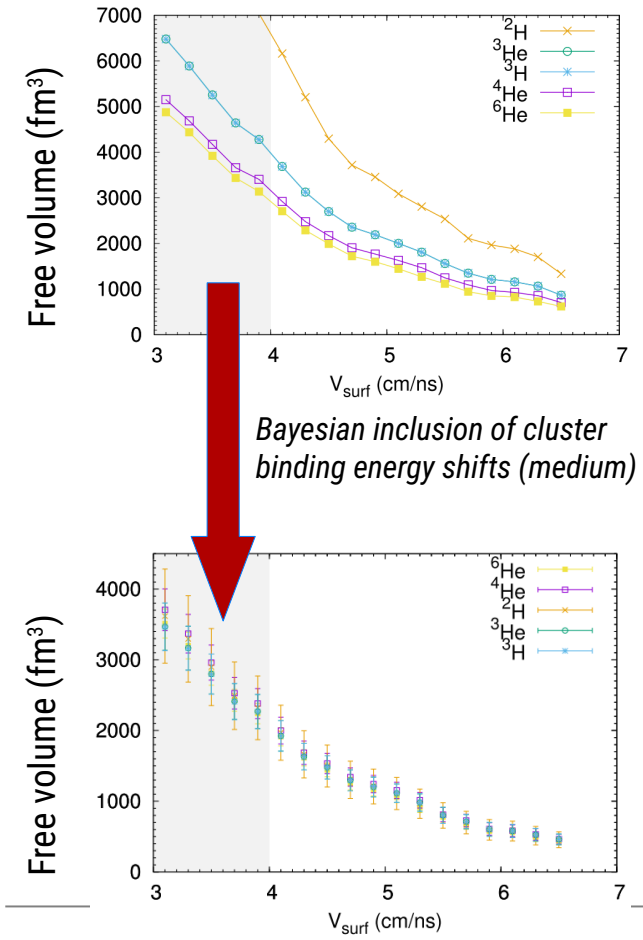

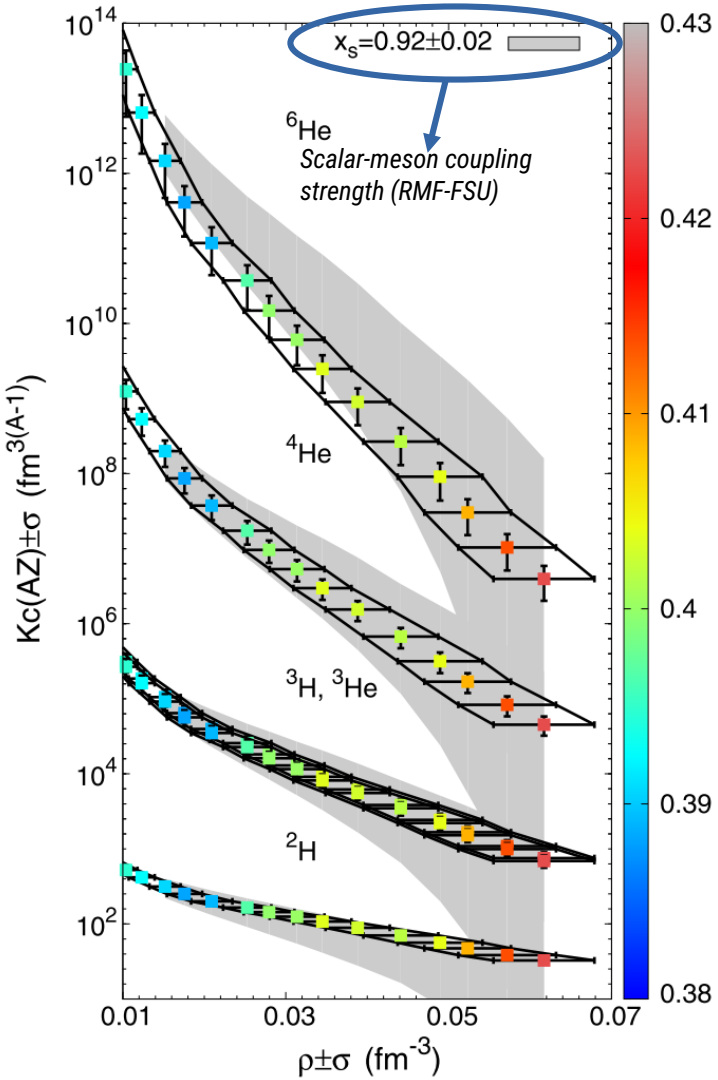

PHYSICAL REVIEW LETTERS **125,** 012701 (2020)

Low Density In-Medium Effects on Light Clusters from Heavy-Ion Data

Helena Pais,[1] Rémi Bougault,[2] Francesca Gulminelli,[2] Constança Providência,[1] Eric Bonnet,[3] Bernard Borderie,[4] Abdelouahad Chbihi,[5] John D. Frankland,[5] Emmanuelle Galichet,[4,6] Diégo Gruyer,[2] Maxime Henri,[5] Nicolas Le Neindre,[2] Olivier Lopez,[2] Loredana Manduci,[2,7] Marian Parlôg,[2] and Giuseppe Verde[8]
[1]*CFisUC, Department of Physics, University of Coimbra, 3004-516 Coimbra, Portugal*
[2]*Normandie University, ENSICAEN, UNICAEN, CNRS/IN2P3, LPC Caen, F-14000 Caen, France*

IOP Publishing — Journal of Physics G: Nuclear and Particle Physics
J. Phys. G: Nucl. Part. Phys. **47** (2020) 105204 (24pp) — https://doi.org/10.1088/1361-6471/aba561

Improved method for the experimental determination of in-medium effects from heavy-ion collisions

Helena Pais[1,9], Rémi Bougault[2], Francesca Gulminelli[2], Constança Providência[1], Eric Bonnet[3], Bernard Borderie[4], Abdelouahad Chbihi[5], John D Frankland[5], Emmanuelle Galichet[4,6], Diégo Gruyer[2], Maxime Henri[5], Nicolas Le Neindre[2], Olivier Lopez[2], Loredana Manduci[2,7], Marian Parlôg[2] and Giuseppe Verde[8]

Conclusions:

- *medium effect less strong (x_s=0.92) than previously thought (x_s=0.85: Qin et al.)*
- *clusters can survive at higher densities*
- *play a larger role in e.g. neutrino opacity*

- *what about heavier clusters?*
- *what if we "measured" the density?*

INDRA Results: The gas phase

LGPT & the QCD phase diagram

Systems	E_{beam}	$K_{tot}^{(c.m.)}$	$\beta_{c.m.}^{(lab)}$	A_{tot}	$Y_p^{(coll)}$
$^{58}Ni + ^{58}Ni$	82	20.3	0.205	116	0.48
$^{58}Ni + ^{58}Ni$	90	22.2	0.215	116	0.48
$^{129}Xe + ^{124}Sn$	80	19.8	0.207	253	0.41
$^{124}Xe + ^{112}Sn$	100	24.6	0.237	236	0.44
$^{124}Xe + ^{124}Sn$	100	24.7	0.226	248	0.42
$^{129}Xe + ^{112}Sn$	100	24.6	0.241	241	0.43
$^{129}Xe + ^{124}Sn$	100	24.7	0.230	253	0.41
$^{124}Xe + ^{124}Sn$	150	36.8	0.273	248	0.42
$^{129}Xe + ^{124}Sn$	150	36.8	0.278	253	0.41
$^{197}Au + ^{197}Au$	80	19.8	0.203	394	0.40
$^{197}Au + ^{197}Au$	100	24.7	0.226	394	0.40
$^{197}Au + ^{197}Au$	150	36.8	0.273	394	0.40

PHYSICAL REVIEW C **111**, 064616 (2025)

Nuclear clustering process in heavy-ion collisions: Experimental constraints on the low-temperature region of the QCD phase diagram

E. Bonnet,[1,*] B. Borderie,[2] R. Bougault,[3] A. Chbihi,[4] Q. Fable,[4] J. D. Frankland,[4] D. Gruyer,[3] M. La Commara,[5,6] A. Le Fèvre,[7] N. Le Neindre,[3] I. Lombardo,[8,9] J. Łukasik,[10] M. Pârlog,[3,11] G. Verde,[9,12] and J. P. Wieleczko[4]
(INDRA Collaboration)

$$n^{(GC)} = d \int \frac{d^2p}{h^2} \left(e^{\frac{E(p)-\mu}{T}} + \kappa \right)^{-1}$$

$$\mu_i = \mu(Z_i, A_i) = A_i \mu_B + Z_i \mu_Q.$$

INDRA Results: The gas phase

LGPT & the QCD phase diagram

Systems	E_{beam}	$K_{tot}^{(c.m.)}$	$\beta_{c.m.}^{(lab)}$	A_{tot}	$Y_p^{(coll)}$
$^{58}Ni + ^{58}Ni$	82	20.3	0.205	116	0.48
$^{58}Ni + ^{58}Ni$	90	22.2	0.215	116	0.48
$^{129}Xe + ^{124}Sn$	80	19.8	0.207	253	0.41
$^{124}Xe + ^{112}Sn$	100	24.6	0.237	236	0.44
$^{124}Xe + ^{124}Sn$	100	24.7	0.226	248	0.42
$^{129}Xe + ^{112}Sn$	100	24.6	0.241	241	0.43
$^{129}Xe + ^{124}Sn$	100	24.7	0.230	253	0.41
$^{124}Xe + ^{124}Sn$	150	36.8	0.273	248	0.42
$^{129}Xe + ^{124}Sn$	150	36.8	0.278	253	0.41
$^{197}Au + ^{197}Au$	80	19.8	0.203	394	0.40
$^{197}Au + ^{197}Au$	100	24.7	0.226	394	0.40
$^{197}Au + ^{197}Au$	150	36.8	0.273	394	0.40

PHYSICAL REVIEW C **111**, 064616 (2025)

Nuclear clustering process in heavy-ion collisions: Experimental constraints on the low-temperature region of the QCD phase diagram

E. Bonnet,[1,*] B. Borderie,[2] R. Bougault,[3] A. Chbihi,[4] Q. Fable,[4] J. D. Frankland,[4] D. Gruyer,[3] M. La Commara,[5,6] A. Le Fèvre,[7] N. Le Neindre,[3] I. Lombardo,[8,9] J. Łukasik,[10] M. Pârlog,[3,11] G. Verde,[9,12] and J. P. Wieleczko[4]
(INDRA Collaboration)

$$n^{(GC)} = d \int \frac{d^2p}{h^2} \left(e^{\frac{E(p)-\mu}{T}} + \kappa \right)^{-1}$$

$$\mu_i = \mu(Z_i, A_i) = A_i \mu_B + Z_i \mu_Q.$$

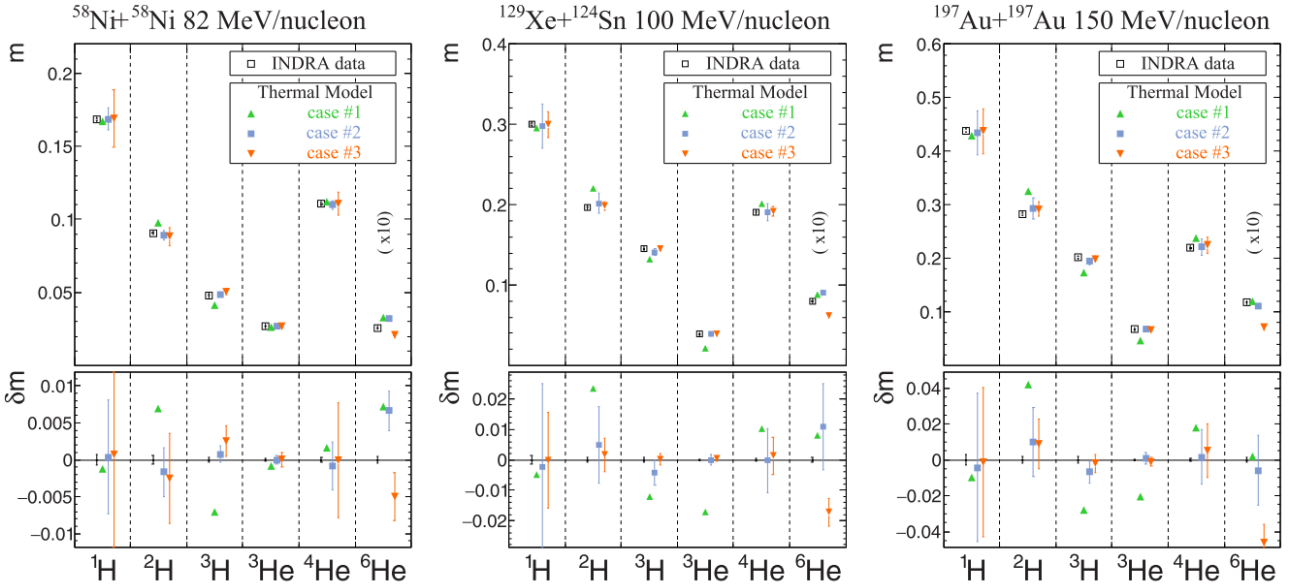

INDRA Results: The gas phase

LGPT & the QCD phase diagram

Nuclear clustering process in heavy-ion collisions: Experimental constraints on the low-temperature region of the QCD phase diagram

E. Bonnet,[1,*] B. Borderie,[2] R. Bougault,[3] A. Chbihi,[4] Q. Fable,[4] J. D. Frankland,[4] D. Gruyer,[3] M. La Commara,[5,6] A. Le Fèvre,[7] N. Le Neindre,[3] I. Lombardo,[8,9] J. Łukasik,[10] M. Pârlog,[3,11] G. Verde,[9,12] and J. P. Wieleczko[4]
(INDRA Collaboration)

Systems	E_{beam}	$K_{tot}^{(c.m.)}$	$\beta_{c.m.}^{(lab)}$	A_{tot}	$Y_p^{(coll)}$
$^{58}Ni+^{58}Ni$	82	20.3	0.205	116	0.48
$^{58}Ni+^{58}Ni$	90	22.2	0.215	116	0.48
$^{129}Xe+^{124}Sn$	80	19.8	0.207	253	0.41
$^{124}Xe+^{112}Sn$	100	24.6	0.237	236	0.44
$^{124}Xe+^{124}Sn$	100	24.7	0.226	248	0.42
$^{129}Xe+^{112}Sn$	100	24.6	0.241	241	0.43
$^{129}Xe+^{124}Sn$	100	24.7	0.230	253	0.41
$^{124}Xe+^{124}Sn$	150	36.8	0.273	248	0.42
$^{129}Xe+^{124}Sn$	150	36.8	0.278	253	0.41
$^{197}Au+^{197}Au$	80	19.8	0.203	394	0.40
$^{197}Au+^{197}Au$	100	24.7	0.226	394	0.40
$^{197}Au+^{197}Au$	150	36.8	0.273	394	0.40

$$n^{(GC)} = d\int \frac{d^2p}{h^2}\left(e^{\frac{E(p)-\mu}{T}}+\kappa\right)^{-1}$$

$$\mu_i = \mu(Z_i, A_i) = A_i\mu_B + Z_i\mu_Q.$$

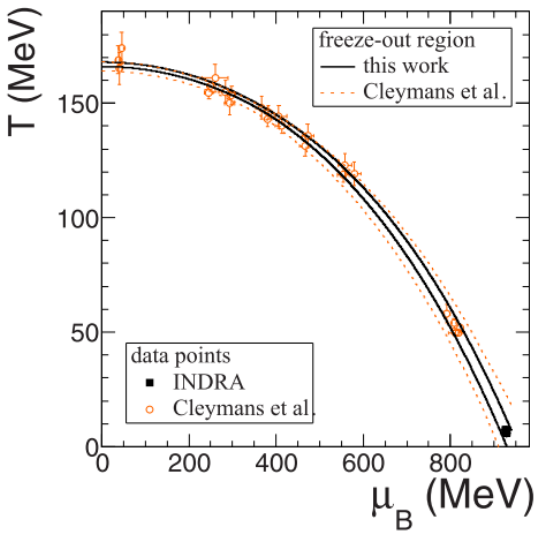

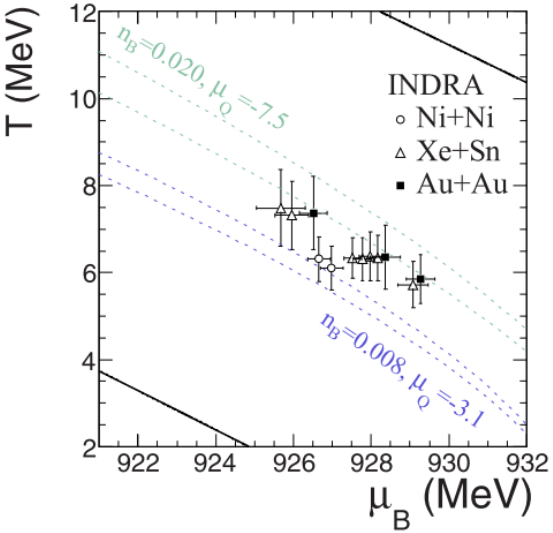

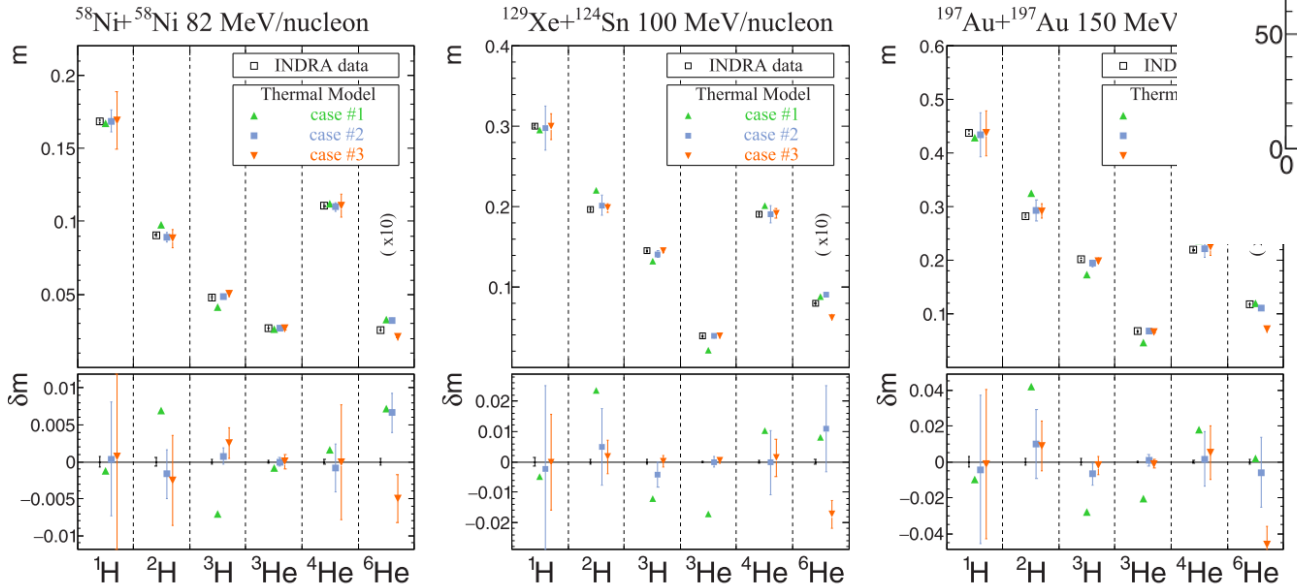

INDRA Results: The gas phase

LGPT & the QCD phase diagram

Systems	E_{beam}	$K_{tot}^{(c.m.)}$	$\beta_{c.m.}^{(lab)}$	A_{tot}	$Y_p^{(coll)}$
$^{58}Ni+^{58}Ni$	82	20.3	0.205	116	0.48
$^{58}Ni+^{58}Ni$	90	22.2	0.215	116	0.48
$^{129}Xe+^{124}Sn$	80	19.8	0.207	253	0.41
$^{124}Xe+^{112}Sn$	100	24.6	0.237	236	0.44
$^{124}Xe+^{124}Sn$	100	24.7	0.226	248	0.42
$^{129}Xe+^{112}Sn$	100	24.6	0.241	241	0.43
$^{129}Xe+^{124}Sn$	100	24.7	0.230	253	0.41
$^{124}Xe+^{124}Sn$	150	36.8	0.273	248	0.42
$^{129}Xe+^{124}Sn$	150	36.8	0.278	253	0.41
$^{197}Au+^{197}Au$	80	19.8	0.203	394	0.40
$^{197}Au+^{197}Au$	100	24.7	0.226	394	0.40
$^{197}Au+^{197}Au$	150	36.8	0.273	394	0.40

Nuclear clustering process in heavy-ion collisions: Experimental constraints on the low-temperature region of the QCD phase diagram

E. Bonnet,[1,*] B. Borderie,[2] R. Bougault,[3] A. Chbihi,[4] Q. Fable,[4] J. D. Frankland,[4] D. Gruyer,[3] M. La Commara,[5,6] A. Le Fèvre,[7] N. Le Neindre,[3] I. Lombardo,[8,9] J. Łukasik,[10] M. Pârlog,[3,11] G. Verde,[9,12] and J. P. Wieleczko[4]
(INDRA Collaboration)

$$n^{(GC)} = d\int \frac{d^2p}{h^2}\left(e^{\frac{E(p)-\mu}{T}}+\kappa\right)^{-1}$$

$$\mu_i = \mu(Z_i, A_i) = A_i\mu_B + Z_i\mu_Q.$$

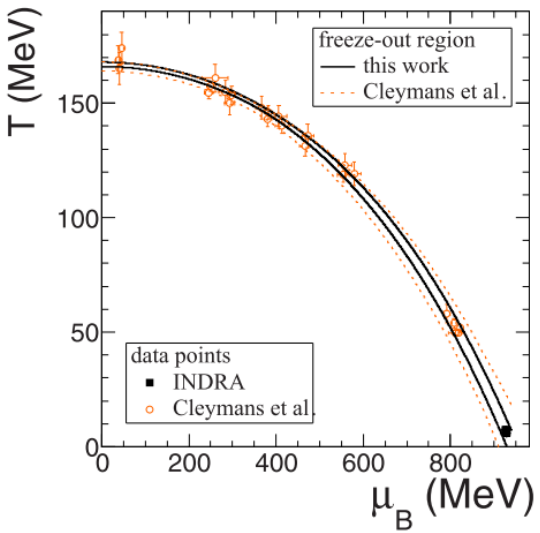

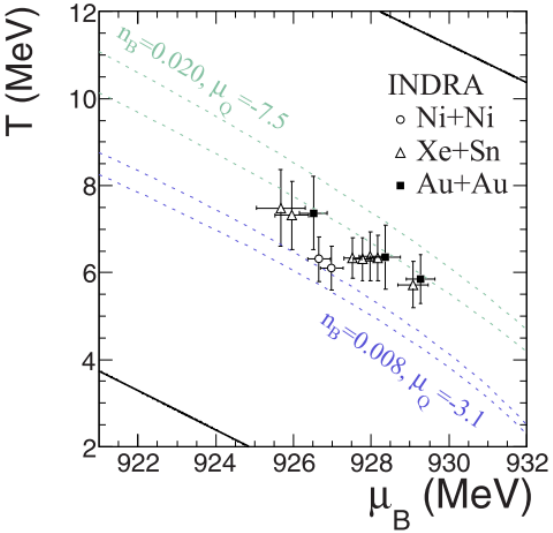

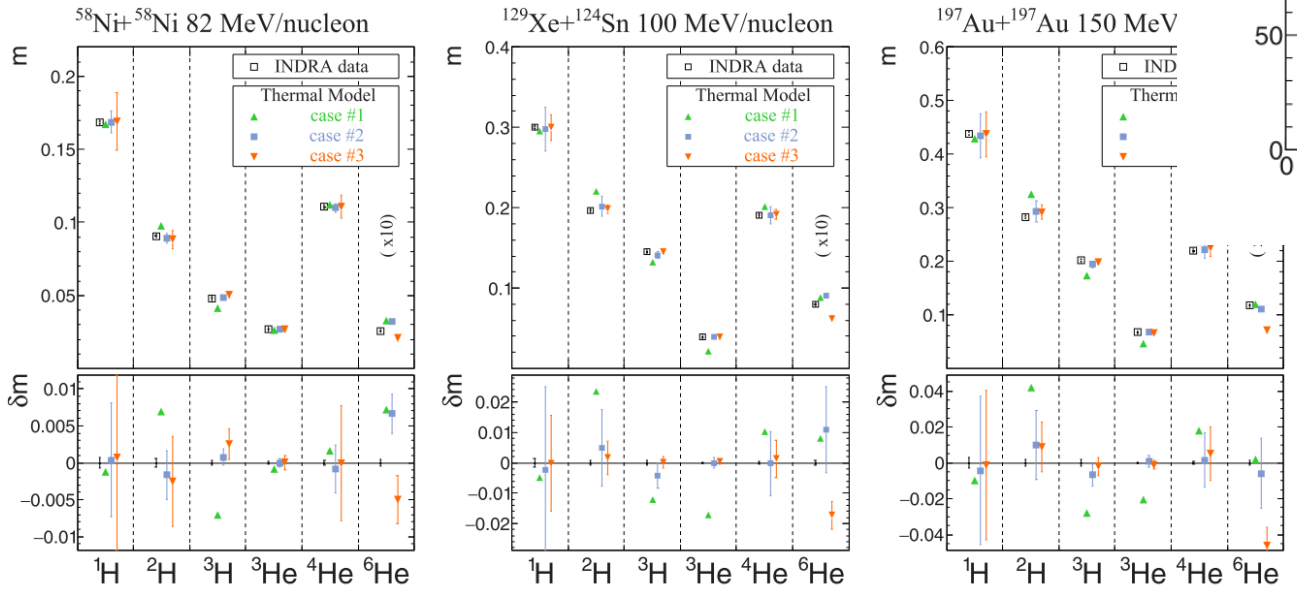

The average multiplicities emitted in the transverse plane of the collision are reproduced by the thermal model describing an ideal gas of free neutrons and protons in chemical equilibrium with clusters. The thermodynamic potentials obtained are consistent with existing results at higher energies and validate the continuity of a universal curve in the QCD phase diagram called the "freeze-out" line linking hadron production and nuclear clustering processes. With re-

LIQUID-GAS PHASE TRANSITIONS IN NUCLEAR MATTER

A (hopefully) pedagogical introduction and overview of experimental achievements in the field

John FRANKLAND

GANIL

cnrs NUCLÉAIRE & PARTICULES

cea

1. INTRODUCTION

- a few “reminders” on equations of state & LGPT in classical systems, associated critical phenomena, realistic nuclear matter EoS & link to multifragmentation, and statistical models in HIC

2. SOME EXPERIMENTAL OBSERVATIONS

- a historical tour from the earliest experiments suggesting strong links between multifragmentation and a liquid-gas phase transition of nuclear matter

3. INDRA RESULTS

- characterizing the gas phase, now including in-medium effects & link to QCD phase diagram
- characterizing the phase transition: convex entropy intruder & all that entails

FiNiTE SYSTEM SiGNALS OF 1st ORDER PHASE TRANSiTiON

Recognising phase transitions in macroscopic systems is easy (put the kettle on!)

Example: macroscopic van der Waals fluid

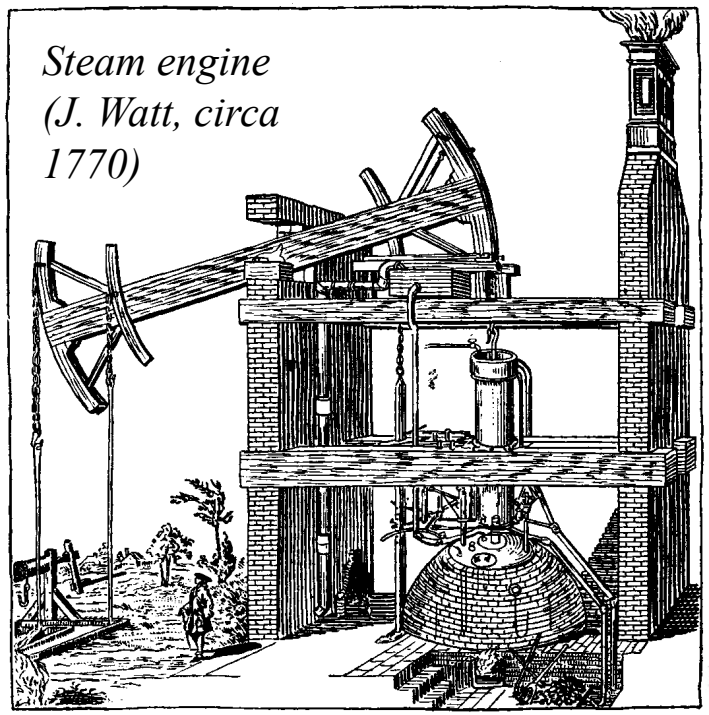

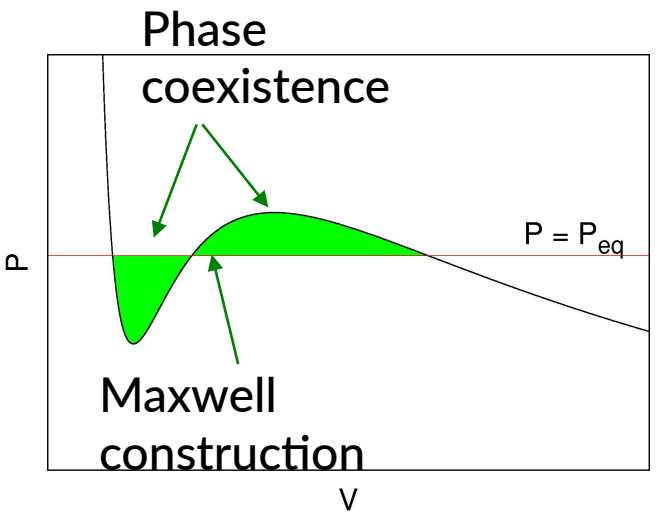

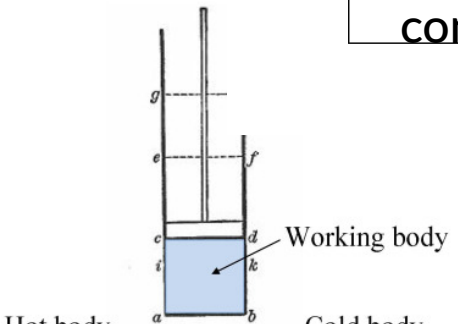

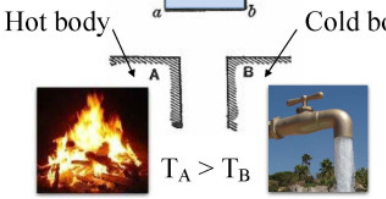

FiNiTE SYSTEM SiGNALS OF 1st ORDER PHASE TRANSiTiON

Recognising phase transitions in macroscopic systems is easy (put the kettle on!)

Example: macroscopic van der Waals fluid

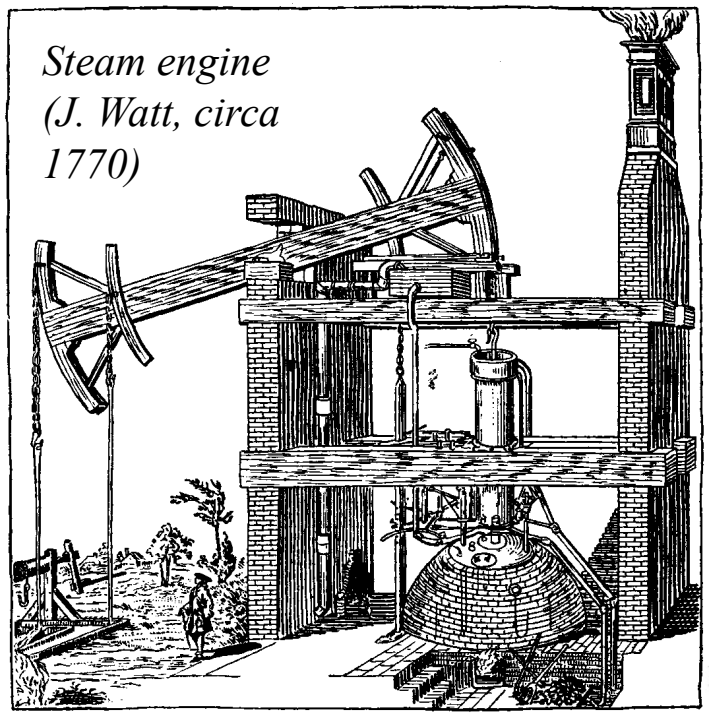

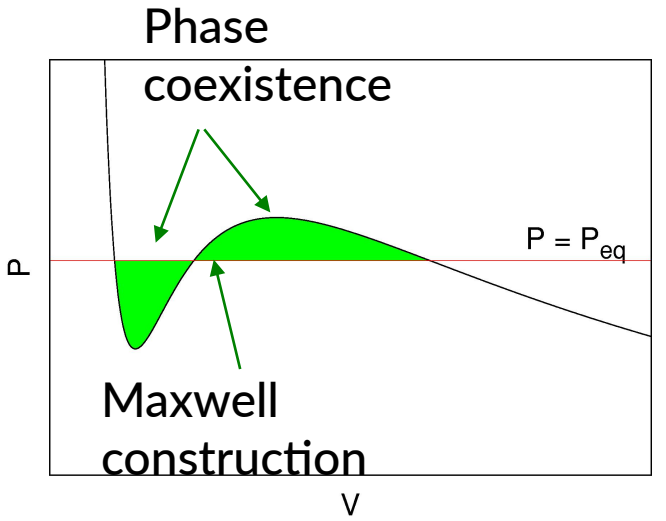

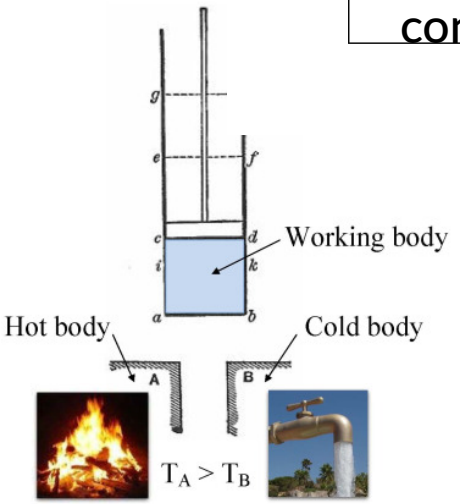

But what if you only had access to microscopic water droplets containing at most a few 100 molecules?

FiNiTE SYSTEM SiGNALS OF 1st ORDER PHASE TRANSiTiON

Recognising phase transitions in macroscopic systems is easy
Recognising phase transitions in small systems requires the right approach!

Example: microscopic Lennard-Jones clusters

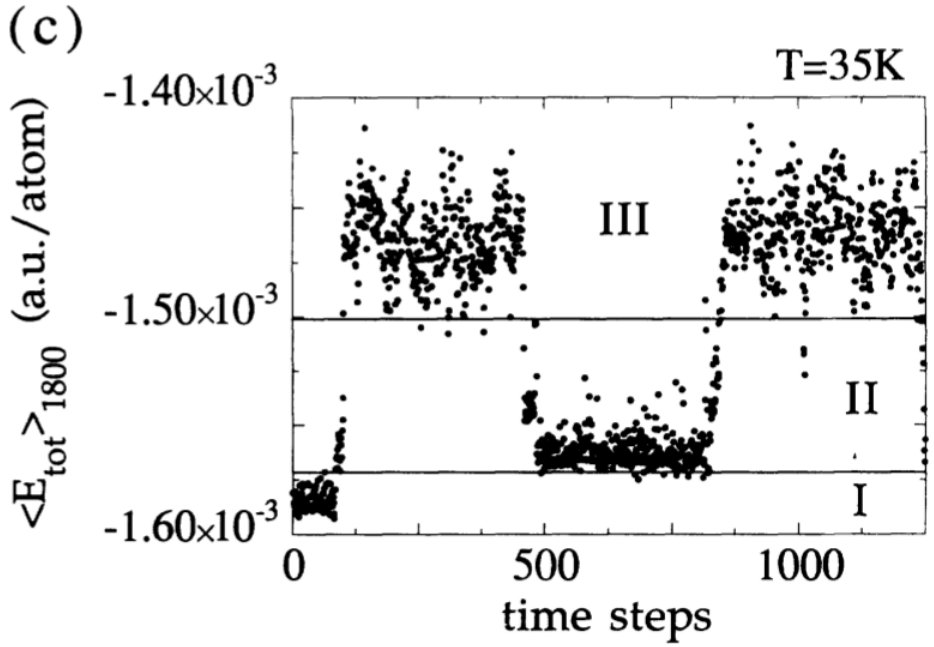

Average energy over time of Ar_{55} cluster near the solid-liquid transition temperature

Dynamic "coexistence" between different energetic states

Kunz, Berry, Phys. Rev. E49 (1994)1895

FiNiTE SYSTEM SiGNALS OF 1st ORDER PHASE TRANSiTiON

Recognising phase transitions in macroscopic systems is easy
Recognising phase transitions in small systems requires the right approach!

Example: microscopic Lennard-Jones clusters

* thermodynamic limit p.t. is well-known
* finite clusters too small for phases or coexistence
* 'phase' precursors are states of different energy, d.o.f.

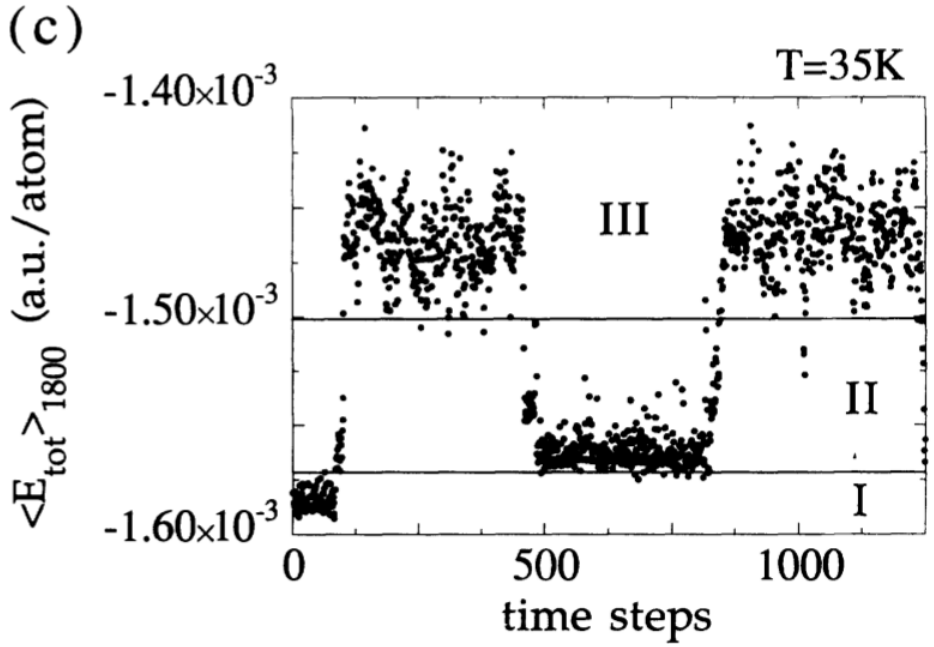

Kunz, Berry, Phys. Rev. E49 (1994)1895

Average energy over time of Ar_{55} cluster near the solid-liquid transition temperature

Dynamic "coexistence" between different energetic states

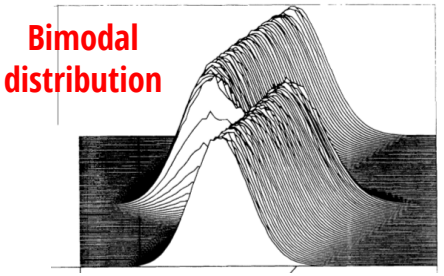

Labastie, Whetten PRL65, 1567(1990)

FiNiTE SYSTEM SiGNALS OF 1st ORDER PHASE TRANSiTiON

Recognising phase transitions in macroscopic systems is easy
Recognising phase transitions in small systems requires the right approach!

* finite (small) systems → large surface effects → non-additivity

NON-ADDITIVE SYSTEMS

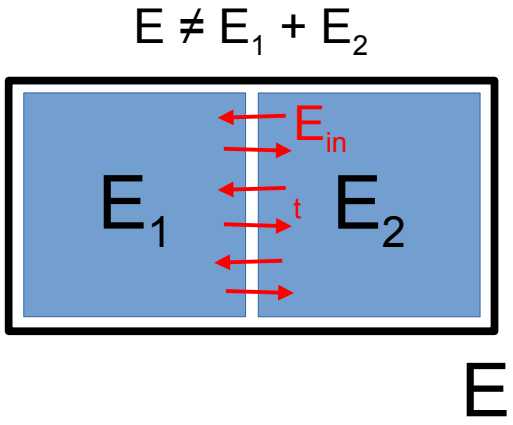

FiNiTE SYSTEM SiGNALS OF 1st ORDER PHASE TRANSiTiON

Recognising phase transitions in macroscopic systems is easy
Recognising phase transitions in small systems requires the right approach!

* finite (small) systems → large surface effects → non-additivity
* non-additivity forbids phase mixing, Maxwell construction

NON-ADDITIVE SYSTEMS

$E \neq E_1 + E_2$

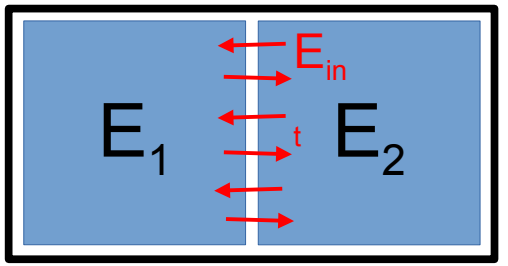

E

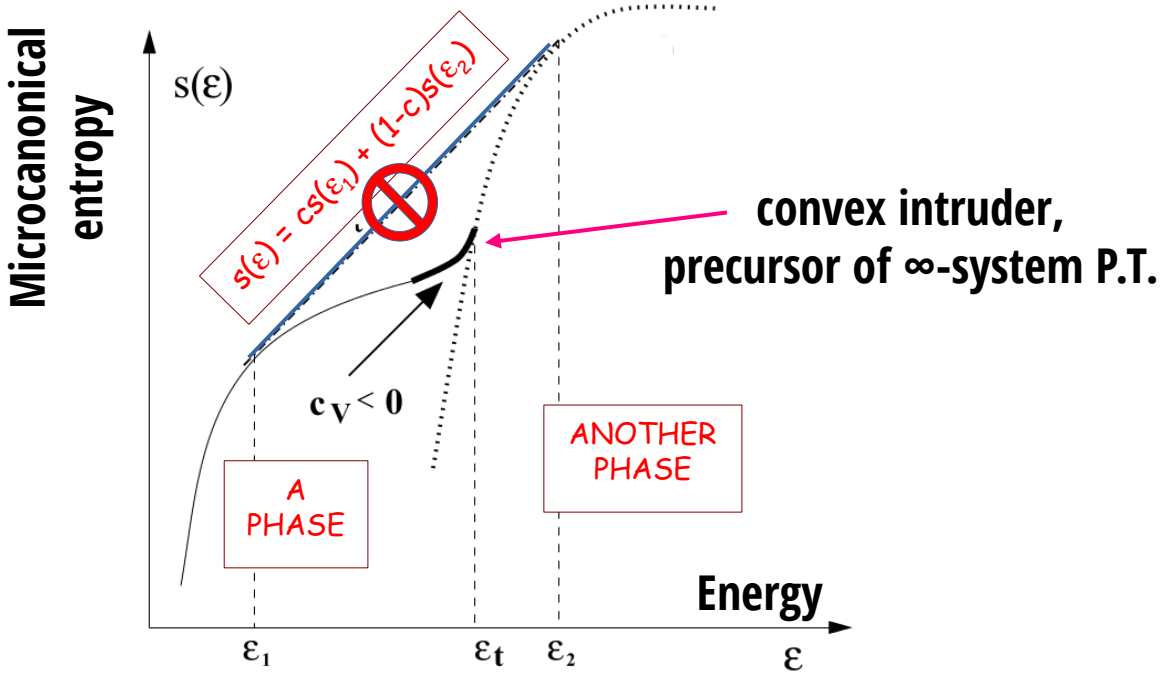

Campa, Dauxois, Ruffo, PhysRep480, 57(2009)

FiNiTE SYSTEM SiGNALS OF 1st ORDER PHASE TRANSiTiON

Recognising phase transitions in macroscopic systems is easy
Recognising phase transitions in small systems requires the right approach!

* finite (small) systems → large surface effects → non-additivity
* non-additivity forbids phase mixing, Maxwell construction
* convex intruder in microcanonical entropy origin of 1st order phase transition signals

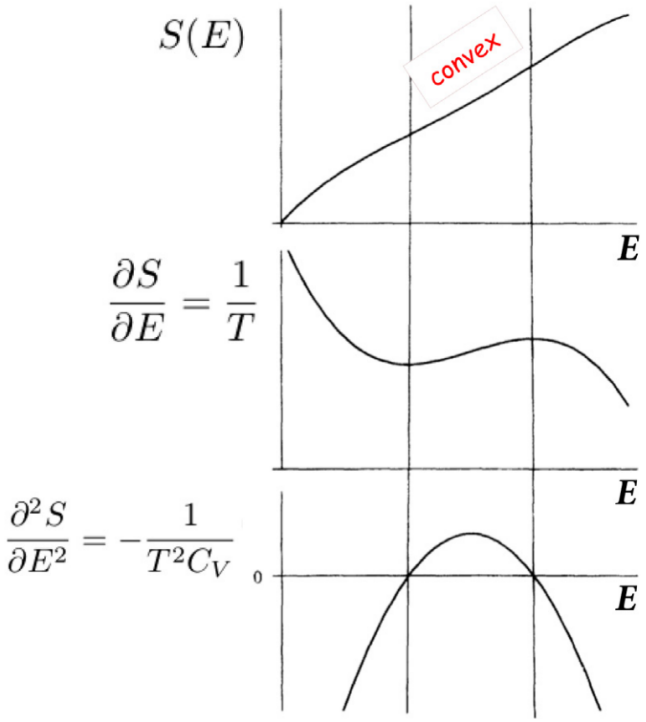

Borderie & Frankland, Prog. Part. Nuc. Phys. 105(2019)82
adapted from Wales & Berry, PRL73, 2875(1994)

FiNiTE SYSTEM SiGNALS OF 1st ORDER PHASE TRANSiTiON

Recognising phase transitions in macroscopic systems is easy
Recognising phase transitions in small systems requires the right approach!

* finite (small) systems → large surface effects → non-additivity
* non-additivity forbids phase mixing, Maxwell construction
* convex intruder in microcanonical entropy origin of 1st order phase transition signals

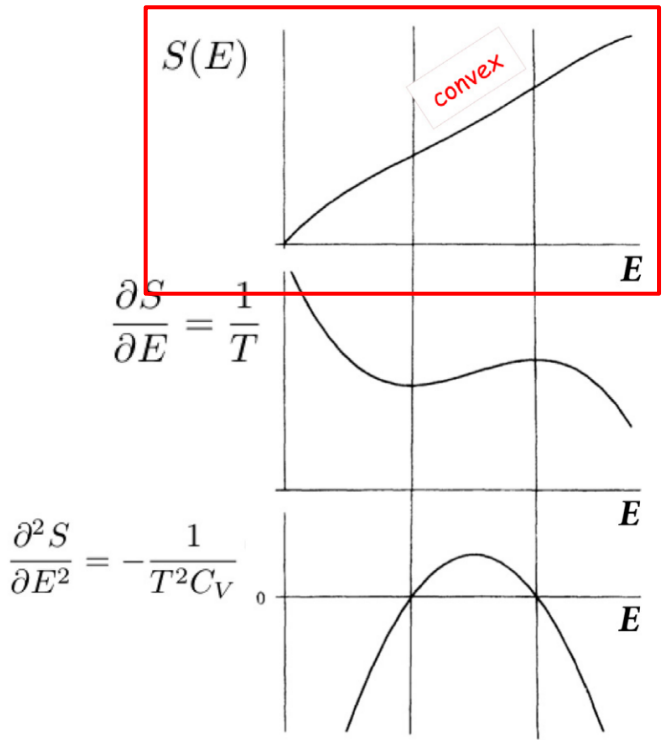

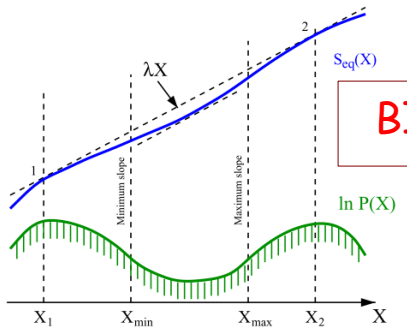

BIMODALITY

Borderie & Frankland, Prog. Part. Nuc. Phys. 105(2019)82
adapted from Wales & Berry, PRL73, 2875(1994)

FiNiTE SYSTEM SiGNALS OF 1st ORDER PHASE TRANSiTiON

Recognising phase transitions in macroscopic systems is easy
Recognising phase transitions in small systems requires the right approach!

* finite (small) systems → large surface effects → non-additivity
* non-additivity forbids phase mixing, Maxwell construction
* convex intruder in microcanonical entropy origin of 1st order phase transition signals

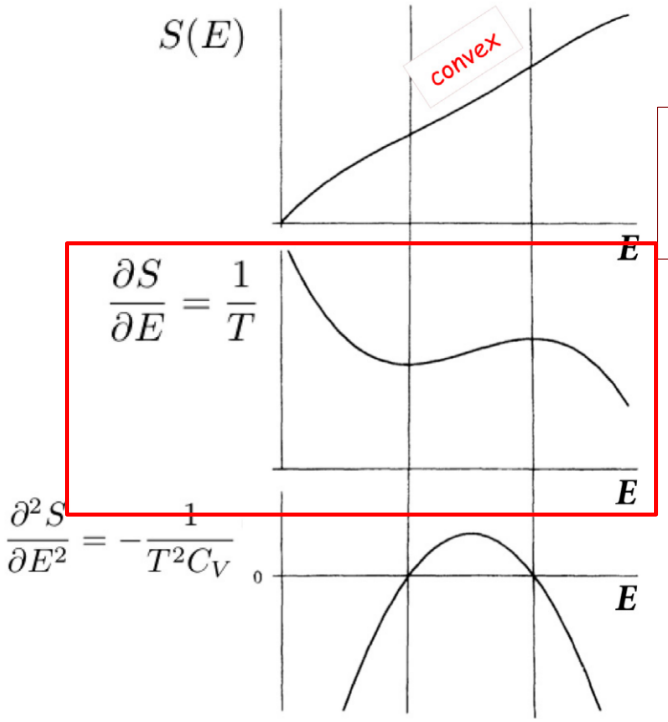

BACK-BENDING CALORIC CURVE

D.H.E. Gross, PhysRep279, 119(1997)

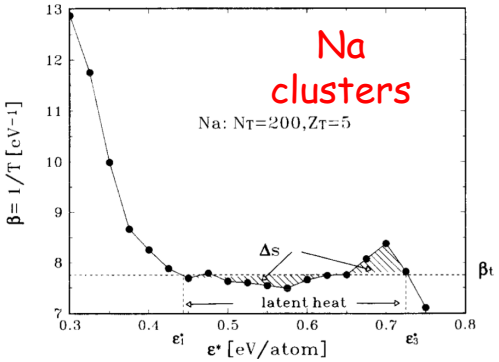

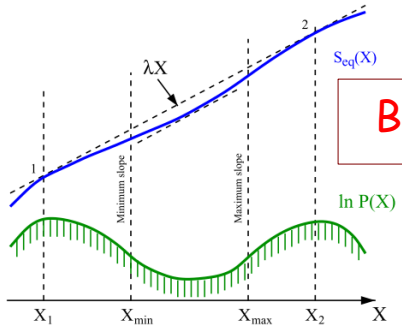

BIMODALITY

Borderie & Frankland, Prog. Part. Nuc. Phys. 105(2019)82
adapted from Wales & Berry, PRL73, 2875(1994)

FiNiTE SYSTEM SiGNALS OF 1st ORDER PHASE TRANSiTiON

Recognising phase transitions in macroscopic systems is easy
Recognising phase transitions in small systems requires the right approach!

* finite (small) systems → large surface effects → non-additivity
* non-additivity forbids phase mixing, Maxwell construction
* convex intruder in microcanonical entropy origin of 1st order phase transition signals

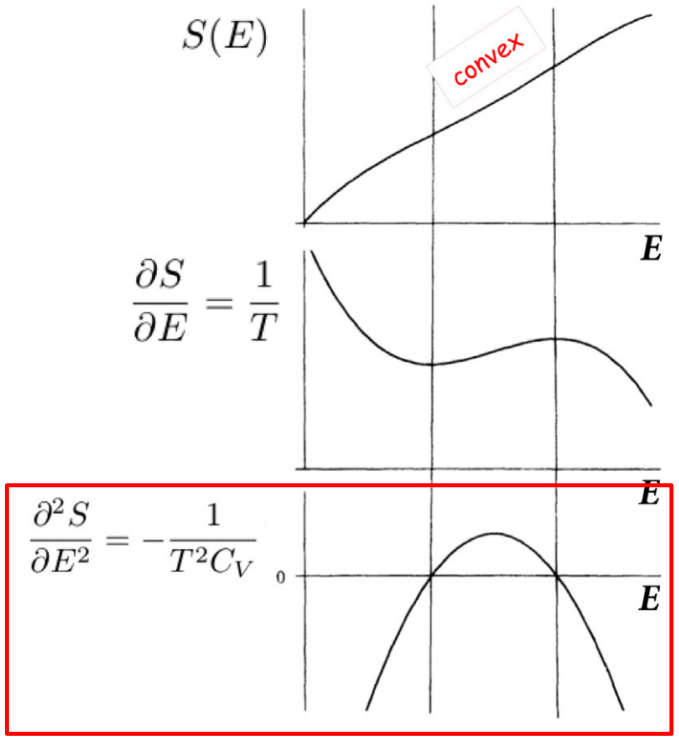

BACK-BENDING CALORIC CURVE

D.H.E. Gross, PhysRep279, 119(1997)

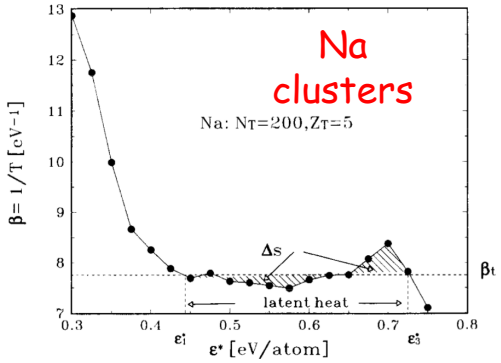

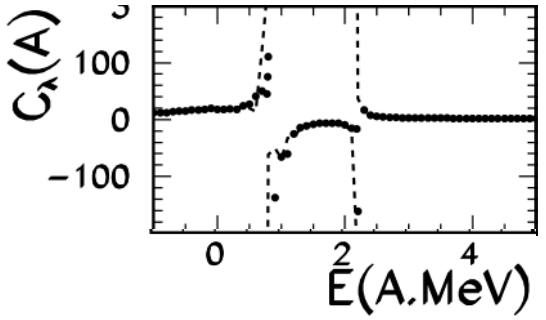

NEGATIVE HEAT CAPACITY

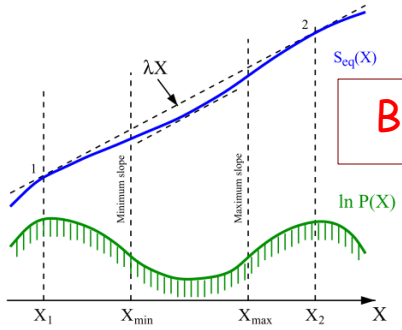

BIMODALITY

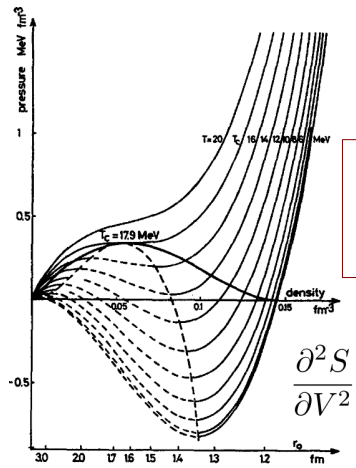

SPINODAL INSTABILITY

$$\frac{\partial^2 S}{\partial V^2} > 0 \Rightarrow \kappa^{-1} \equiv -V\frac{\partial P}{\partial V} < 0$$

Borderie & Frankland, Prog. Part. Nuc. Phys. 105(2019)82
adapted from Wales & Berry, PRL73, 2875(1994)

Chomaz, Duflot, Gulminelli , PRL85, 3587(2000)

BiMODALiTY iN NUCLEAR MULTiFRAGMENTATiON DATA

For the liquid-gas transition both the energy and
the mass/charge of the largest "cluster" are bimodal

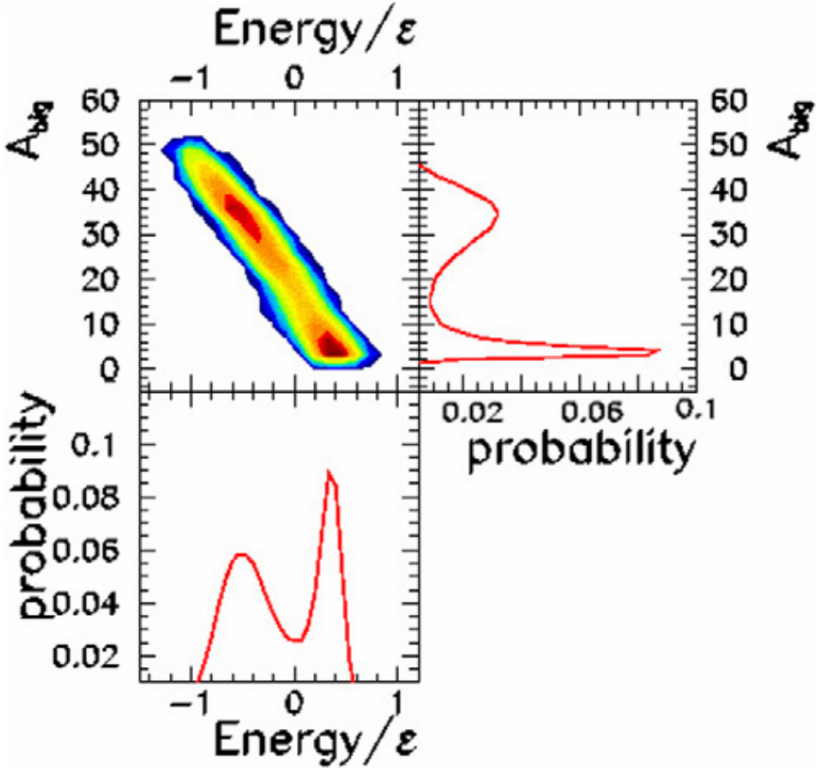

Lattice Gas Model calculation
Chomaz, Gulminelli in Nucl. Phys. A779(2006)267

BiMODALiTY iN NUCLEAR MULTiFRAGMENTATiON DATA

For the liquid-gas transition both the energy and the mass/charge of the largest "cluster" are bimodal

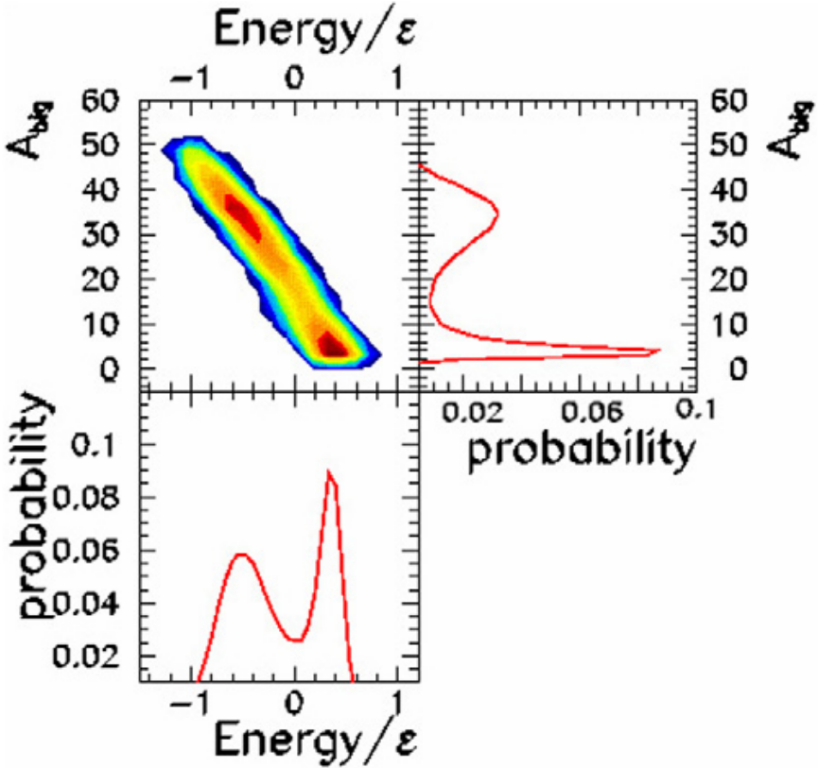

Lattice Gas Model calculation
Chomaz, Gulminelli in Nucl. Phys. A779(2006)267

First studies: asymmetry of 2 largest fragments of each event, events sorted according to dissipation/centrality

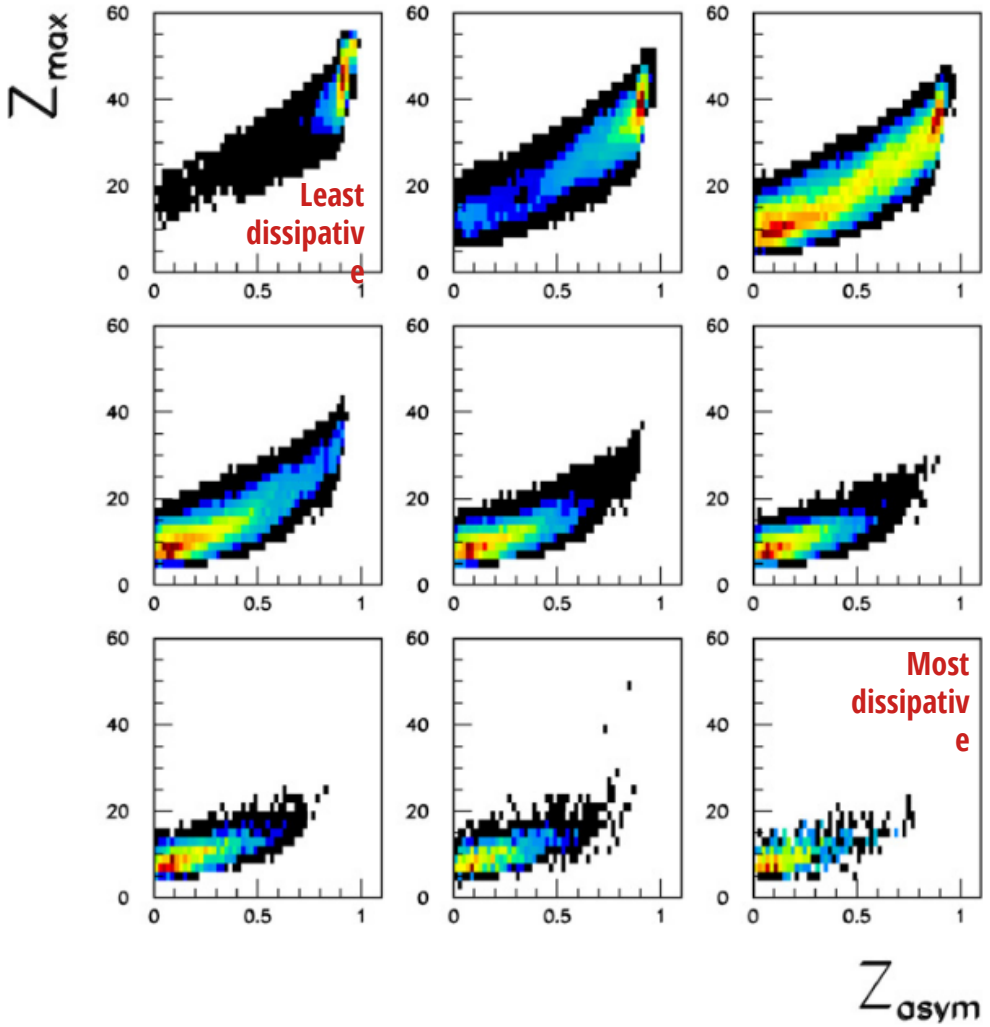

INDRA-ALADIN (GSI) Xe+Sn 80AMeV

Multifragmentation of Xe quasi-projectile spectators

$$Z_{max} > Z_2 > Z_3 > \dots$$

$$Z_{asym} = \frac{Z_{max} - Z_2}{Z_{max} + Z_2}$$

M. Pichon, B. Tamain et al. (INDRA-ALADIN) Nucl. Phys. A779(2006)267

BiMODALiTY iN NUCLEAR MULTiFRAGMENTATiON DATA

For the liquid-gas transition both the energy and the mass/charge of the largest "cluster" are bimodal

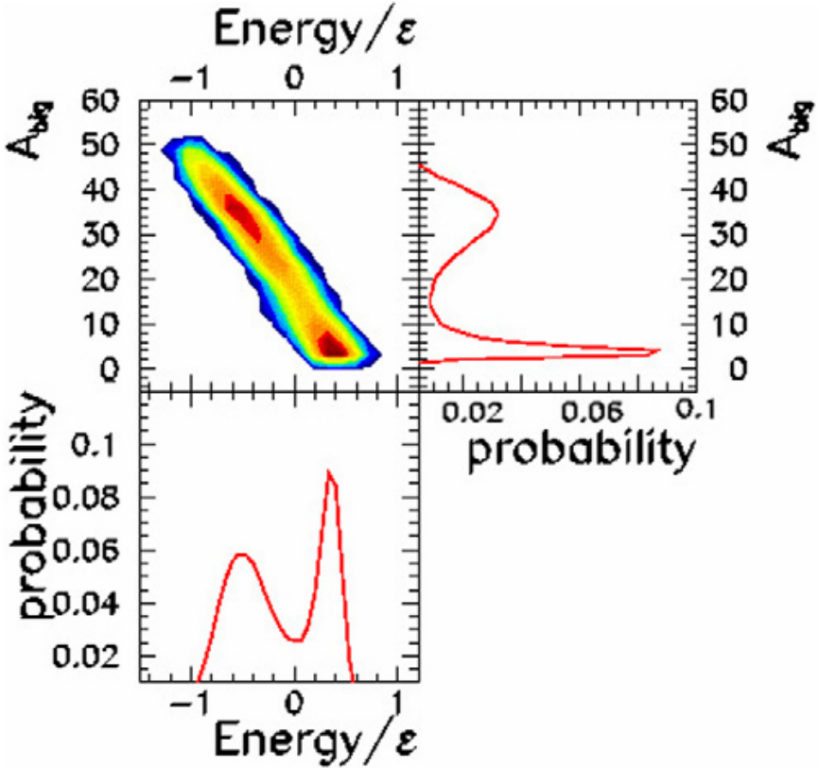

Lattice Gas Model calculation
Chomaz, Gulminelli in Nucl. Phys. A779(2006)267

M. Bruno et al. / Nuclear Physics A 807 (2008) 48–60

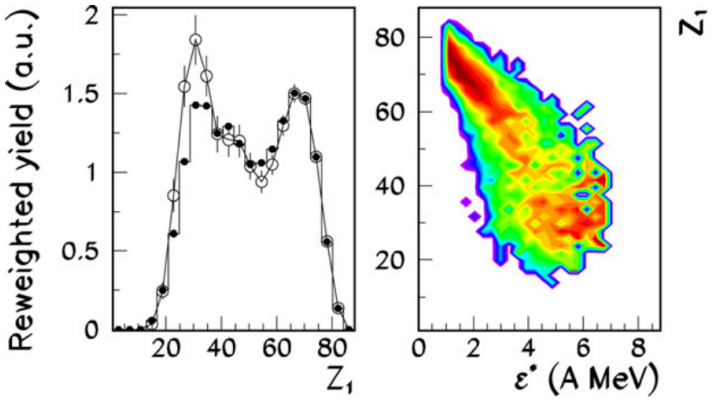

MULTICS/
MINIBALL
(MSU)
Au+Au 35AMeV

Multifragmentation of Au quasi-projectile spectators

INDRA (GSI)
Au+Au
80AMeV

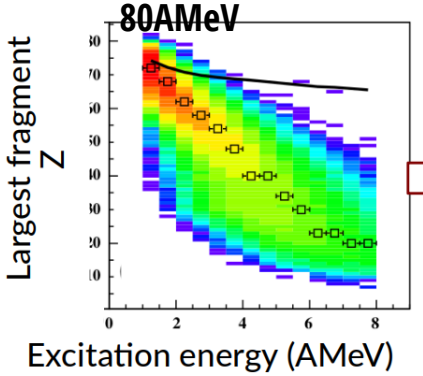

Reweighting of experimental E* distribution (experiment not performed in canonical ensemble)

F. Gulminelli NPA791(2007)165

Pseudo-canonical probability distributions

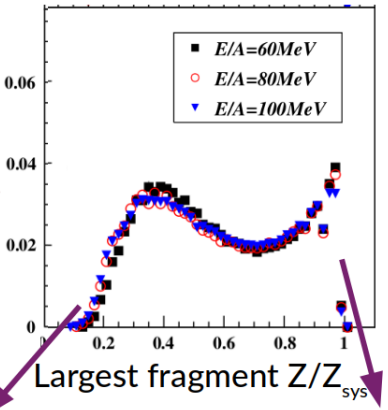

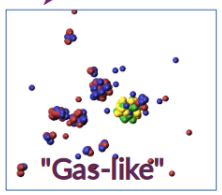

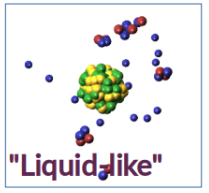

INDRA collaboration (E. Bonnet et al.)
Phys. Rev. Lett. 103(2009)072701

CALORiC CURVES

Evidence for the boiling of hot nuclei?

Bondorf, Donangelo, Schulz & Sneppen
Phys. Lett. B162(1985)30

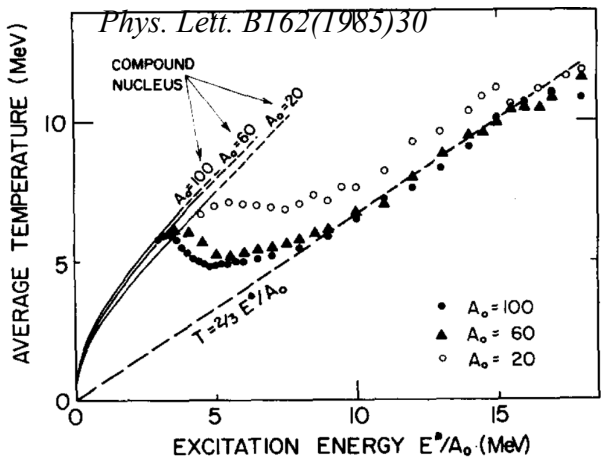

Statistical Multifragmentation Model (SMM) calculations

J. Pochodzalla et al.
Phys. Rev. Lettt. 75(1995)1040

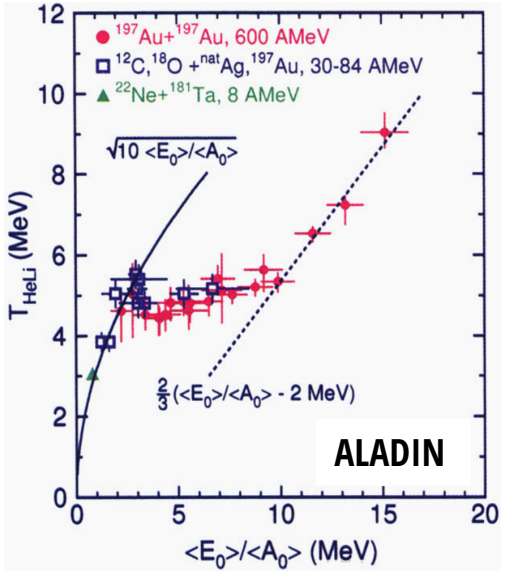

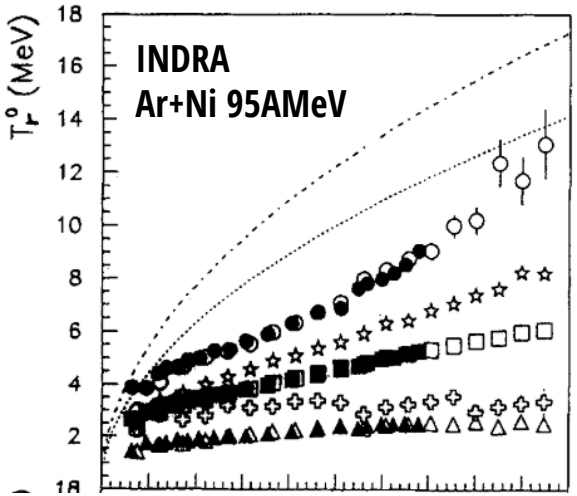

Y.G. Ma et al.
Phys. Lettt. B390(1997)41

Texas A&M + others

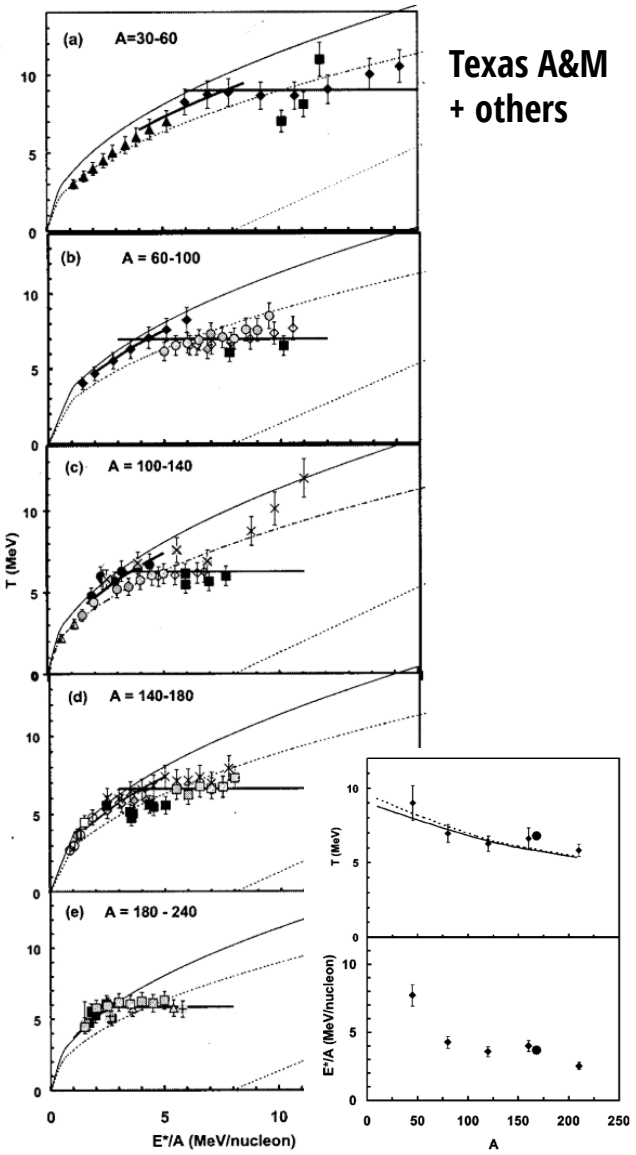

J.B. Natowitz, R. Wada, K. Hagel, et al.
Phys. Rev. C65(2002)034618

CALORiC CURVES

Ambiguous signals

Chomaz, Duflot, Gulminelli,
Phys. Rev. Lett. 85(2000)3587

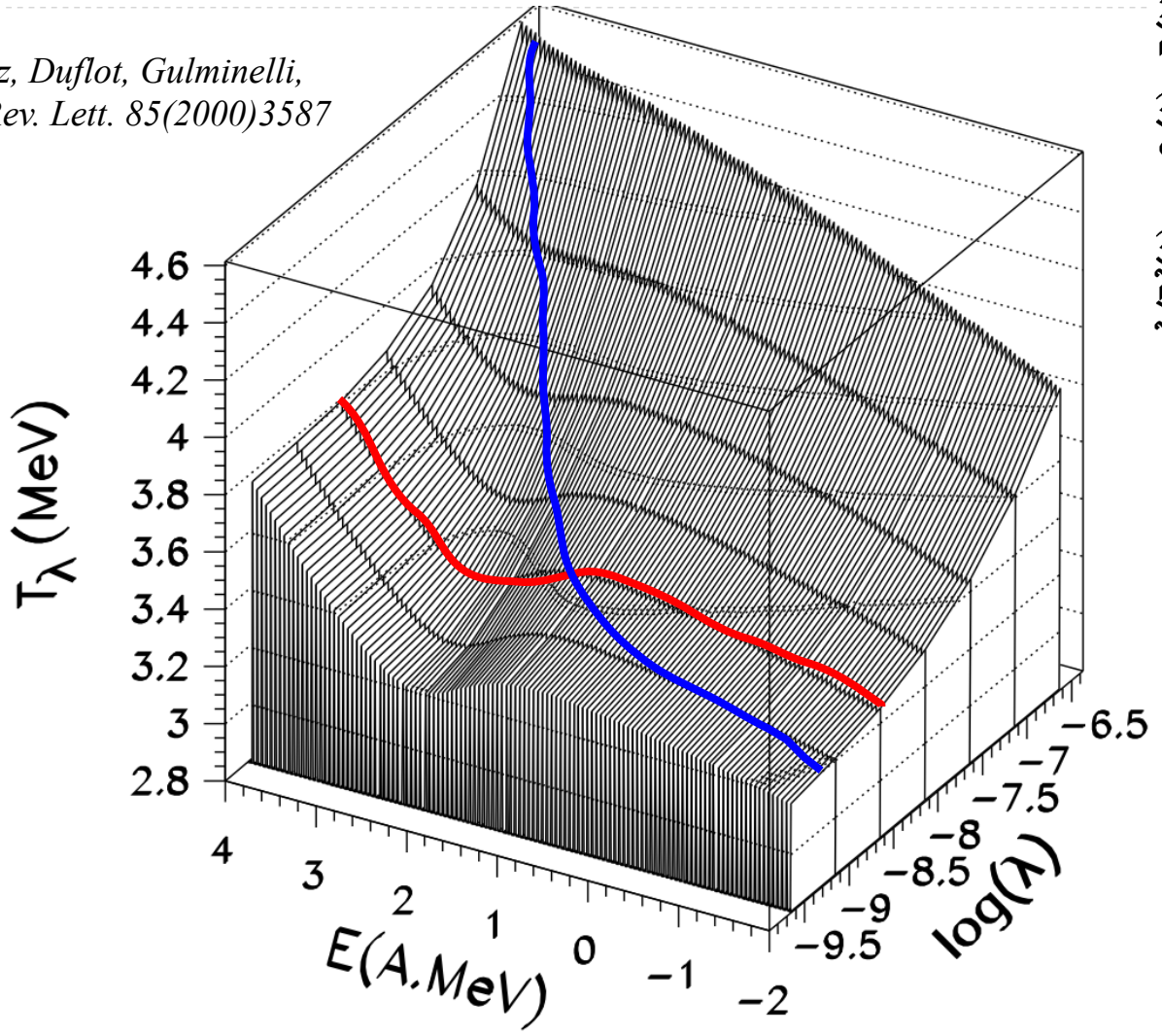

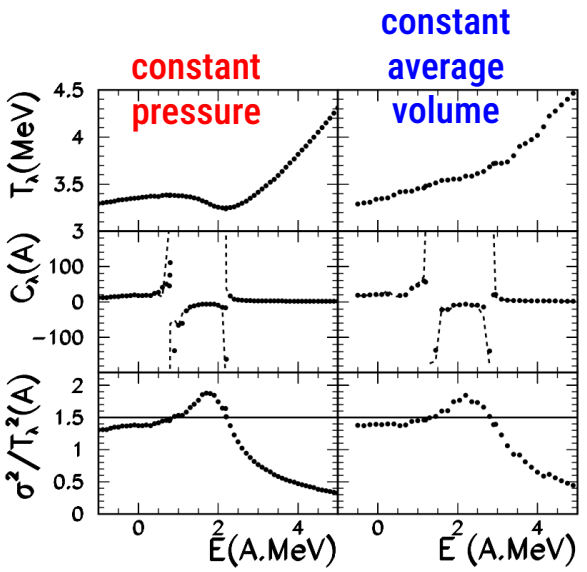

Microcanonical lattice-gas calculations
with fixed mean volumes

$$S = -\sum p_i \log p_i + \lambda \langle V \rangle$$

Pressure $P_\lambda = T_\lambda \lambda$

The shape of the observed caloric curve depends how the EoS is sampled
i.e. how not only temperature but also how volume depends on excitation energy

This is in principle impossible to control experimentally

CONSTRAiNED CALORiC CURVES

A posteriori control of experimental conditions

Simulations were used to reconstruct freeze-out properties (configuration of excited primary fragments and light particles) for quasi-fused sources in **Xe+Sn central collisions 32-50 MeV/u (INDRA)**.

INDRA Collaboration (S. Piantelli et al.)
*Nucl. Phys. **A809**(2008)111*

CONSTRAiNED CALORiC CURVES

A posteriori control of experimental conditions

Simulations were used to reconstruct freeze-out properties (configuration of excited primary fragments and light particles) for quasi-fused sources in **Xe+Sn central collisions 32-50 MeV/u (INDRA)**.

INDRA Collaboration (S. Piantelli et al.)
*Nucl. Phys. **A809**(2008)111*

The use of a limiting temperature for fragments (vanishing level density at high E*) was mandatory (velocity widths):

$$\frac{1}{T_f} = \frac{1}{T_{kin}} + \frac{1}{T_{lim}},\ T_{lim} = 9\mathrm{MeV}$$

S.E. Koonin, J. Randrup
*Nucl. Phys. **A474**(1987)173*

CONSTRAiNED CALORiC CURVES

A posteriori control of experimental conditions

Simulations were used to reconstruct freeze-out properties (configuration of excited primary fragments and light particles) for quasi-fused sources in **Xe+Sn central collisions 32-50 MeV/u (INDRA)**.

INDRA Collaboration (S. Piantelli et al.)
*Nucl. Phys. **A809**(2008)111*

The use of a limiting temperature for fragments (vanishing level density at high E*) was mandatory (velocity widths):

$$\frac{1}{T_f} = \frac{1}{T_{kin}} + \frac{1}{T_{lim}},\ T_{lim} = 9\mathrm{MeV}$$

S.E. Koonin, J. Randrup
*Nucl. Phys. **A474**(1987)173*

Then, using exact microcanonical expressions for pressure, temperature depending only on **total multiplicity M_c** and **total kinetic energy K** at freeze-out:

$$T^{-1} = \left(\frac{\partial S}{\partial E}\right) = \left\langle \frac{3M_C - 5}{2K} \right\rangle$$

$$P = T\left(\frac{\partial S}{\partial V}\right) = \frac{\langle M_C \rangle T}{V}$$

Al. H. Raduta, Ad. R. Raduta
*Nucl. Phys. **A703**(2002)876*

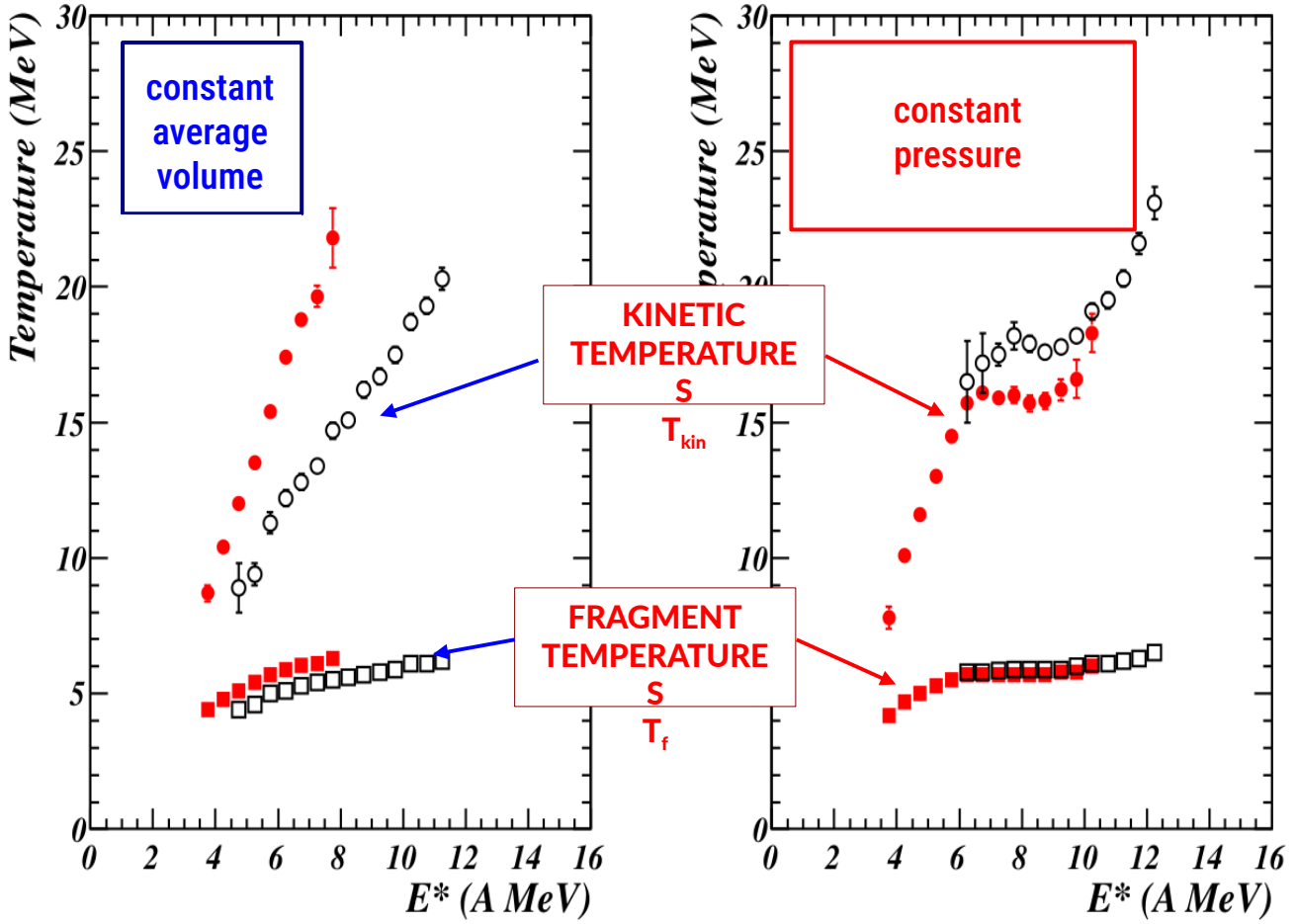

B. Borderie et al.,
*Phys. Lett. B**723**(2013)140*

NEGATiVE HEAT CAPACiTiES

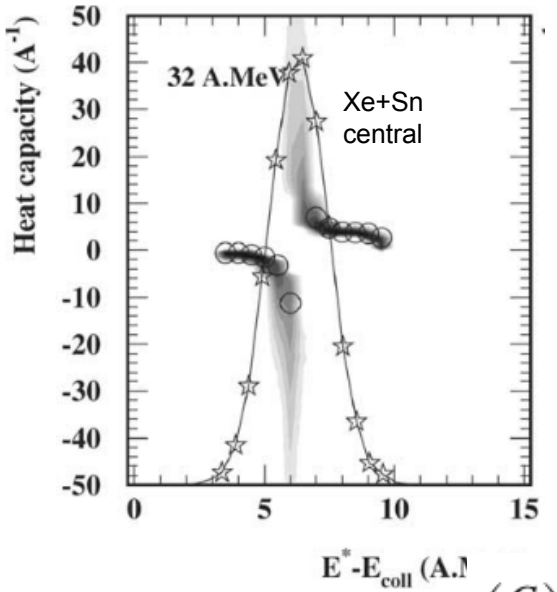

M. D'Agostino, R. Bougault et al.
Nucl. Phys. A699, 795(2002)

Chomaz, Gulminelli
Nucl. Phys. A647, 153 (1999)

$$\left(\frac{C}{A}\right)_{\text{micro}} \simeq C_k + C_p \simeq \frac{C_k^2}{C_k - \frac{A\sigma_k^2}{T^2}}$$

N. Le Neindre et al,
Nucl. Phys. A795, 47(2007)

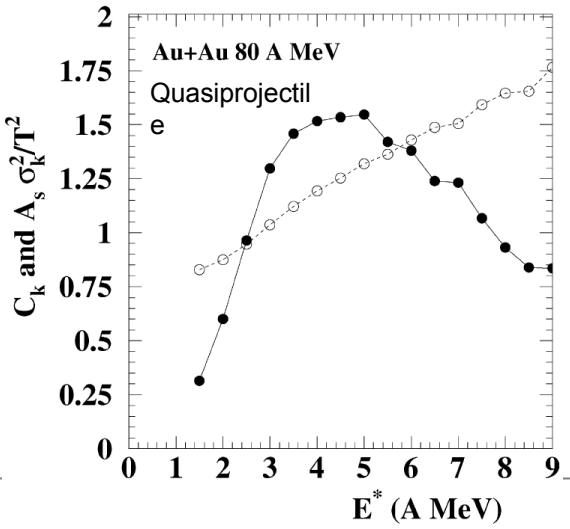

NEGATiVE HEAT CAPACiTiES

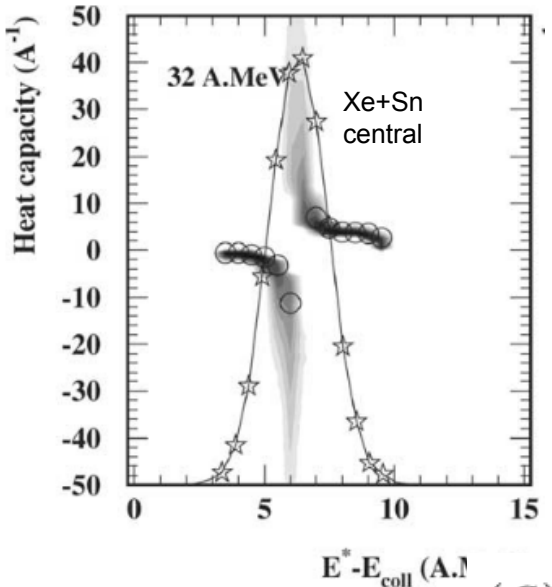

M. D'Agostino, R. Bougault et al.
Nucl. Phys. A699, 795(2002)

Chomaz, Gulminelli
Nucl. Phys. A647, 153 (1999)

$$\left(\frac{C}{A}\right)_{\text{micro}} \simeq C_k + C_p \simeq \frac{C_k^2}{C_k - \frac{A\sigma_k^2}{T^2}}$$

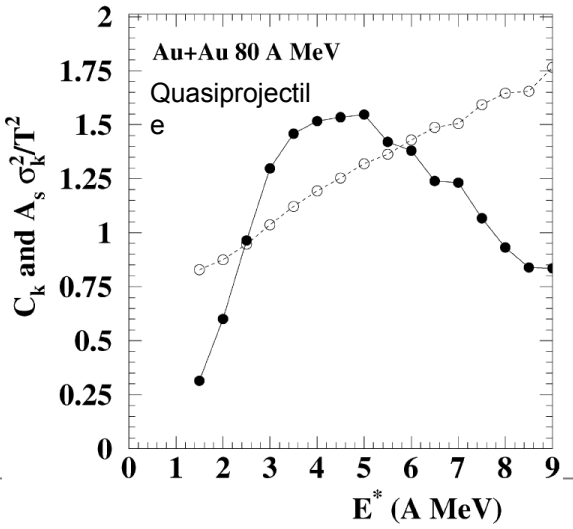

N. Le Neindre et al,
Nucl. Phys. A795, 47(2007)

SPINODAL INSTABILITIES

Circumstancial evidence: bulk effect in multifragmentation

M.F. Rivet et al.
Phys. Lett. B430(1998)217

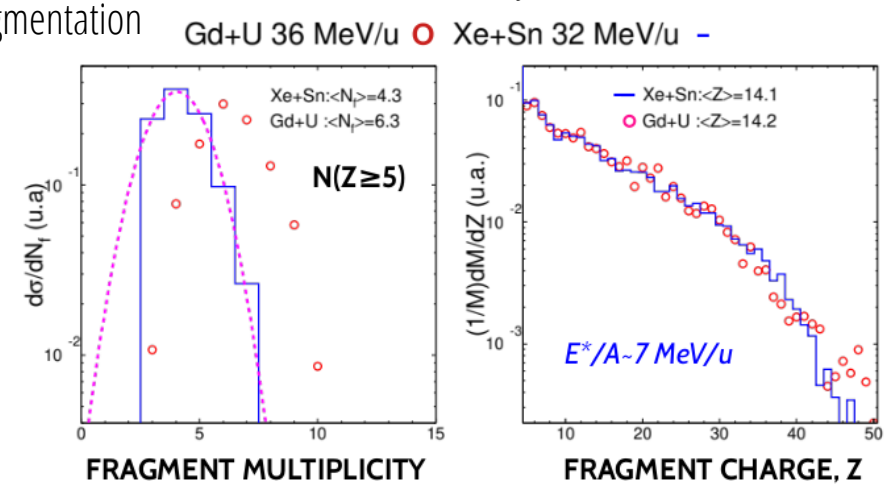

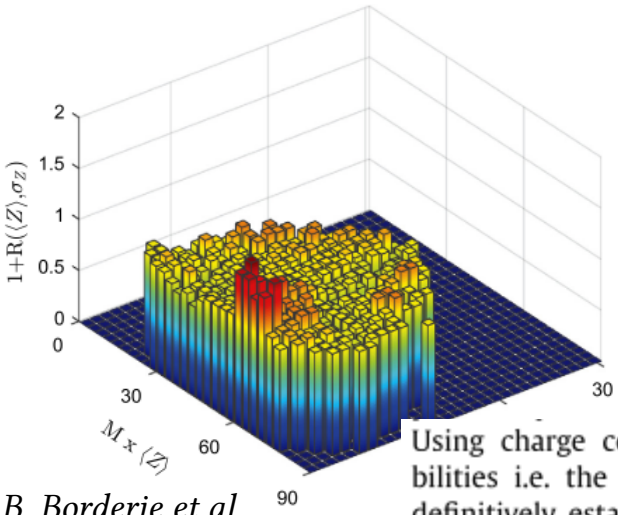

B. Borderie et al.
Phys. Lett. B782(2018)291

Smoking gun: abnormal production of equal-size fragments

$$\sigma_Z^2 = \frac{1}{M}\sum n_Z (Z - \langle Z \rangle)^2$$

$$1 + R(\sigma_Z, \langle Z \rangle) = \frac{Y(\sigma_Z, \langle Z \rangle)}{Y'(\sigma_Z, \langle Z \rangle)}\Big|_M$$

Using charge correlations the fossil signature of spinodal instabilities i.e. the abnormal presence of equal-sized fragments was definitively established at a confidence level of around 6–7 sigma units for both reactions at 32 *A* MeV incident energy. At higher

WHY DO YOU HAVE TO BE SO CRITICAL ALL THE TIME?

Much early evidence and studies concentrated on the similarity between multifragmentation and (macroscopic) critical phenomena...

J.E. Finn et al. PRL49, 1321(1982)

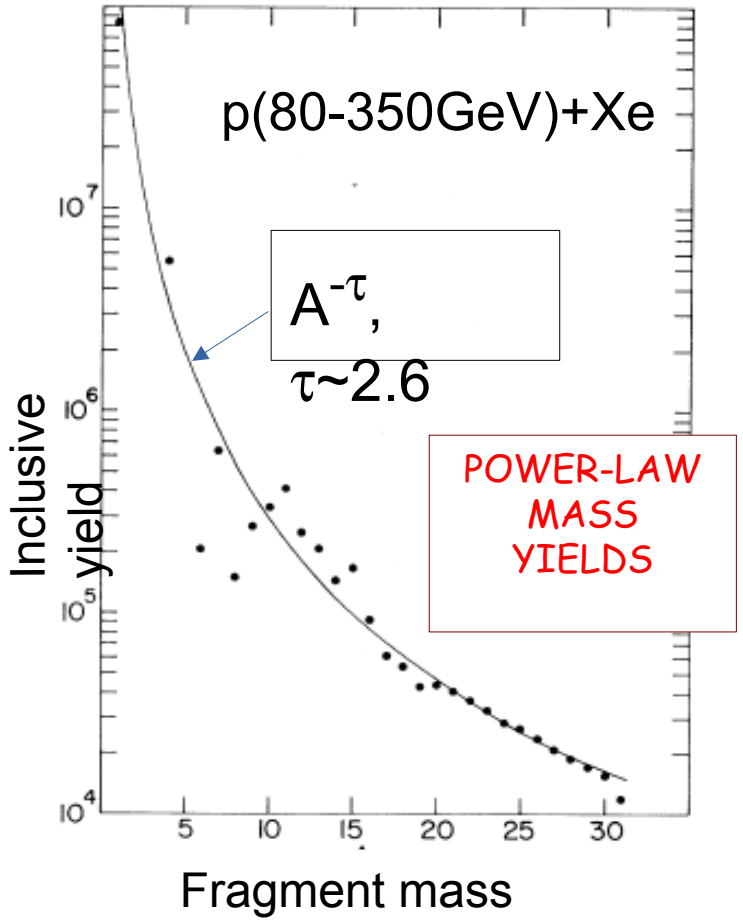

Gilkes & al PRL73, 1590(1994)
Elliott & al PLB381, 35(1996)

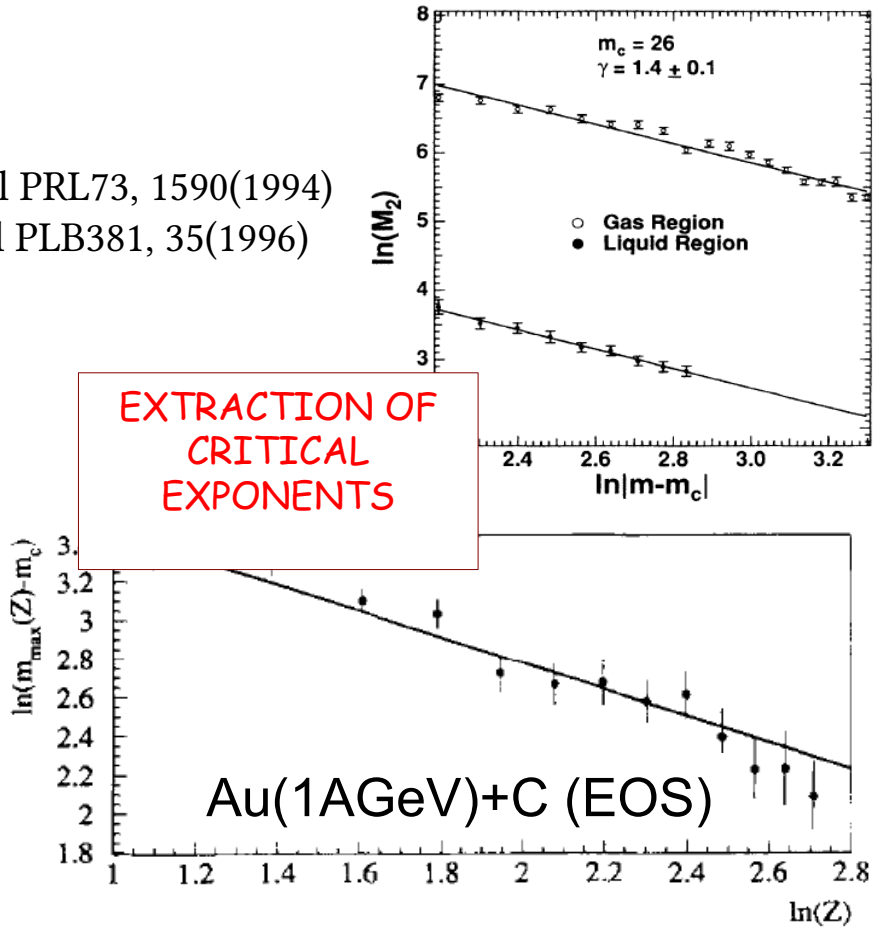

WHY DO YOU HAVE TO BE SO CRITICAL ALL THE TIME?

Much early evidence and studies concentrated on the similarity between multifragmentation and (macroscopic) critical phenomena...

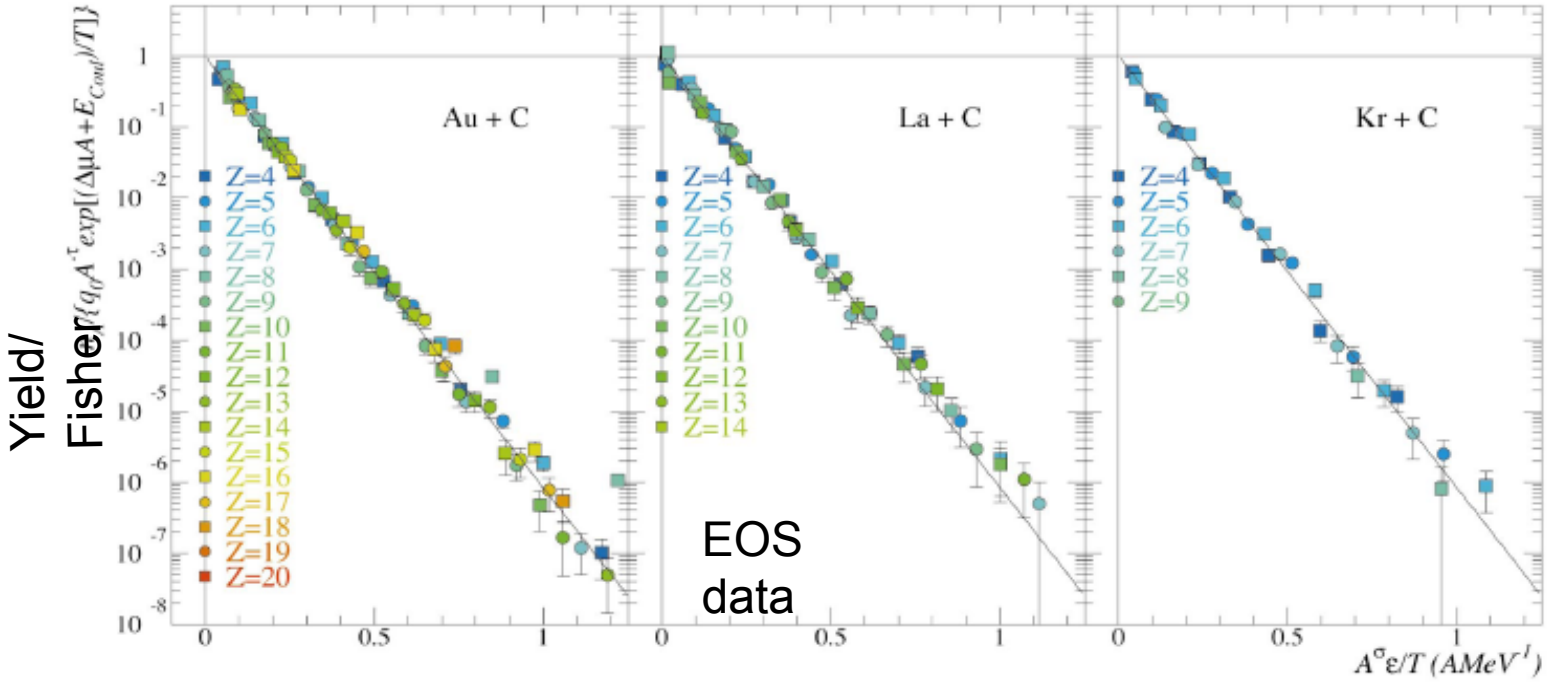

Elliott & al PRC67, 024609(2003)

FISHER DROPLET MODEL

$$n_A = q_0 A^{-\tau} \exp\left[\frac{\Delta\mu A}{T} - \frac{c_0 \varepsilon A^{\sigma}}{T}\right]$$

Cluster size distribution for condensation in near-critical fluid

Fisher, Physics 3, 41(1967)

"FISHER SCALING"

- fragment yields follow Fisher law for all $T<T_C$

WHY DO YOU HAVE TO BE SO CRITICAL ALL THE TIME?

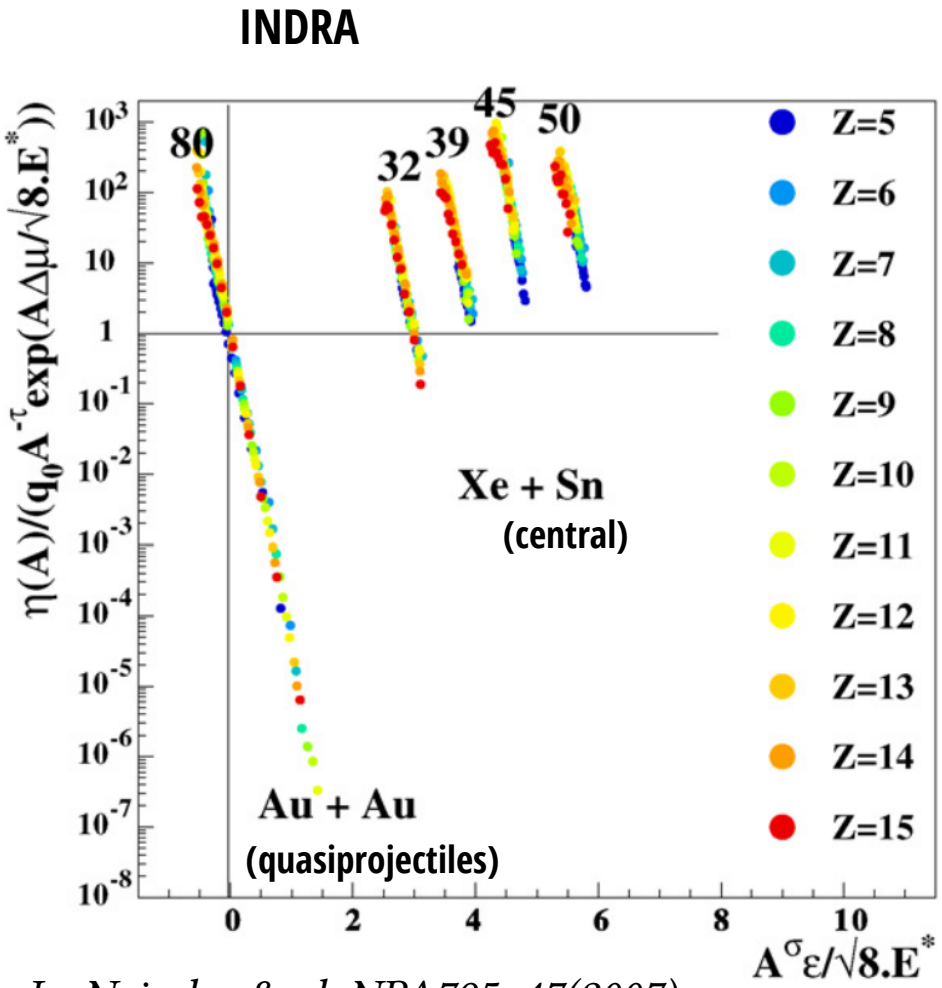

Le Neindre & al, NPA795, 47(2007)

Much early evidence and studies concentrated on the similarity between multifragmentation and (macroscopic) critical phenomena...

But on closer inspection, inconsistencies appear...

"FISHER INCONSISTENCY"

INDRA data: fragment yields follow Fisher law... even (especially) above the critical temperature ???

WHY DO YOU HAVE TO BE SO CRITICAL ALL THE TIME?

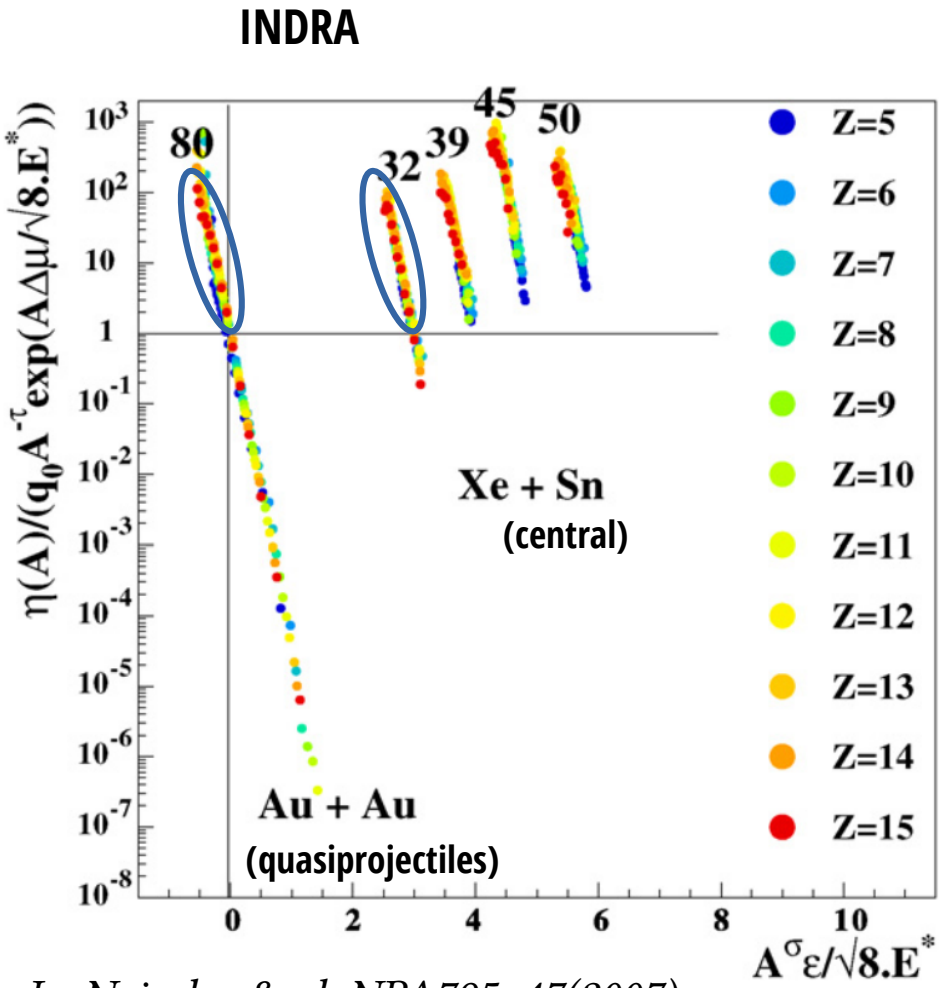

Le Neindre & al, NPA795, 47(2007)

Much early evidence and studies concentrated on the similarity between multifragmentation and (macroscopic) critical phenomena...

But on closer inspection, inconsistencies appear...

"FISHER INCONSISTENCY"

INDRA data: fragment yields follow Fisher law... even (especially) above the critical temperature ???

THE ORDER IS NOT WHAT IT SEEMS…

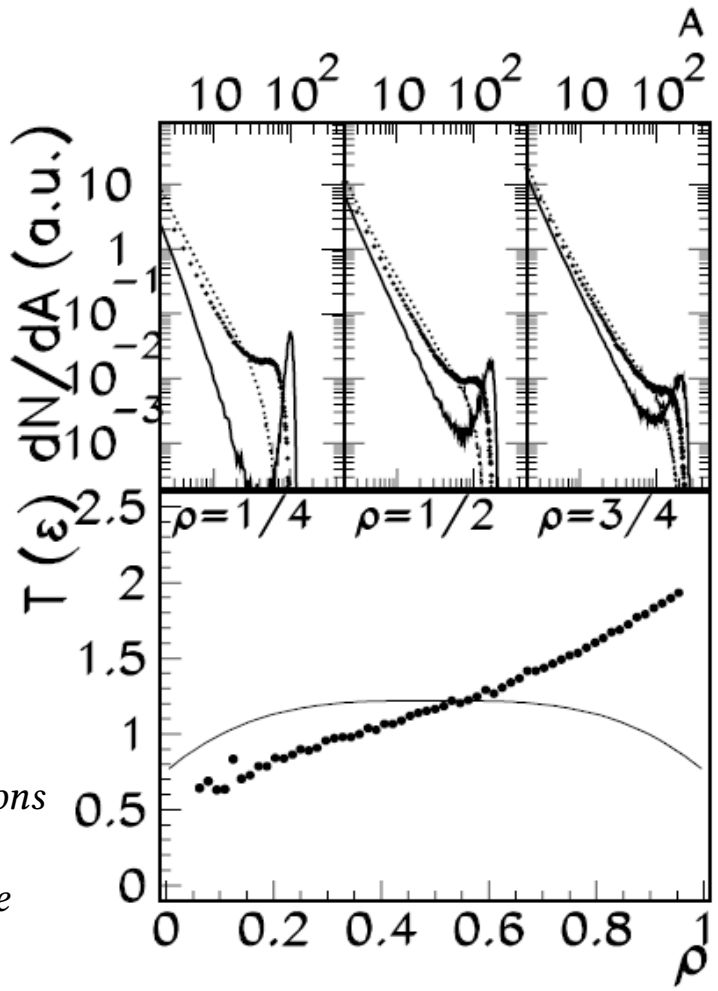

Lattice Gas Model calculations showing line of points where mass distributions appear "critical" inside coexistence zone

Gulminelli, Chomaz, Phys. Rev. Lett. 82(1999)1402

Phase transitions which are **1st order in the thermodynamic limit** can exhibit all the critical behaviour and scalings of continuous/2nd order transitions **when they manifest in a finite system**

This can be understood intuitively:

- in infinite systems, critical behaviour occurs when the correlation length becomes comparable to the system size, i.e. infinite
- in finite systems, correlations only need be comparable to the system size for them to become "**pseudocritical**"

+ due to non-additivity, phases cannot coexist. These are "**1st order phase transitions without coexistence**". Which sounds a lot like a continuous phase transition.

UNIVERSAL FLUCTUATIONS AND AN OLD QUESTION

Therefore we can use approaches developed for continuous phase transitions (as long we are careful with the interpretations) without any contradiction with the 1st order nature of the nuclear liquid-gas phase transition!

PHYSICAL REVIEW E VOLUME 62, NUMBER 2 AUGUST 2000

Universal features of the order-parameter fluctuations: Reversible and irreversible aggregation

Robert Botet[1] and Marek Płoszajczak[2]
[1]*Laboratoire de Physique des Solides, CNRS, Bâtiment 510, Université Paris–Sud, Centre d'Orsay, F-91405 Orsay, France*
[2]*Grand Accélérateur National d'Ions Lourds (GANIL), CEA/DSM–CNRS/IN2P3, Boîte Postale 5027, F-14021 Caen Cedex, France*

A $\langle m \rangle^{\Delta} P_N[m] = \Phi(z_{(\Delta)}) = \Phi\left(\frac{m - \langle m \rangle}{\langle m \rangle^{\Delta}}\right)$

B $\sigma^2 \sim \langle m \rangle^{2\Delta}$

UNIVERSAL FLUCTUATIONS AND AN OLD QUESTION

Therefore we can use approaches developed for continuous phase transitions (as long we are careful with the interpretations) without any contradiction with the 1st order nature of the nuclear liquid-gas phase transition!

"An observable m whose probability distributions can be scaled according to **A** and for whom the exponent Δ in the fluctuation scaling law **B** changes as a function of energy or temperature is behaving as the order parameter of a pseudocritical phase transition"

A $\langle m \rangle^{\Delta} P_N[m] = \Phi(z_{(\Delta)}) = \Phi\left(\frac{m - \langle m \rangle}{\langle m \rangle^{\Delta}}\right)$

B $\sigma^2 \sim \langle m \rangle^{2\Delta}$

UNIVERSAL FLUCTUATIONS AND AN OLD QUESTION

Therefore we can use approaches developed for continuous phase transitions (as long we are careful with the interpretations) without any contradiction with the 1st order nature of the nuclear liquid-gas phase transition!

"An observable m whose probability distributions can be scaled according to **A** and for whom the exponent Δ in the fluctuation scaling law **B** changes as a function of energy or temperature is behaving as the order parameter of a pseudocritical phase transition"

A $$\langle m \rangle^{\Delta} P_N[m] = \Phi(z_{(\Delta)}) = \Phi\left(\frac{m - \langle m \rangle}{\langle m \rangle^{\Delta}}\right)$$

B $$\sigma^2 \sim \langle m \rangle^{2\Delta}$$

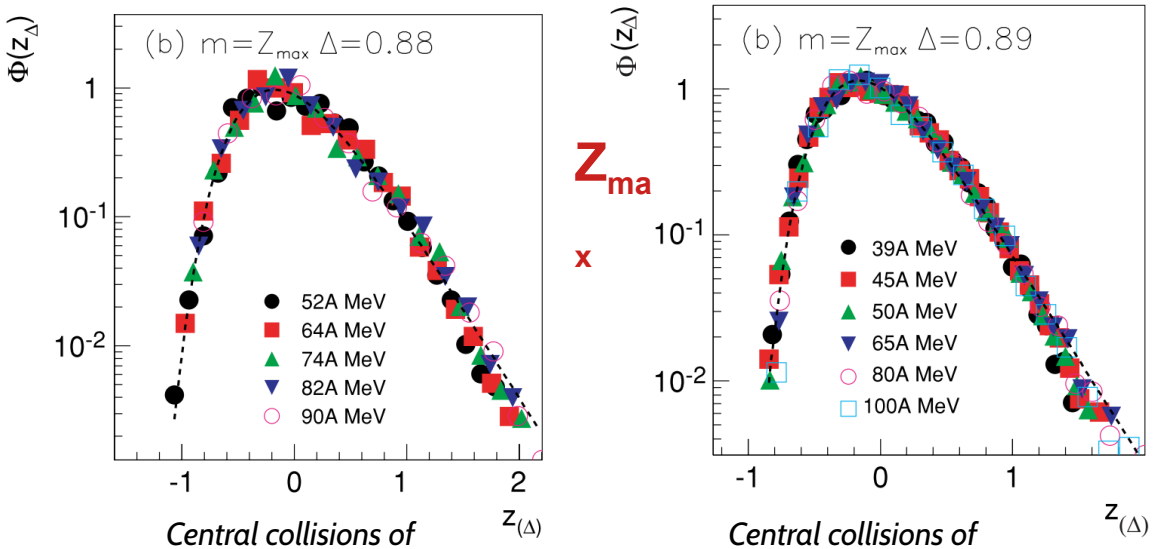

Central collisions of
^{58}Ni+^{58}Ni E/A=52-90 MeV
[INDRA 2nd campaign, 1994]

Central collisions of
^{129}Xe+^{x}Sn E/A=39-100 MeV
[INDRA 1st & 4th (GSI) campaigns]

UNIVERSAL FLUCTUATIONS AND AN OLD QUESTION

Therefore we can use approaches developed for continuous phase transitions (as long we are careful with the interpretations) without any contradiction with the 1st order nature of the nuclear liquid-gas phase transition!

"An observable m whose probability distributions can be scaled according to **A** and for whom the exponent Δ in the fluctuation scaling law **B** changes as a function of energy or temperature is behaving as the order parameter of a pseudocritical phase transition"

A $\langle m \rangle^{\Delta} P_N[m] = \Phi(z_{(\Delta)}) = \Phi\left(\frac{m - \langle m \rangle}{\langle m \rangle^{\Delta}}\right)$

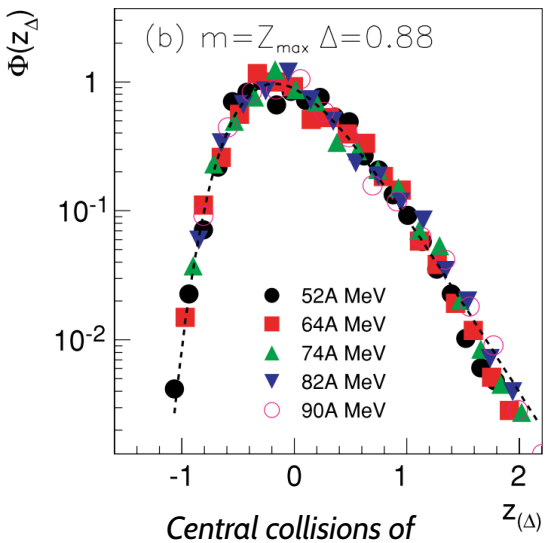

Central collisions of
^{58}Ni+^{58}Ni E/A=52-90 MeV
[INDRA 2nd campaign, 1994]

Z_max
x

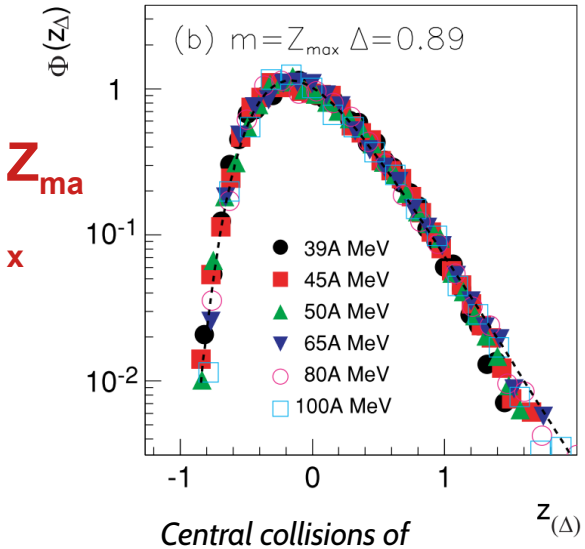

Central collisions of
^{129}Xe+^{x}Sn E/A=39-100 MeV
[INDRA 1st & 4th (GSI) campaigns]

B $\sigma^2 \sim \langle m \rangle^{2\Delta}$

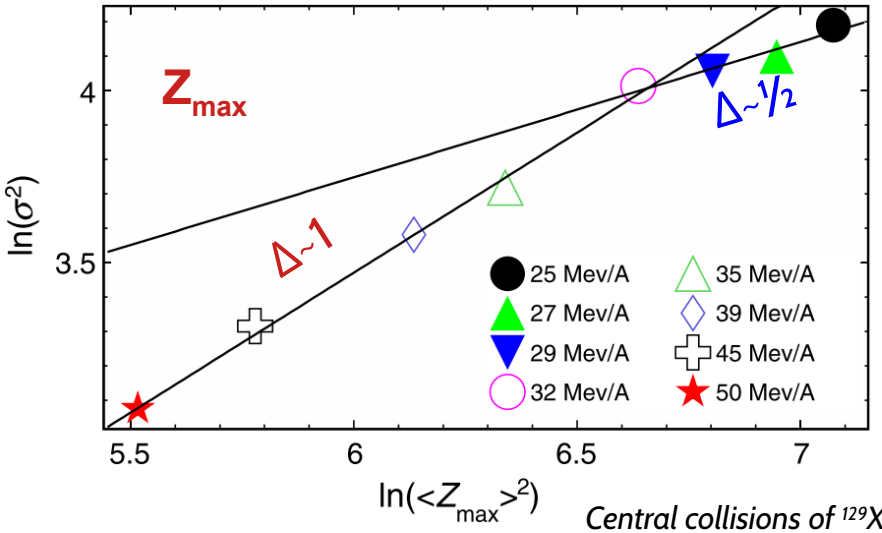

Botet *et al.*
PRL86(2001)

Frankland *et al.*
(INDRA/ALADIN)
PRC71(2005)

Gruyer *et al.*
(INDRA collab.)
PRL110(2013)

Central collisions of ^{129}Xe+^{119}Sn
[INDRA 1st & 5th campaigns, 1993, 2001]

UNIVERSAL FLUCTUATIONS AND AN OLD QUESTION

Therefore we can use approaches developed for continuous phase transitions (as long we are careful with the interpretations) without any contradiction with the 1st order nature of the nuclear liquid-gas phase transition!

"An observable m whose probability distributions can be scaled according to **A** and for whom the exponent Δ in the fluctuation scaling law **B** changes as a function of energy or temperature is behaving as the order parameter of a pseudocritical phase transition"

A $\langle m \rangle^{\Delta} P_N[m] = \Phi(z_{(\Delta)}) = \Phi\left(\frac{m - \langle m \rangle}{\langle m \rangle^{\Delta}}\right)$

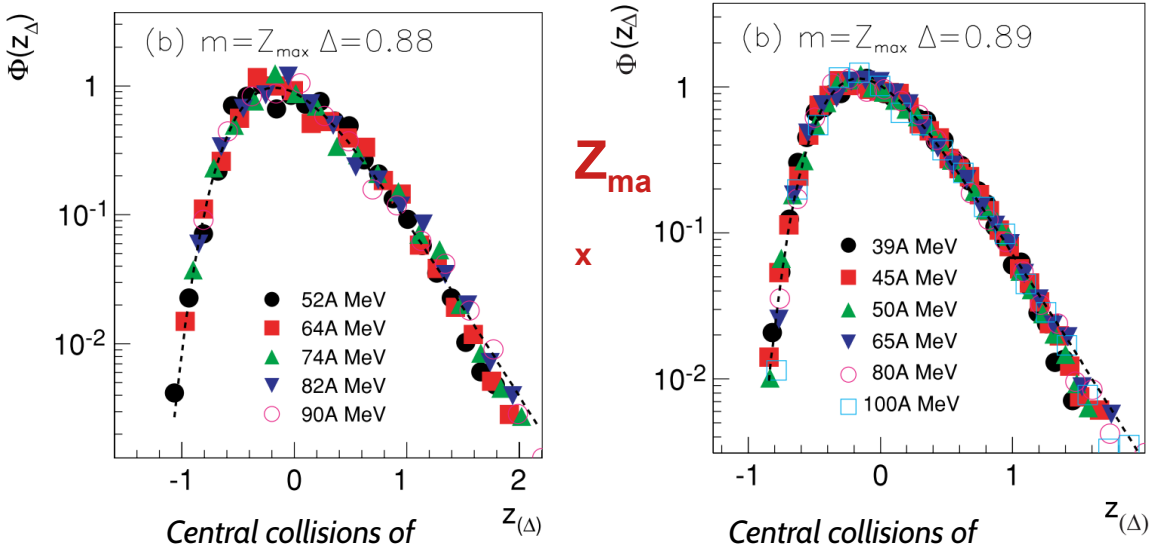

Central collisions of $^{58}Ni+^{58}Ni$ E/A=52-90 MeV [INDRA 2nd campaign, 1994]

Central collisions of $^{129}Xe+^{x}Sn$ E/A=39-100 MeV [INDRA 1st & 4th (GSI) campaigns]

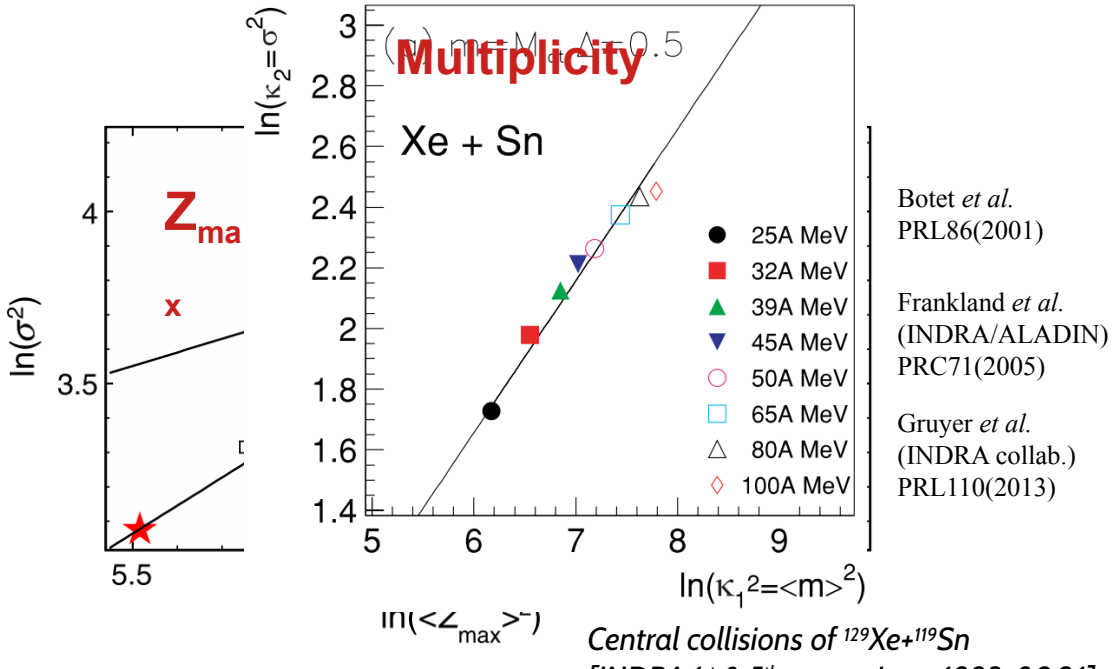

Botet *et al.* PRL86(2001)

Frankland *et al.* (INDRA/ALADIN) PRC71(2005)

Gruyer *et al.* (INDRA collab.) PRL110(2013)

Central collisions of $^{129}Xe+^{119}Sn$ [INDRA 1st & 5th campaigns, 1993, 2001]

UNIVERSAL FLUCTUATIONS AND AN OLD QUESTION

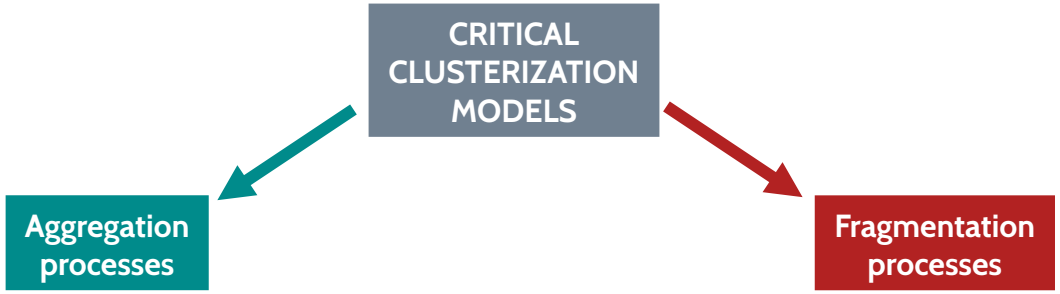

UNIVERSAL FLUCTUATIONS AND AN OLD QUESTION

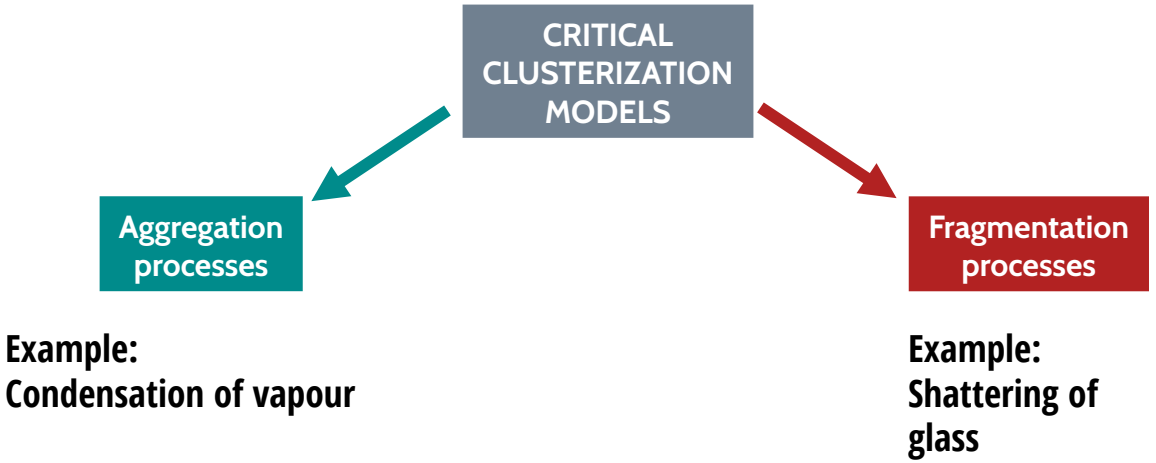

UNIVERSAL FLUCTUATIONS AND AN OLD QUESTION

Example:
Condensation of vapour

Example:
Shattering of glass

Volume 136B, number 1,2 PHYSICS LETTERS 23 February 1984

FRAGMENTATION REACTIONS ON NUCLEI:
CONDENSATION OF VAPOUR OR SHATTERING OF GLASS? ☆

J. AICHELIN[1] and J. HUEFNER
Institut für Theoretische Physik der Universität Heidelberg, Heidelberg, Fed. Rep. Germany
and Max-Planck-Institut für Kernphysik, Heidelberg, Fed. Rep. Germany

UNIVERSAL FLUCTUATIONS AND AN OLD QUESTION

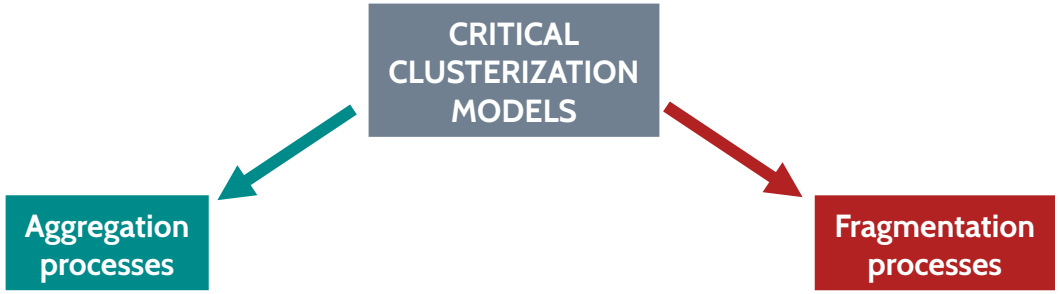

Example:
Condensation of vapour

Order parameter:
Largest cluster size

Example:
Shattering of glass

Order parameter:
Number of clusters

Volume 136B, number 1,2 PHYSICS LETTERS 23 February 1984

FRAGMENTATION REACTIONS ON NUCLEI: CONDENSATION OF VAPOUR OR SHATTERING OF GLASS? ☆

J. AICHELIN[1] and J. HUEFNER
Institut für Theoretische Physik der Universität Heidelberg, Heidelberg, Fed. Rep. Germany and Max-Planck-Institut für Kernphysik, Heidelberg, Fed. Rep. Germany

UNIVERSAL FLUCTUATIONS AND AN OLD QUESTION

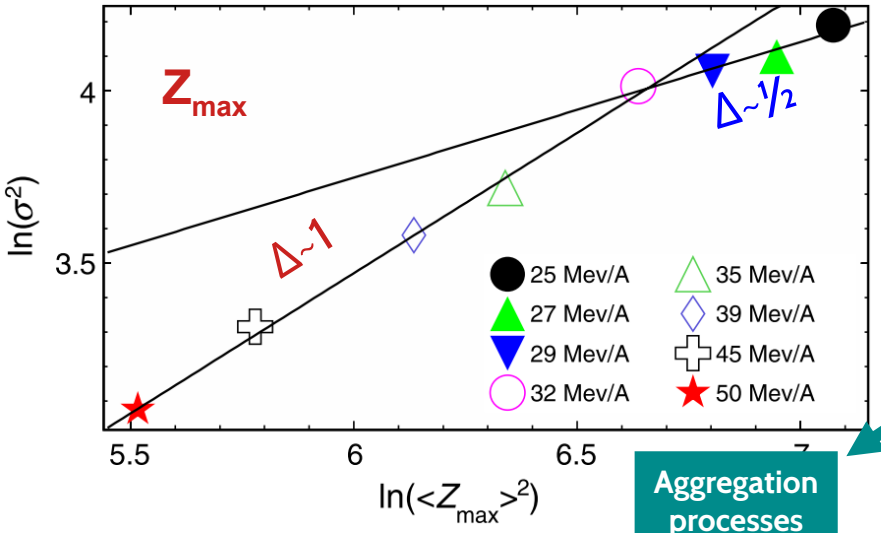

CRITICAL CLUSTERIZATION MODELS

Aggregation processes

Fragmentation processes

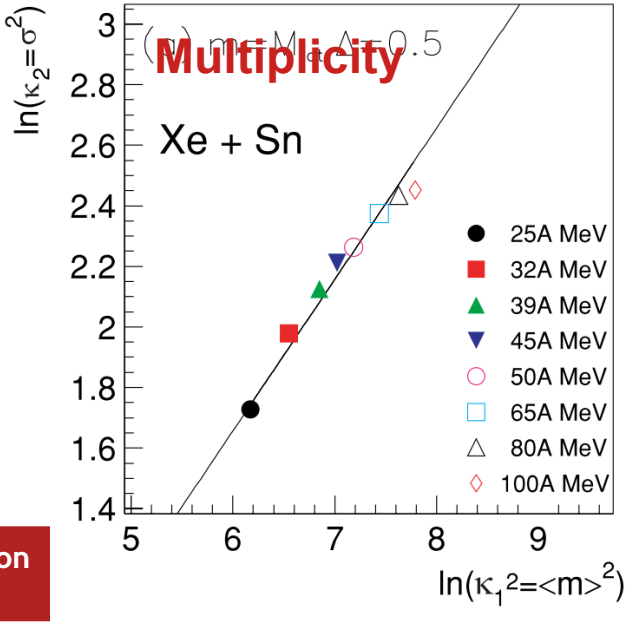

Example:
Condensation of vapour

Order parameter:
Largest cluster size

Example:
Shattering of glass

Order parameter:
Number of clusters

Volume 136B, number 1,2 PHYSICS LETTERS 23 February 1984

FRAGMENTATION REACTIONS ON NUCLEI:
CONDENSATION OF VAPOUR OR SHATTERING OF GLASS?☆

J. AICHELIN[1] and J. HUEFNER
Institut für Theoretische Physik der Universität Heidelberg, Heidelberg, Fed. Rep. Germany
and Max-Planck-Institut für Kernphysik, Heidelberg, Fed. Rep. Germany

LIQUID-GAS PHASE TRANSITIONS IN NUCLEAR MATTER

A (hopefully) pedagogical introduction and overview of experimental achievements in the field

John FRANKLAND

GANIL

cnrs NUCLÉAIRE & PARTICULES

cea

1. EoS & Liquid-gas phase transition

- non-ideal fluids (e.g. Van der Waals) exhibit LGPT with low/high-density phases, coexistence, spinodal instability and critical point
- nuclear matter calculations (HF+Skyrme, & many more) exhibit very similar phenomenology
- clear link between multifragmentation/vaporization and NM EoS

2. Historic experimental observations

- power-law mass distribution suggests critical phenomenon
- critical exponents shown close to LGPT universality class (but ambiguous)
- caloric curve apparently compatible with 1st order PT (plateau → coexistence) (but ambiguous)
- multifragmentation onset E*~3 MeV/u
- quasi-simultaneous break-up at low density ($\rho \sim \rho_0/3$)

3. INDRA results

- characterization of gas phase:
  - weakly-interacting (non-ideal) gas fermions/bosons
  - density-dependence of chemical constants indicate weak in-medium effect on clusters
  - LGPT in QCD phase diagram: continuity between hadronization and nuclear clustering in HIC
- characterization of the phase transition:
  - in finite systems LGPT → convex intruder in 'system' entropy/event population
  - coherent signals of negative heat capacity, bimodality, spinodal decomposition were observed
  - ambiguity of "caloric curves" removed by a posteriori control of phase space trajectory
  - finite size → pseudocritical behaviour
  - universal fluctuations → Z_{max} order parameter → multifragmentation = aggregation/coalescence/condensation